

Inverse Seesaw with flavour and CP symmetries and its phenomenology

Based on “Charged lepton flavour violation from inverse seesaw with flavour and CP symmetries”
(FPDM, C. Hagedorn, '24) ;

“Lepton mixing and cLFV from ISS with non-degenerate heavy states”
(FPDM, C.Hagedorn, '25)



GENERALITAT
VALENCIANA

CSIC

VNIVERSITAT
D VALÈNCIA



EXCELENCIA
SEVERO
OCHOA

Flash Introduction to Neutrino Physics

- 1930 : Pauli's hypothesis to explain β -decay

(<https://neutrinos.fnal.gov/history/>)

Flash Introduction to Neutrino Physics

- 1930 : Pauli's hypothesis to explain β -decay
- 1956: Discovered at Los Alamos (Reines and Cowan)

(<https://neutrinos.fnal.gov/history/>)

Flash Introduction to Neutrino Physics

- 1930 : Pauli's hypothesis to explain β -decay
- 1956: Discovered at Los Alamos (Reines and Cowan)
- 1958: Neutrinos are only LH (Southpaw)

(<https://neutrinos.fnal.gov/history/>)

Flash Introduction to Neutrino Physics

- 1930 : Pauli's hypothesis to explain β -decay
- 1956: Discovered at Los Alamos (Reines and Cowan)
- 1958: Neutrinos are only LH (Southpaw)



Formulation of GSW theory of EW interactions (approx 1960-1970): LH and massless neutrinos

(<https://neutrinos.fnal.gov/history/>)

Flash Introduction to Neutrino Physics

- 1930 : Pauli's hypothesis to explain β -decay
- 1956: Discovered at Los Alamos (Reines and Cowan)
- 1958: Neutrinos are only LH (Southpaw)
- 1962: Discovery of muon neutrino (Lederman)



Formulation of GSW theory of EW interactions (approx 1960-1970): LH and massless neutrinos

(<https://neutrinos.fnal.gov/history/>)

Flash Introduction to Neutrino Physics

- 1930 : Pauli's hypothesis to explain β -decay
- 1956: Discovered at Los Alamos (Reines and Cowan)
- 1958: Neutrinos are only LH (Southpaw)
- 1962: Discovery of muon neutrino (Lederman)
- 1968 : Detection of Solar Neutrinos (Homestake exp.)
 - Only 1/3 of electron neutrinos observed...
- 1985 : Detection of Atmospheric Neutrinos (Kamiokande and IMB)
 - Smaller ratio of muon neutrinos to electron neutrinos observed
- 1998 : First evidence of Atmospheric Neutrino Oscillations (Super-Kamiokande)



Formulation of GSW theory of EW interactions (approx 1960-1970): LH and massless neutrinos

(<https://neutrinos.fnal.gov/history/>)

Flash Introduction to Neutrino Physics

- 1930 : Pauli's hypothesis to explain β -decay
- 1956: Discovered at Los Alamos (Reines and Cowan)
- 1958: Neutrinos are only LH (Southpaw)
- 1962: Discovery of muon neutrino (Lederman)
- 1968 : Detection of Solar Neutrinos (Homestake exp.)
 - Only 1/3 of electron neutrinos observed...
- 1985 : Detection of Atmospheric Neutrinos (Kamiokande and IMB)
 - Smaller ratio of muon neutrinos to electron neutrinos observed
- 1998 : First evidence of Atmospheric Neutrino Oscillations (Super-Kamiokande)
- 2000 : Discovery of Tau neutrino (DONUT collaboration)



Formulation of GSW theory of EW interactions (approx 1960-1970): LH and massless neutrinos

(<https://neutrinos.fnal.gov/history/>)

Flash Introduction to Neutrino Physics

- 1930 : Pauli's hypothesis to explain β -decay
- 1956: **Discovered at Los Alamos (Reines and Cowan)**
- 1958: Neutrinos are only LH (Southpaw)
- 1962: **Discovery of muon neutrino (Lederman)**
- 1968 : Detection of Solar Neutrinos (Homestake exp.)
 - Only 1/3 of electron neutrinos observed...
- 1985 : Detection of Atmospheric Neutrinos (Kamiokande and IMB)
 - Smaller ratio of muon neutrinos to electron neutrinos observed
- 1998 : First evidence of Atmospheric Neutrino Oscillations (Super-Kamiokande)
- 2000 : **Discovery of Tau neutrino (DONUT collaboration)**

Formulation of GSW theory of EW interactions (approx 1960-1970): LH and massless neutrinos

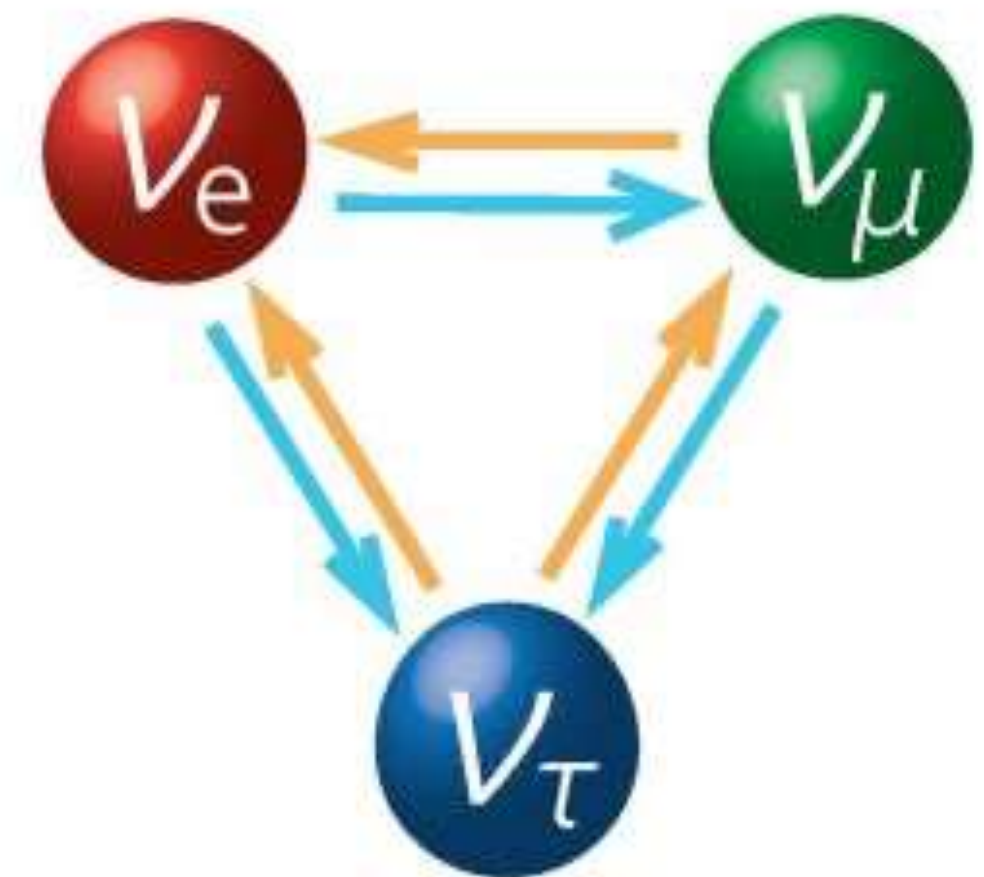


(<https://neutrinos.fnal.gov/history/>)

Flash Introduction to Neutrino Physics

- 1930 : Pauli's hypothesis to explain β -decay
- 1956: Discovered at Los Alamos (Reines and Cowan)
- 1958: Neutrinos are only LH (Southpaw)
- 1962: Discovery of muon neutrino (Lederman)
- 1968 : Detection of Solar Neutrinos (Homestake exp.)
 - Only 1/3 of electron neutrinos observed...
- 1985 : Detection of Atmospheric Neutrinos (Kamiokande and IMB)
 - Smaller ratio of muon neutrinos to electron neutrinos observed
- 1998 : First evidence of Atmospheric Neutrino Oscillations (Super-Kamiokande)
- 2000 : Discovery of Tau neutrino (DONUT collaboration)

Formulation of GSW theory of EW interactions (approx 1960-1970): LH and massless neutrinos



(<https://neutrinos.fnal.gov/history/>)

Flash Introduction to Neutrino Physics

- 1930 : Pauli's hypothesis to explain β -decay
- 1956: Discovered at Los Alamos (Reines and Cowan)
- 1958: Neutrinos are only LH (Southpaw)
- 1962: Discovery of muon neutrino (Lederman)
- 1968 : Detection of Solar Neutrinos (Homestake exp.)
 - Only 1/3 of electron neutrinos observed...
- 1985 : Detection of Atmospheric Neutrinos (Kamiokande and IMB)
 - Smaller ratio of muon neutrinos to electron neutrinos observed
- 1998 : First evidence of Atmospheric Neutrino Oscillations (Super-Kamiokande)
- 2000 : Discovery of Tau neutrino (DONUT collaboration)



Formulation of GSW theory of EW interactions (approx 1960-1970): LH and massless neutrinos



Evidences of oscillation in the neutrino sector is incompatible with massless neutrinos!

Flavour dynamics needs explanations!!

(<https://neutrinos.fnal.gov/history/>)

First Problem: Neutrino Masses

- SM does not predict Majorana Neutrino masses at renormalizable level

First Problem: Neutrino Masses

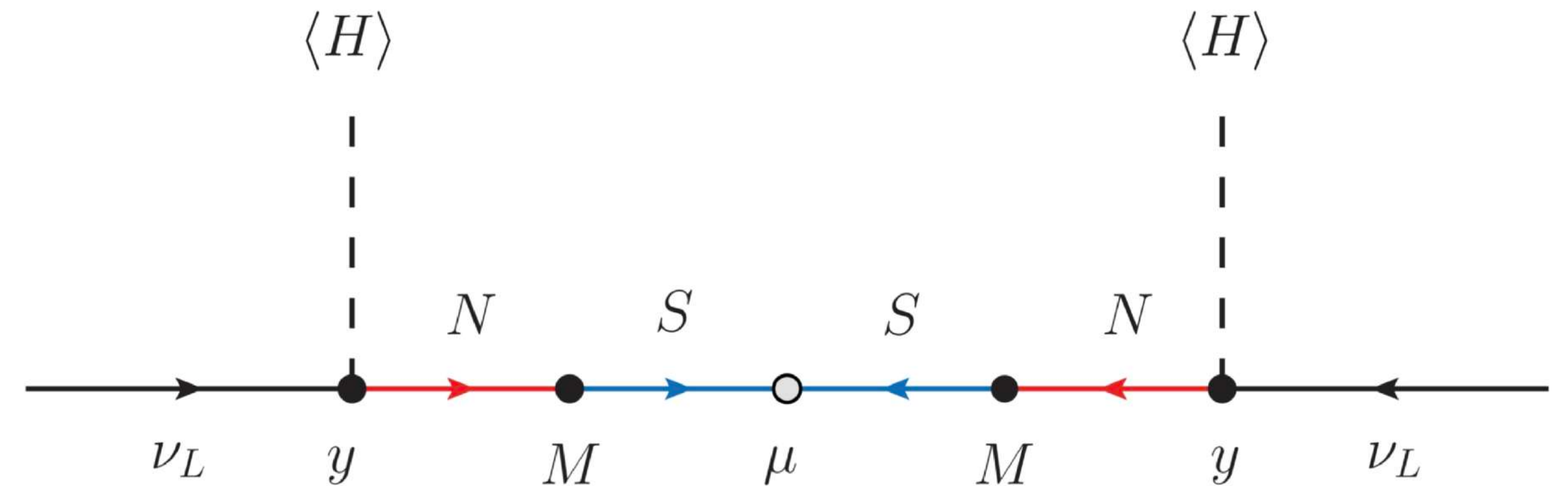
- SM does not predict Majorana Neutrino masses at renormalizable level
- Majorana Masses generated via Weinberg operators

$$\mathcal{O}_W^{(5)} = \frac{1}{\Lambda} \langle LLHH \rangle$$

First Problem: Neutrino Masses

- SM does not predict Majorana Neutrino masses at renormalizable level
- Majorana Masses generated via Weinberg operators
- In this talk: **Inverse Seesaw**

$$\mathcal{O}_W^{(5)} = \frac{1}{\Lambda} \langle LLHH \rangle$$



$$\mathcal{L}_m = -\bar{L}^c Y_D H N^c - \bar{N} M_{NS} S - \frac{1}{2} \bar{S}^c \mu_S S + h.c. = -(\bar{\nu}_L \quad \bar{N}^c \quad \bar{S})^c \mathcal{M} \begin{pmatrix} \nu_L \\ N^c \\ S \end{pmatrix}$$

$$\mathcal{M} = \begin{pmatrix} \emptyset & m_D & \emptyset \\ m_D^T & \emptyset & M_{NS} \\ \emptyset & M_{NS}^T & \mu_S \end{pmatrix}$$

$$|\mu_0| \ll |m_D| \ll M_{NS}$$

First Problem: Neutrino Masses

The Inverse Seesaw (ISS)

$$\mathcal{L}_m = -\bar{L}^c Y_D H N^c - \bar{N} M_{NS} S - \frac{1}{2} \bar{S}^c \mu_S S + h.c. = -(\bar{\nu}_L \quad \bar{N}^c \quad \bar{S})^c \mathcal{M} \begin{pmatrix} \nu_L \\ N^c \\ S \end{pmatrix}$$

$$|\mu_0| \ll |m_D| \ll M_{NS}$$

$$\mathcal{M} = \begin{pmatrix} \emptyset & m_D & \emptyset \\ m_D^T & \emptyset & M_{NS} \\ \emptyset & M_{NS}^T & \mu_S \end{pmatrix}$$

(R. N. Mohapatra and J. W. F. Valle, ('86); R. N. Mohapatra ('86); J. Bernabeu, A. Santamaria, J. Vidal, A. Mendez and J. W. F. Valle, ('87))

First Problem: Neutrino Masses

The Inverse Seesaw (ISS)

$$|\mu_0| \ll |m_D| \ll M_{NS}$$

$$\mathcal{L}_m = -\bar{L}^c Y_D H N^c - \bar{N} M_{NS} S - \frac{1}{2} \bar{S}^c \mu_S S + h.c. = -(\bar{\nu}_L \quad \bar{N}^c \quad \bar{S})^c \mathcal{M} \begin{pmatrix} \nu_L \\ N^c \\ S \end{pmatrix} \quad \mathcal{M} = \begin{pmatrix} \emptyset & m_D & \emptyset \\ m_D^T & \emptyset & M_{NS} \\ \emptyset & M_{NS}^T & \mu_S \end{pmatrix}$$

(R. N. Mohapatra and J. W. F. Valle, ('86); R. N. Mohapatra ('86); J. Bernabeu, A. Santamaria, J. Vidal, A. Mendez and J. W. F. Valle, ('87))

$$\mathcal{U}^T \mathcal{M} \mathcal{U} = \mathcal{M}^{(diag)}$$

$$\mathcal{U} = \begin{pmatrix} \tilde{U}_\nu & S \\ T & V \end{pmatrix}$$

$$m_\nu \approx m_D (M_{NS}^{-1})^T \mu_S M_{NS}^{-1} m_D^T \sim y^2 \frac{\mu_0}{M_0^2} v^2$$

First Problem: Neutrino Masses

The Inverse Seesaw (ISS)

$$|\mu_0| \ll |m_D| \ll M_{NS}$$

$$\mathcal{L}_m = -\bar{L}^c Y_D H N^c - \bar{N} M_{NS} S - \frac{1}{2} \bar{S}^c \mu_S S + h.c. = -(\bar{\nu}_L \quad \bar{N}^c \quad \bar{S})^c \mathcal{M} \begin{pmatrix} \nu_L \\ N^c \\ S \end{pmatrix} \quad \mathcal{M} = \begin{pmatrix} \emptyset & m_D & \emptyset \\ m_D^T & \emptyset & M_{NS} \\ \emptyset & M_{NS}^T & \mu_S \end{pmatrix}$$

(R. N. Mohapatra and J. W. F. Valle, ('86); R. N. Mohapatra ('86); J. Bernabeu, A. Santamaria, J. Vidal, A. Mendez and J. W. F. Valle, ('87))

$$\mathcal{U}^T \mathcal{M} \mathcal{U} = \mathcal{M}^{(diag)}$$

$$\mathcal{U} = \begin{pmatrix} \tilde{U}_\nu & S \\ T & V \end{pmatrix}$$

$$m_\nu \approx m_D (M_{NS}^{-1})^T \mu_S M_{NS}^{-1} m_D^T \sim y^2 \frac{\mu_0}{M_0^2} v^2$$

First Problem: Neutrino Masses

The Inverse Seesaw (ISS)

$$\mathcal{L}_m = -\bar{L}^c Y_D H N^c - \bar{N} M_{NS} S - \frac{1}{2} \bar{S}^c \mu_S S + h.c. = -(\bar{\nu}_L \quad \bar{N}^c \quad \bar{S})^c \mathcal{M} \begin{pmatrix} \nu_L \\ N^c \\ S \end{pmatrix}$$

$$|\mu_0| \ll |m_D| \ll M_{NS}$$

$$\mathcal{M} = \begin{pmatrix} \emptyset & m_D & \emptyset \\ m_D^T & \emptyset & M_{NS} \\ \emptyset & M_{NS}^T & \mu_S \end{pmatrix}$$

(R. N. Mohapatra and J. W. F. Valle, ('86); R. N. Mohapatra ('86); J. Bernabeu, A. Santamaria, J. Vidal, A. Mendez and J. W. F. Valle, ('87))

$$m_\nu \approx m_D (M_{NS}^{-1})^T \mu_S M_{NS}^{-1} m_D^T \sim y^2 \frac{\mu_0}{M_0^2} v^2$$

In the basis in which charged lepton mass matrix is diagonal,

\tilde{U}_ν is the **(non-unitary)** leptonic mixing matrix

$$\tilde{U}_\nu = (1 - \eta) U_0$$

First Problem: Neutrino Masses

The Inverse Seesaw (ISS)

$$|\mu_0| \ll |m_D| \ll M_{NS}$$

$$\mathcal{L}_m = -\bar{L}^c Y_D H N^c - \bar{N} M_{NS} S - \frac{1}{2} \bar{S}^c \mu_S S + h.c. = -(\bar{\nu}_L \quad \bar{N}^c \quad \bar{S})^c \mathcal{M} \begin{pmatrix} \nu_L \\ N^c \\ S \end{pmatrix}$$

$$\mathcal{M} = \begin{pmatrix} \emptyset & m_D & \emptyset \\ m_D^T & \emptyset & M_{NS} \\ \emptyset & M_{NS}^T & \mu_S \end{pmatrix}$$

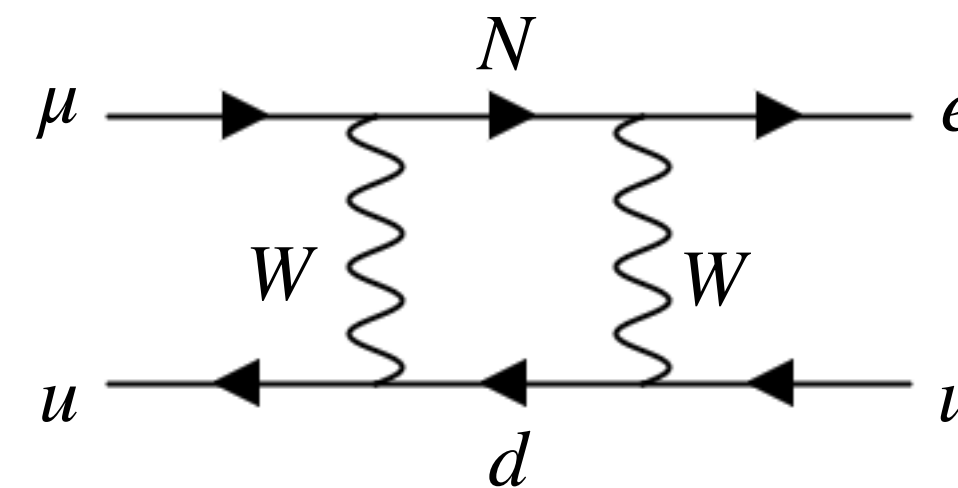
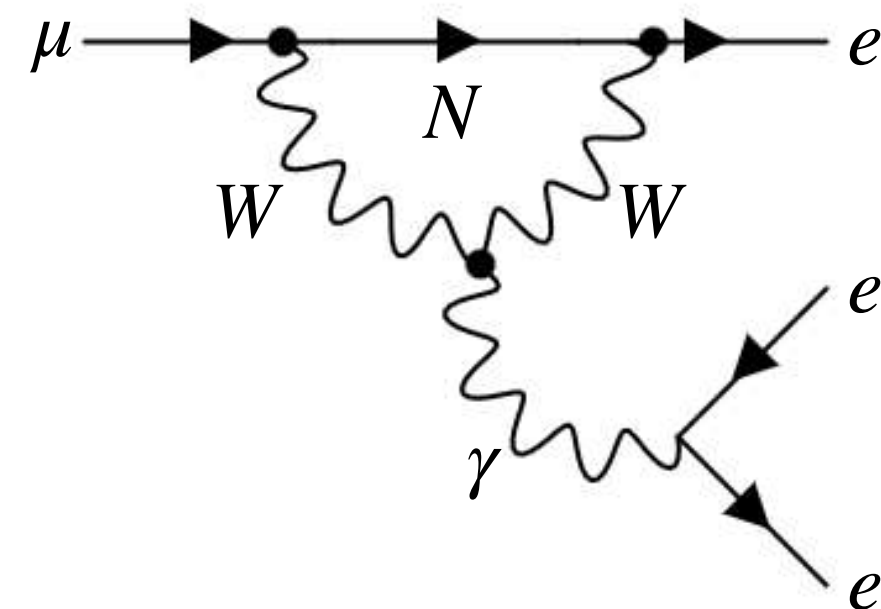
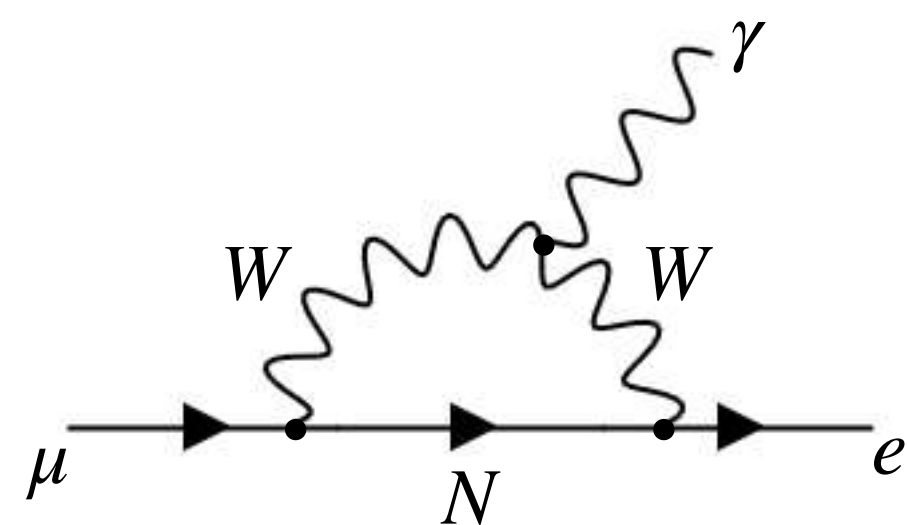
(R. N. Mohapatra and J. W. F. Valle, ('86); R. N. Mohapatra ('86); J. Bernabeu, A. Santamaria, J. Vidal, A. Mendez and J. W. F. Valle, ('87))

$$m_\nu \approx m_D (M_{NS}^{-1})^T \mu_S M_{NS}^{-1} m_D^T \sim y^2 \frac{\mu_0}{M_0^2} v^2$$

S, T describe the mixing of light and sterile neutrinos

$(S, T \ll \tilde{U}_\nu) \Rightarrow$ **Can induce cLFV processes**

(R. Alonso, M. Dhen, M. B. Gavela, T. Hambye ('12))

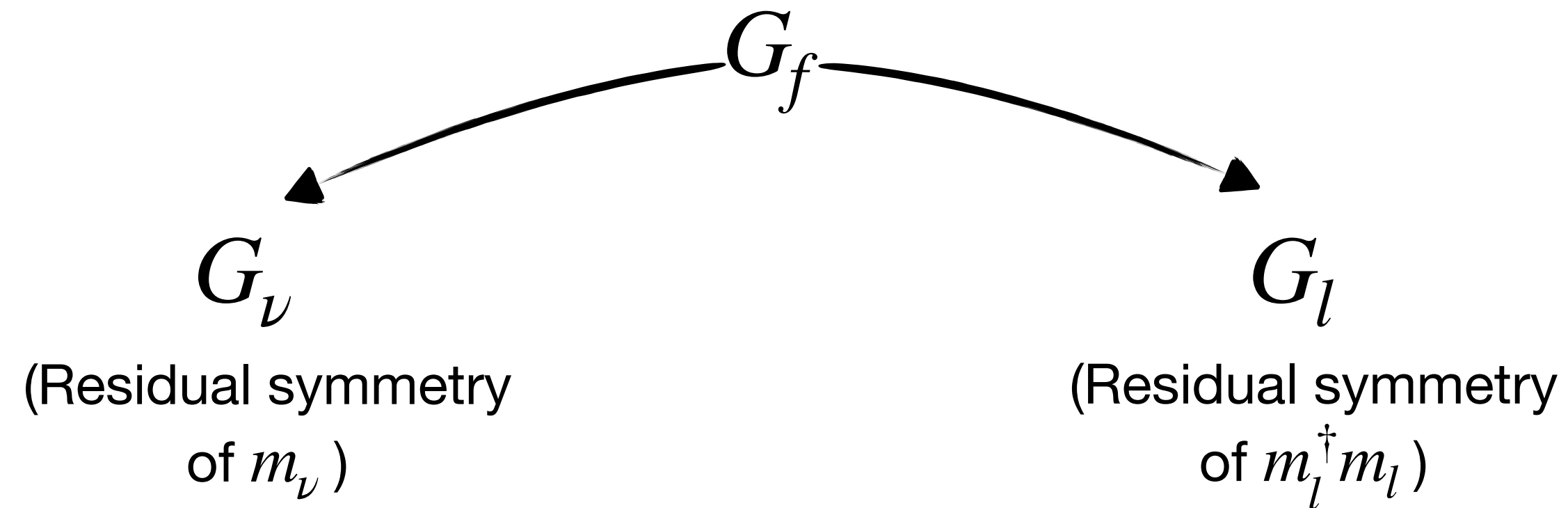


First Problem: Neutrino Masses

That explains the masses, but...
What about the mixing?

\mathcal{L}_m
(R. N. M)

$\left. \begin{matrix} \emptyset \\ M_{NS} \\ \mu_S \end{matrix} \right\}$



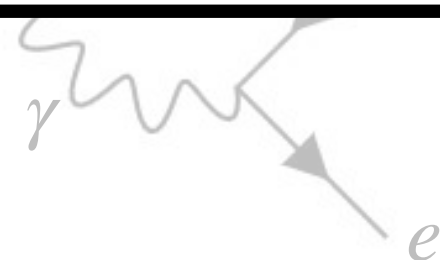
$$\text{diag}\{m_e^2, m_\mu^2, m_\tau^2\} = U_l^\dagger m_l^\dagger m_l U_l$$

$$m_\nu^{(diag)} = U_\nu^\dagger m_\nu U_\nu^*$$

$$U_{PMNS} = U_l^\dagger U_\nu$$

m_ν , $m_l^\dagger m_l$ and the mixing U_{PMNS} is completely fixed by the symmetry!

bye ('12))

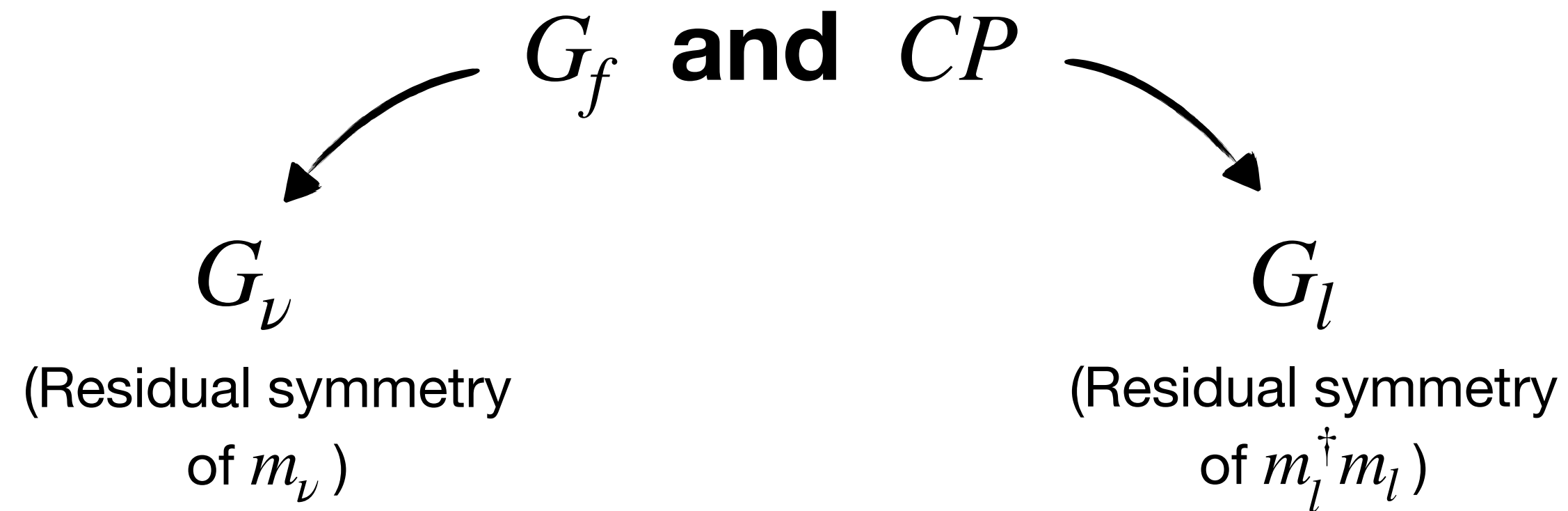


First Problem: Neutrino Masses

That explains the masses, but...
What about the mixing?

\mathcal{L}_m
(R. N. M)

$\left. \begin{matrix} \emptyset \\ M_{NS} \\ \mu_S \end{matrix} \right\}$



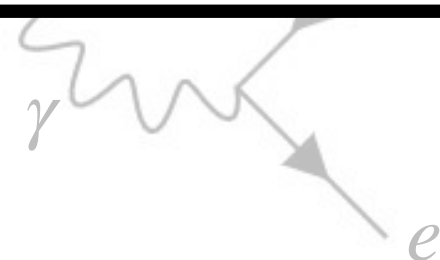
$$\text{diag}\{m_e^2, m_\mu^2, m_\tau^2\} = U_l^\dagger m_l^\dagger m_l U_l$$

$$m_\nu^{(diag)} = U_\nu^\dagger m_\nu U_\nu^*$$

$$U_{PMNS} = U_l^\dagger U_\nu$$

m_ν , $m_l^\dagger m_l$ and the mixing U_{PMNS} is completely fixed by the symmetry!

bye ('12))



What about the Mixing?

$\Delta(3n^2)$, $\Delta(6n^2)$ and CP

What about the Mixing?

$\Delta(3n^2)$, $\Delta(6n^2)$ and CP

$\Delta(3n^2)$ ($\Delta(6n^2)$) is a non-Abelian finite subgroup of $SU(3)$ of order $3n^2$ ($6n^2$): $\Delta(6n^2) \sim (Z_n \times Z_n) \rtimes S_3$ (J.A. Escobar, C. Luhn ('07, '08))

Here, we consider only $n \nmid 3$ (not divisible by 3)

What about the Mixing?

$\Delta(3n^2)$, $\Delta(6n^2)$ and CP

(J.A. Escobar, C. Luhn ('07, '08))

$\Delta(3n^2)$ ($\Delta(6n^2)$) is a non-Abelian finite subgroup of $SU(3)$ of order $3n^2$ ($6n^2$): $\Delta(6n^2) \sim (Z_n \times Z_n) \rtimes S_3$

Here, we consider only $n \nmid 3$ (not divisible by 3)

Generators for $\Delta(3n^2)$:

$$a^3 = 1 \quad c^n = d^n = 1$$

$$cd = dc$$

$$aca^{-1} = c^{-1}d^{-1} \quad ada^{-1} = c$$

General element of the group is written:

$$g = a^\alpha c^\gamma d^\delta \quad \alpha, \gamma, \delta \in N$$

What about the Mixing?

$\Delta(3n^2)$, $\Delta(6n^2)$ and CP

(J.A. Escobar, C. Luhn ('07, '08))

$\Delta(3n^2)$ ($\Delta(6n^2)$) is a non-Abelian finite subgroup of $SU(3)$ of order $3n^2$ ($6n^2$): $\Delta(6n^2) \sim (Z_n \times Z_n) \rtimes S_3$

Here, we consider only $n \nmid 3$ (not divisible by 3)

Generators for $\Delta(6n^2)$:

$$a^3 = 1 \quad c^n = d^n = 1 \quad b^2 = 1$$

$$cd = dc \quad (ab)^2 = 1$$
$$aca^{-1} = c^{-1}d^{-1} \quad ada^{-1} = d$$

$$bcb^{-1} = d^{-1} \quad bsdb^{-1} = c^{-1}$$

(Add a further generator b)

General element of the group is written:

$$g = a^\alpha b^\beta c^\gamma d^\delta \quad \alpha, \beta, \gamma, \delta \in N$$

What about the Mixing?

$\Delta(3n^2), \Delta(6n^2)$ and CP

Charged Leptons:

$$G_l = \text{diag} (Z_3 \times Z_3^{\text{aux}})$$

Neutral leptons

$$G_\nu = Z_2 \times CP$$

(J.A. Escobar, C. Luhn ('07, '08))

$\Delta(3n^2)$ ($\Delta(6n^2)$) is a non-Abelian finite subgroup of $SU(3)$ of order $3n^2$ ($6n^2$): $\Delta(6n^2) \sim (Z_n \times Z_n) \rtimes S_3$

Here, we consider only $n \nmid 3$ (not divisible by 3)

Generators for $\Delta(6n^2)$:

$$a^3 = 1 \quad c^n = d^n = 1 \quad b^2 = 1$$

$$cd = dc \quad (ab)^2 = 1$$

$$aca^{-1} = c^{-1}d^{-1} \quad ada^{-1} = d$$

$$bcb^{-1} = d^{-1} \quad bsdb^{-1} = c^{-1}$$

(Add a further generator b)

General element of the group is written:

$$g = a^\alpha b^\beta c^\gamma d^\delta \quad \alpha, \beta, \gamma, \delta \in N$$

What about the Mixing?

$\Delta(3n^2), \Delta(6n^2)$ and CP

Charged Leptons:

$$G_l = \text{diag} (Z_3 \times Z_3^{\text{aux}})$$

Neutral leptons

$$G_\nu = Z_2 \times CP$$

Three possible ways of choosing generators of the residual symmetries:

Case 1) $Z = c^{n/2} \quad X = abc^s d^{2s} X_0$

Case 2) $Z = c^{n/2} \quad X = c^s d^t X_0$

Case 3) $Z = bc^m d^m \quad X = bc^s d^{n-s} X_0$

$$X_0 = \begin{pmatrix} 1 & 0 & 0 \\ 0 & 0 & 1 \\ 0 & 1 & 0 \end{pmatrix} \quad (\text{F. Feruglio, C. Hagedorn, R. Ziegler, ('13)})$$

Form of the generators depends on the particular representation chosen.

What about the Mixing?

$\Delta(3n^2), \Delta(6n^2)$ and CP

Charged Leptons:

$$G_l = \text{diag} (Z_3 \times Z_3^{\text{aux}})$$

Neutral leptons

$$G_\nu = Z_2 \times CP$$

Three possible ways of choosing generators of the residual symmetries:

Case 1) $Z = c^{n/2} \quad X = abc^s d^{2s} X_0$

Case 2) $Z = c^{n/2} \quad X = c^s d^t X_0$

Case 3) $Z = bc^m d^m \quad X = bc^s d^{n-s} X_0$

$$X_0 = \begin{pmatrix} 1 & 0 & 0 \\ 0 & 0 & 1 \\ 0 & 1 & 0 \end{pmatrix} \quad (\text{F. Feruglio, C. Hagedorn, R. Ziegler, ('13)})$$

Form of the generators depends on the particular representation chosen.

(J.A. Escobar, C. Luhn ('07, '08))

G_f has a variety of 3-dim. representations 3_l

$3 = 3_1$ Complex, Faithful three-dim. representation

$3' = 3_5$ Real, Unfaithful three-dim. representation

What about the Mixing?

$\Delta(3n^2), \Delta(6n^2)$ and CP

Charged Leptons:

$$G_l = \text{diag} (Z_3 \times Z_3^{\text{aux}})$$

Neutral leptons

$$G_\nu = Z_2 \times CP$$

$$\mathcal{L}_m = -\bar{L}^c Y_D H N^c - \bar{N} M_{NS} S - \frac{1}{2} \bar{S}^c \mu_S S + h.c.$$

What about the Mixing?

$\Delta(3n^2), \Delta(6n^2)$ and CP

Charged Leptons:

$$G_l = \text{diag} (Z_3 \times Z_3^{\text{aux}})$$

Neutral leptons

$$G_\nu = Z_2 \times CP$$

$$\mathcal{L}_m = -\bar{L}^c Y_D H N^c - \bar{N} M_{NS} S - \frac{1}{2} \bar{S}^c \mu_S S + h.c.$$

What about the Mixing?

$\Delta(3n^2), \Delta(6n^2)$ and CP

Charged Leptons:

$$G_l = \text{diag} (Z_3 \times Z_3^{aux})$$

Neutral leptons

$$G_\nu = Z_2 \times CP$$

$$\mathcal{L}_m = -\bar{L}^c Y_D H N^c - \bar{N} M_{NS} S - \boxed{\frac{1}{2} \bar{S}^c \mu_S S} + h.c.$$

(C. Hagedorn, J. Kriewald, J. Orloff, A. M. Teixeira, ('21))

$$Y_D = y_0 \frac{\langle H \rangle}{M_0} \begin{pmatrix} 1 & 0 & 0 \\ 0 & 1 & 0 \\ 0 & 0 & 1 \end{pmatrix}$$

$$M_{NS} = M_0 \begin{pmatrix} 1 & 0 & 0 \\ 0 & 1 & 0 \\ 0 & 0 & 1 \end{pmatrix}$$

$$\mu_S = U_S^*(\theta_S) \begin{pmatrix} \mu_1 & 0 & 0 \\ 0 & \mu_2 & 0 \\ 0 & 0 & \mu_3 \end{pmatrix} U_S^T(\theta_S)$$

What about the Mixing?

$\Delta(3n^2), \Delta(6n^2)$ and CP

Charged Leptons:

$$G_l = \text{diag} (Z_3 \times Z_3^{\text{aux}})$$

Neutral leptons

$$G_\nu = Z_2 \times CP$$

$$\mathcal{L}_m = -\boxed{\bar{L}^c Y_D H N^c} - \bar{N} M_{NS} S - \frac{1}{2} \bar{S}^c \mu_S S + h.c.$$

(FPDM, C. Hagedorn, ('24))

$$M_{NS} = M_0 \begin{pmatrix} 1 & 0 & 0 \\ 0 & 1 & 0 \\ 0 & 0 & 1 \end{pmatrix} \quad \mu_S = \mu_0 \begin{pmatrix} 1 & 0 & 0 \\ 0 & 0 & 1 \\ 0 & 1 & 0 \end{pmatrix}$$

$$m_D = \langle H \rangle U_L^*(\theta_L) \begin{pmatrix} y_1 & 0 & 0 \\ 0 & y_2 & 0 \\ 0 & 0 & y_3 \end{pmatrix} U_R^T(\theta_R)$$

What about the Mixing?

$\Delta(3n^2), \Delta(6n^2)$ and CP

Charged Leptons:

$$G_l = \text{diag} (Z_3 \times Z_3^{\text{aux}})$$

Neutral leptons

$$G_\nu = Z_2 \times CP$$

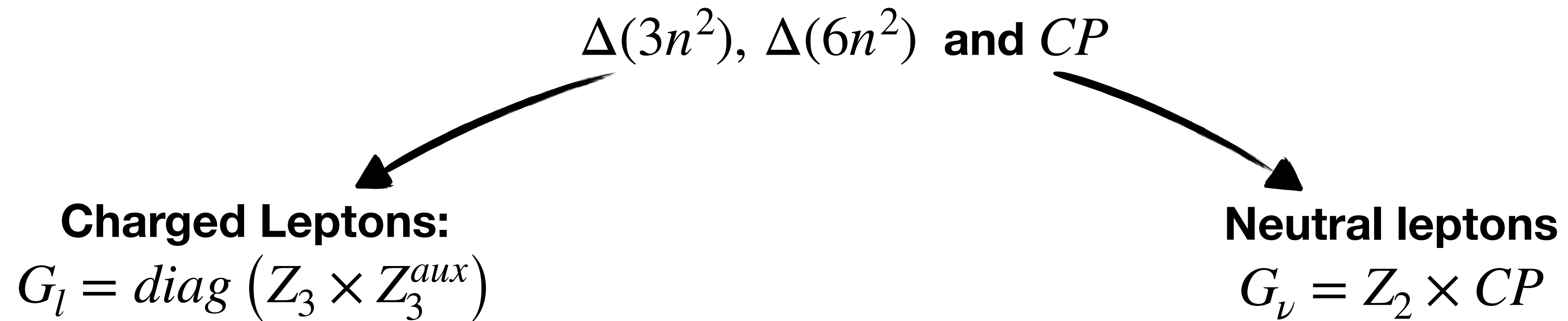
$$\mathcal{L}_m = -\bar{L}^c Y_D H N^c - \boxed{\bar{N} M_{NS} S} - \frac{1}{2} \bar{S}^c \mu_S S + h.c.$$

(FPDM, C. Hagedorn, ('25, To appear soon!))

$$Y_D = y_0 \begin{pmatrix} 1 & 0 & 0 \\ 0 & 1 & 0 \\ 0 & 0 & 1 \end{pmatrix} \quad \mu_S = \mu_0 \begin{pmatrix} 1 & 0 & 0 \\ 0 & 0 & 1 \\ 0 & 1 & 0 \end{pmatrix}$$

$$M_{NS} = U_N(\theta_N) \begin{pmatrix} M_1 & 0 & 0 \\ 0 & M_2 & 0 \\ 0 & 0 & M_3 \end{pmatrix} U_S^\dagger(\theta_S)$$

What about the Mixing?



$$\mathcal{L}_m = -\boxed{\bar{L}^c Y_D H N^c} - \boxed{\bar{N} M_{NS} S} - \frac{1}{2} \bar{S}^c \mu_S S + h.c.$$

In this discussion, we focus on Options 2 and 3

Option 2

$$m_\nu \approx \frac{1}{M_0^2} m_D \mu_S m_D^T = \langle H \rangle \frac{\mu_0}{M_0^2} U_L^*(\theta_L) \left[\begin{pmatrix} y_1 & 0 & 0 \\ 0 & y_2 & 0 \\ 0 & 0 & y_3 \end{pmatrix} U_R^T(\theta_R) \begin{pmatrix} 1 & 0 & 0 \\ 0 & 0 & 1 \\ 0 & 1 & 0 \end{pmatrix} U_R(\theta_R) \begin{pmatrix} y_1 & 0 & 0 \\ 0 & y_2 & 0 \\ 0 & 0 & y_3 \end{pmatrix} \right] U_L^\dagger(\theta_L)$$

Heavy neutral states mass matrix:

$$M_h \approx \begin{pmatrix} \emptyset & M_{NS} \\ M_{NS}^T & \mu_S \end{pmatrix}$$

Heavy neutral states spectrum: **Three almost degenerate Pseudo-Dirac Pairs**

$$m_{(i=4,5,6)} \approx M_0 - \frac{1}{2} \mu_0 \quad m_{(i=7,8,9)} \approx M_0 + \frac{1}{2} \mu_0$$

Remember the ISS condition:

$$|\mu_0| \ll |m_D| \ll M_{NS}$$

Option 2

$$m_\nu \approx \frac{1}{M_0^2} m_D \mu_S m_D^T = \langle H \rangle \frac{\mu_0}{M_0^2} U_L^*(\theta_L) \left[\begin{pmatrix} y_1 & 0 & 0 \\ 0 & y_2 & 0 \\ 0 & 0 & y_3 \end{pmatrix} U_R^T(\theta_R) \begin{pmatrix} 1 & 0 & 0 \\ 0 & 0 & 1 \\ 0 & 1 & 0 \end{pmatrix} U_R(\theta_R) \begin{pmatrix} y_1 & 0 & 0 \\ 0 & y_2 & 0 \\ 0 & 0 & y_3 \end{pmatrix} \right] U_L^\dagger(\theta_L)$$

$$U_L(\theta_L) = \Omega(3) R_{ij}(\theta_L)$$

$$U_R(\theta_R) = \Omega(3') R_{kl}(\theta_R) \left(P_{kl}^{ij} \right)^T$$

Option 2

$$m_\nu \approx \frac{1}{M_0^2} m_D \mu_S m_D^T = \langle H \rangle \frac{\mu_0}{M_0^2} U_L^*(\theta_L) \left[\begin{array}{c} \begin{pmatrix} y_1 & 0 & 0 \\ 0 & y_2 & 0 \\ 0 & 0 & y_3 \end{pmatrix} U_R^T(\theta_R) \begin{pmatrix} 1 & 0 & 0 \\ 0 & 0 & 1 \\ 0 & 1 & 0 \end{pmatrix} U_R(\theta_R) \begin{pmatrix} y_1 & 0 & 0 \\ 0 & y_2 & 0 \\ 0 & 0 & y_3 \end{pmatrix} \end{array} \right] U_L^\dagger(\theta_L)$$

$$U_L(\theta_L) = \Omega(3) R_{ij}(\theta_L)$$

$$U_R(\theta_R) = \Omega(3') R_{kl}(\theta_R) \left(P_{kl}^{ij} \right)^T$$

$\Omega(3), \Omega(3')$ are unitary

Are determined by residual symmetry (specified by the **CASE** and n, s, t) and its embedding in G_f .

Option 2

$$m_\nu \approx \frac{1}{M_0^2} m_D \mu_S m_D^T = \langle H \rangle \frac{\mu_0}{M_0^2} U_L^*(\theta_L) \left[\begin{pmatrix} y_1 & 0 & 0 \\ 0 & y_2 & 0 \\ 0 & 0 & y_3 \end{pmatrix} U_R^T(\theta_R) \begin{pmatrix} 1 & 0 & 0 \\ 0 & 0 & 1 \\ 0 & 1 & 0 \end{pmatrix} U_R(\theta_R) \begin{pmatrix} y_1 & 0 & 0 \\ 0 & y_2 & 0 \\ 0 & 0 & y_3 \end{pmatrix} \right] U_L^\dagger(\theta_L)$$

$$U_L(\theta_L) = \Omega(3) R_{ij}(\theta_L)$$

$$U_R(\theta_R) = \Omega(3') R_{kl}(\theta_R) \left(P_{kl}^{ij} \right)^T$$

$\Omega(3), \Omega(3')$ are unitary

Are determined by residual symmetry (specified by the **CASE** and n, s, t) and its embedding in G_f .

$R_{ij}(\theta_{L,R})$ is a rotation on the ij plane

Option 2

$$m_\nu \approx \frac{1}{M_0^2} m_D \mu_S m_D^T = \langle H \rangle \frac{\mu_0}{M_0^2} U_L^*(\theta_L) \left[\begin{array}{c} \begin{pmatrix} y_1 & 0 & 0 \\ 0 & y_2 & 0 \\ 0 & 0 & y_3 \end{pmatrix} U_R^T(\theta_R) \begin{pmatrix} 1 & 0 & 0 \\ 0 & 0 & 1 \\ 0 & 1 & 0 \end{pmatrix} U_R(\theta_R) \begin{pmatrix} y_1 & 0 & 0 \\ 0 & y_2 & 0 \\ 0 & 0 & y_3 \end{pmatrix} \end{array} \right] U_L^\dagger(\theta_L)$$

Parameters of the theory:

$$M_0, \mu_0, y_i, \theta_L, \theta_R$$

Option 2

$$m_\nu \approx \frac{1}{M_0^2} m_D \mu_S m_D^T = \langle H \rangle \frac{\mu_0}{M_0^2} U_L^*(\theta_L) \left[\begin{pmatrix} y_1 & 0 & 0 \\ 0 & y_2 & 0 \\ 0 & 0 & y_3 \end{pmatrix} U_R^T(\theta_R) \begin{pmatrix} 1 & 0 & 0 \\ 0 & 0 & 1 \\ 0 & 1 & 0 \end{pmatrix} U_R(\theta_R) \begin{pmatrix} y_1 & 0 & 0 \\ 0 & y_2 & 0 \\ 0 & 0 & y_3 \end{pmatrix} \right] U_L^\dagger(\theta_L)$$

- In our numerical analysis:
 $M_0 \in [150 \text{ GeV}; 10 \text{ TeV}]$

Option 2

$$m_\nu \approx \frac{1}{M_0^2} m_D \mu_S m_D^T = \langle H \rangle \frac{\mu_0}{M_0^2} U_L^*(\theta_L) \left[\begin{pmatrix} y_1 & 0 & 0 \\ 0 & y_2 & 0 \\ 0 & 0 & y_3 \end{pmatrix} U_R^T(\theta_R) \begin{pmatrix} 1 & 0 & 0 \\ 0 & 0 & 1 \\ 0 & 1 & 0 \end{pmatrix} U_R(\theta_R) \begin{pmatrix} y_1 & 0 & 0 \\ 0 & y_2 & 0 \\ 0 & 0 & y_3 \end{pmatrix} \right] U_L^\dagger(\theta_L)$$

- In our numerical analysis:

$$M_0 \in [150 \text{ GeV}; 10 \text{ TeV}] \quad \mu_0 \in [0.1 \text{ keV}; 10^2 \text{ keV}]$$

Option 2

$$m_\nu \approx \frac{1}{M_0^2} m_D \mu_S m_D^T = \langle H \rangle \frac{\mu_0}{M_0^2} U_L^*(\theta_L) \left[\begin{pmatrix} y_1 & 0 & 0 \\ 0 & y_2 & 0 \\ 0 & 0 & y_3 \end{pmatrix} U_R^T(\theta_R) \begin{pmatrix} 1 & 0 & 0 \\ 0 & 0 & 1 \\ 0 & 1 & 0 \end{pmatrix} U_R(\theta_R) \begin{pmatrix} y_1 & 0 & 0 \\ 0 & y_2 & 0 \\ 0 & 0 & y_3 \end{pmatrix} \right] U_L^\dagger(\theta_L)$$

- In our numerical analysis:

$$M_0 \in [150 \text{ GeV}; 10 \text{ TeV}] \quad \mu_0 \in [0.1 \text{ keV}; 10^2 \text{ keV}] \quad \theta_R \in [0; 2\pi]$$

Option 2

$$m_\nu \approx \frac{1}{M_0^2} m_D \mu_S m_D^T = \langle H \rangle \frac{\mu_0}{M_0^2} U_L^*(\theta_L) \left[\begin{pmatrix} y_1 & 0 & 0 \\ 0 & y_2 & 0 \\ 0 & 0 & y_3 \end{pmatrix} U_R^T(\theta_R) \begin{pmatrix} 1 & 0 & 0 \\ 0 & 0 & 1 \\ 0 & 1 & 0 \end{pmatrix} U_R(\theta_R) \begin{pmatrix} y_1 & 0 & 0 \\ 0 & y_2 & 0 \\ 0 & 0 & y_3 \end{pmatrix} \right] U_L^\dagger(\theta_L)$$

- In our numerical analysis:

$$M_0 \in [150 \text{ GeV}; 10 \text{ TeV}] \quad \mu_0 \in [0.1 \text{ keV}; 10^2 \text{ keV}] \quad \theta_R \in [0; 2\pi]$$

- Fixed by fitting LO predictions of the masses to experimental values

Option 2

$$m_\nu \approx \frac{1}{M_0^2} m_D \mu_S m_D^T = \langle H \rangle \frac{\mu_0}{M_0^2} U_L^*(\theta_L) \left[\begin{pmatrix} y_1 & 0 & 0 \\ 0 & y_2 & 0 \\ 0 & 0 & y_3 \end{pmatrix} U_R^T(\theta_R) \begin{pmatrix} 1 & 0 & 0 \\ 0 & 0 & 1 \\ 0 & 1 & 0 \end{pmatrix} U_R(\theta_R) \begin{pmatrix} y_1 & 0 & 0 \\ 0 & y_2 & 0 \\ 0 & 0 & y_3 \end{pmatrix} \right] U_L^\dagger(\theta_L)$$

- In our numerical analysis:

$$M_0 \in [150 \text{ GeV}; 10 \text{ TeV}] \quad \mu_0 \in [0.1 \text{ keV}; 10^2 \text{ keV}] \quad \theta_R \in [0; 2\pi]$$

- Fixed by fitting LO predictions of the masses to experimental values
- Fixed by fitting prediction of mixing to lepton mixing data

Option 2

$$m_\nu \approx \frac{1}{M_0^2} m_D \mu_S m_D^T = \langle H \rangle \frac{\mu_0}{M_0^2} U_L^*(\theta_L) \left[\begin{pmatrix} y_1 & 0 & 0 \\ 0 & y_2 & 0 \\ 0 & 0 & y_3 \end{pmatrix} U_R^T(\theta_R) \begin{pmatrix} 1 & 0 & 0 \\ 0 & 0 & 1 \\ 0 & 1 & 0 \end{pmatrix} U_R(\theta_R) \begin{pmatrix} y_1 & 0 & 0 \\ 0 & y_2 & 0 \\ 0 & 0 & y_3 \end{pmatrix} \right] U_L^\dagger(\theta_L)$$

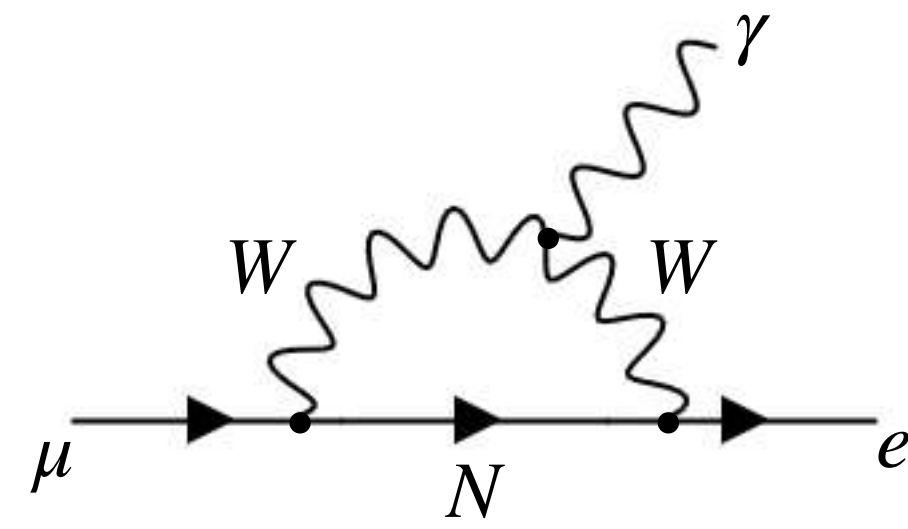
- In our numerical analysis:

$$M_0 \in [150 \text{ GeV}; 10 \text{ TeV}] \quad \mu_0 \in [0.1 \text{ keV}; 10^2 \text{ keV}] \quad \theta_R \in [0; 2\pi]$$

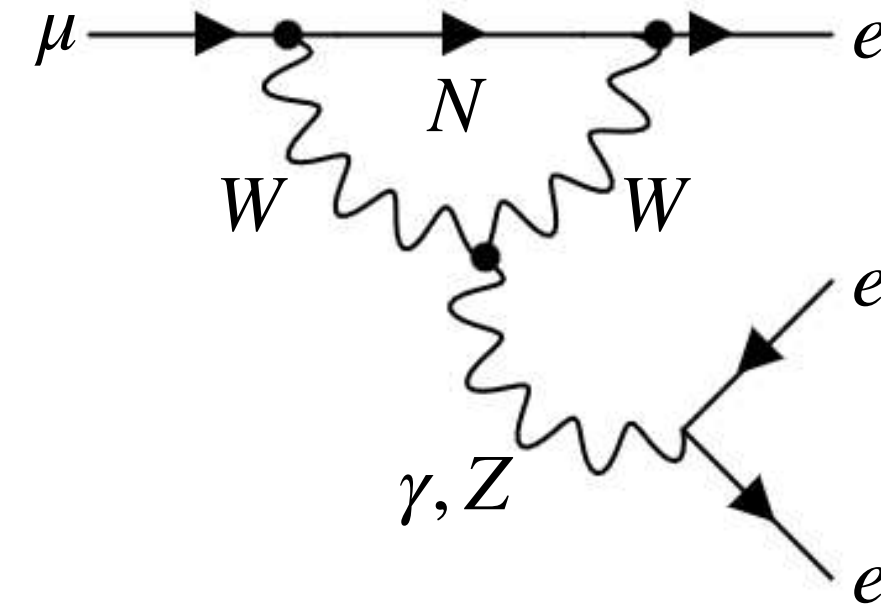
- Fixed by fitting LO predictions of the masses to experimental values
- Fixed by fitting prediction of mixing to lepton mixing data
- We consider $m_0 = 0.03(0.015) \text{ eV}$ for NO(IO)

Option 2

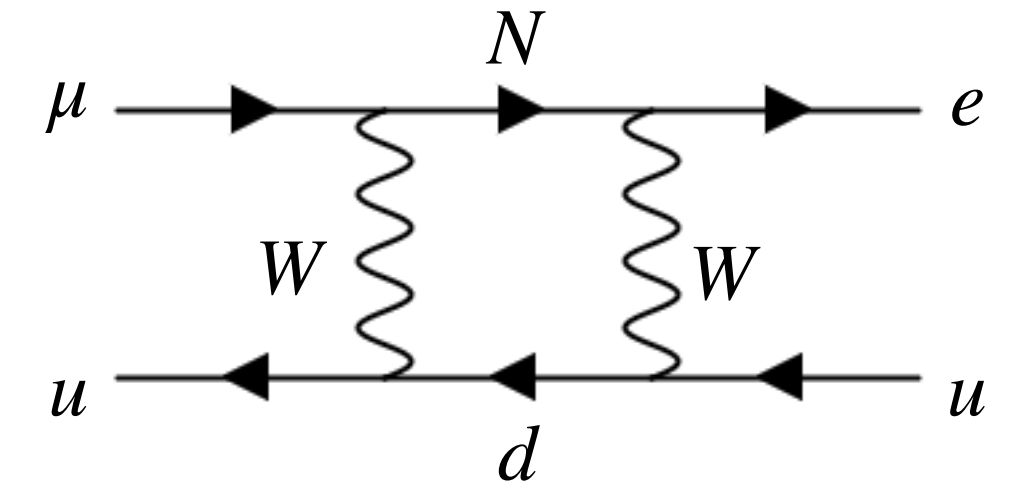
cLFV in the ISS



$$\mu \rightarrow e \gamma$$



$$\mu \rightarrow 3e$$

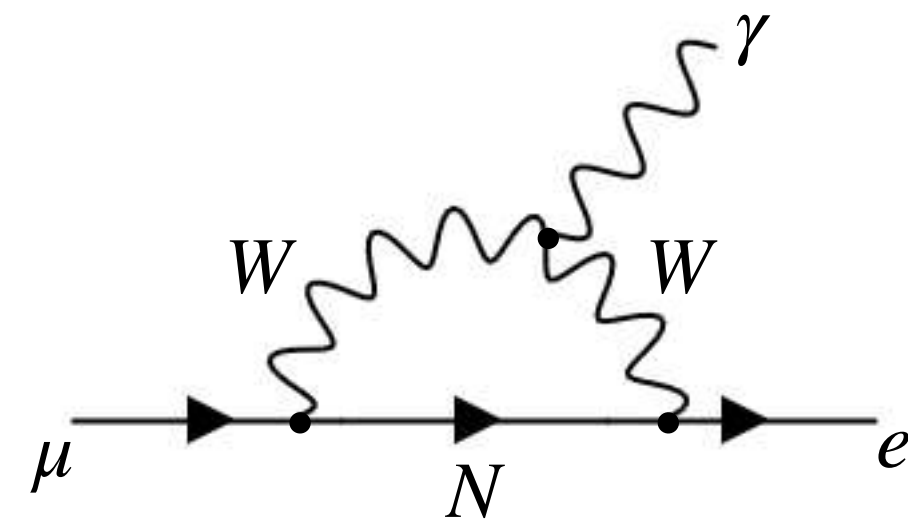


$$\mu - e \text{ Conversion}$$

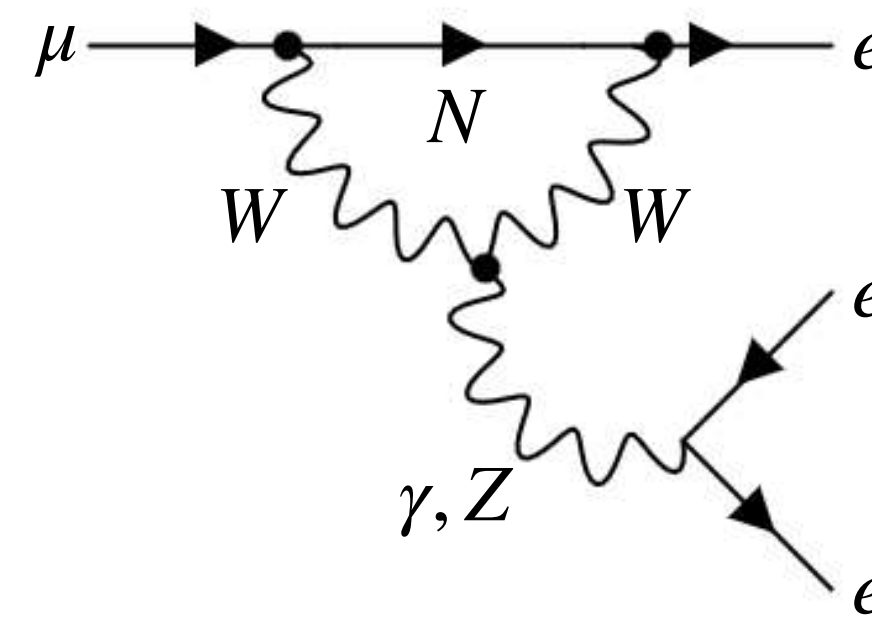
Heavy sterile states and their mixing with light neutrinos can lead to unsuppressed processes that violate flavour in the Charged Lepton Sector!

Option 2

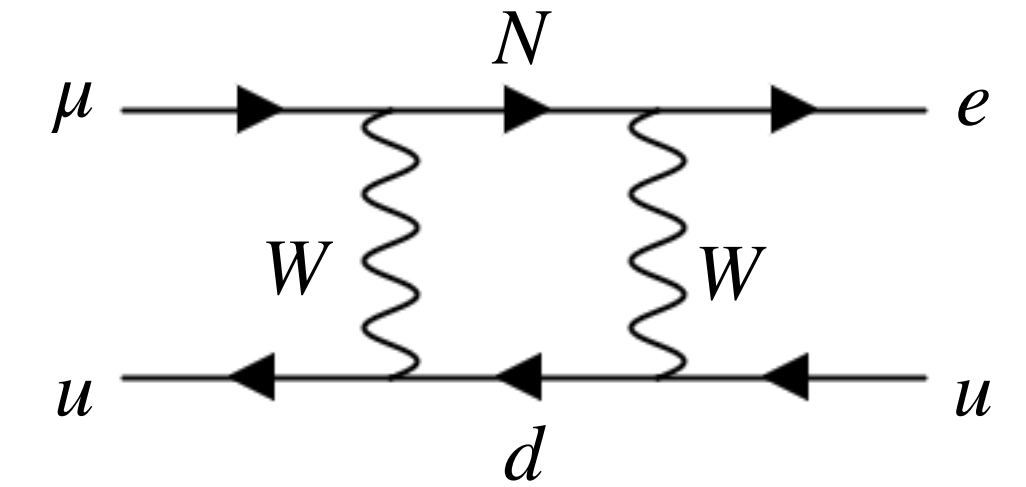
cLFV in the ISS



$$\mu \rightarrow e \gamma$$



$$\mu \rightarrow 3e$$



$$\mu - e \text{ Conversion}$$

Present bounds are non-constraining.

$$BR(\mu \rightarrow e \gamma) \lesssim 6 \times 10^{-14} \quad \text{Meg-II}$$

Main constraints come from future bounds:

$$BR(\mu \rightarrow 3e) \lesssim 20(1) \times 10^{-16} \quad \text{Mu3E Phase-I (II)}$$

$$CR(\mu - e, Al) \lesssim 7.0(8.0) \times 10^{-17} \quad \text{COMET Phase-II (Mu2E)}$$

Option 2: Case 2

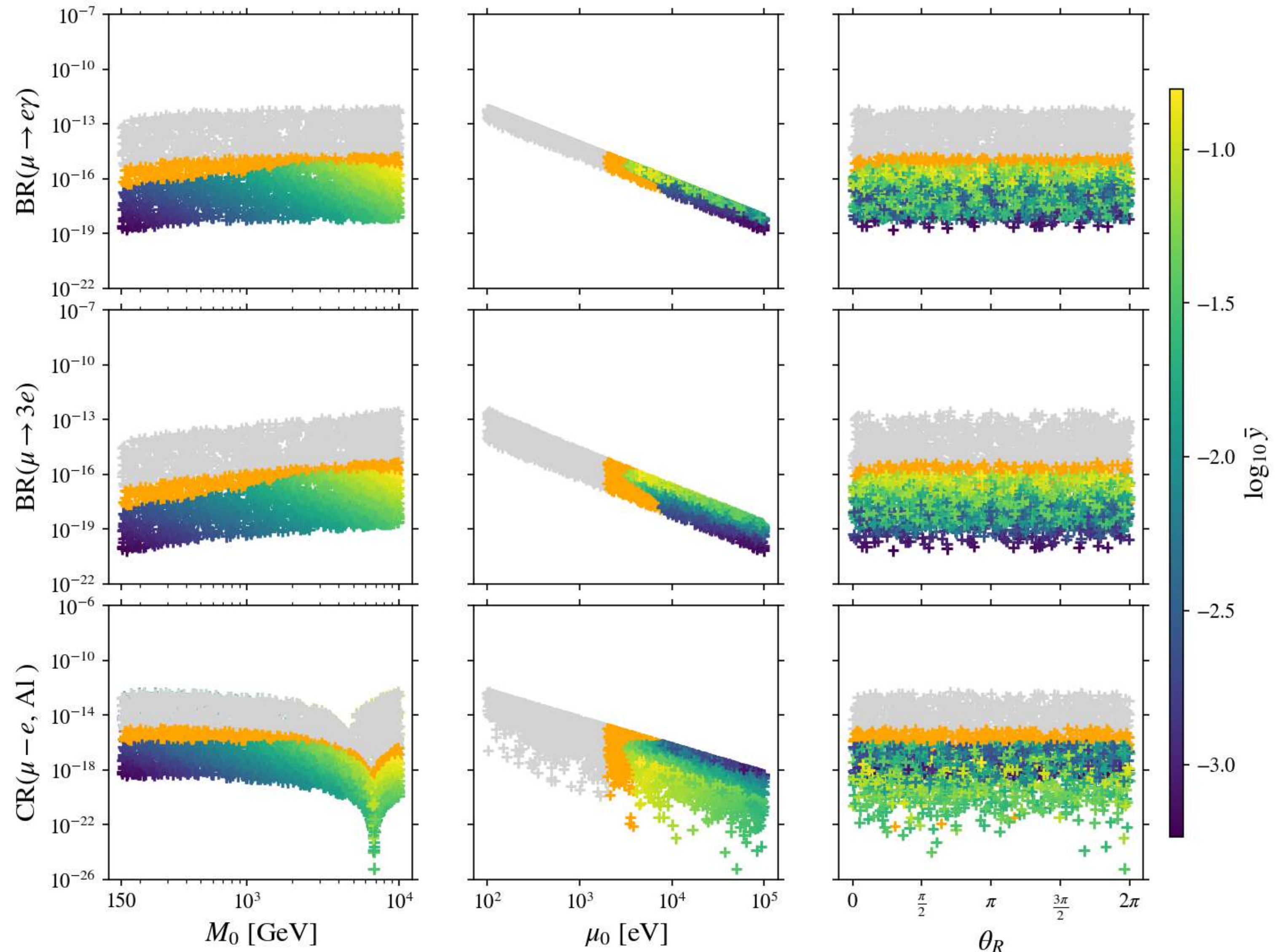
(FPDM, C. Hagedorn, ('24))

Predictions are bounded by both experimental bounds on **cLFV processes** as by bounds on **unitarity violation**

$$\eta \lesssim \begin{pmatrix} 1.3 \times 10^{-3} \\ 1.2 \times 10^{-5} & 1.1 \times 10^{-5} \\ 9.0 \times 10^{-4} & 5.7 \times 10^{-5} & 1.0 \times 10^{-3} \end{pmatrix}$$

(M. Blennow, E. Fernández-Martínez, J. Hernández-García, J. López-Pavón, X., D. Naredo-Tuero ('23))

Case 2), $n=14, s=1, t=2 (u=0)$, NO



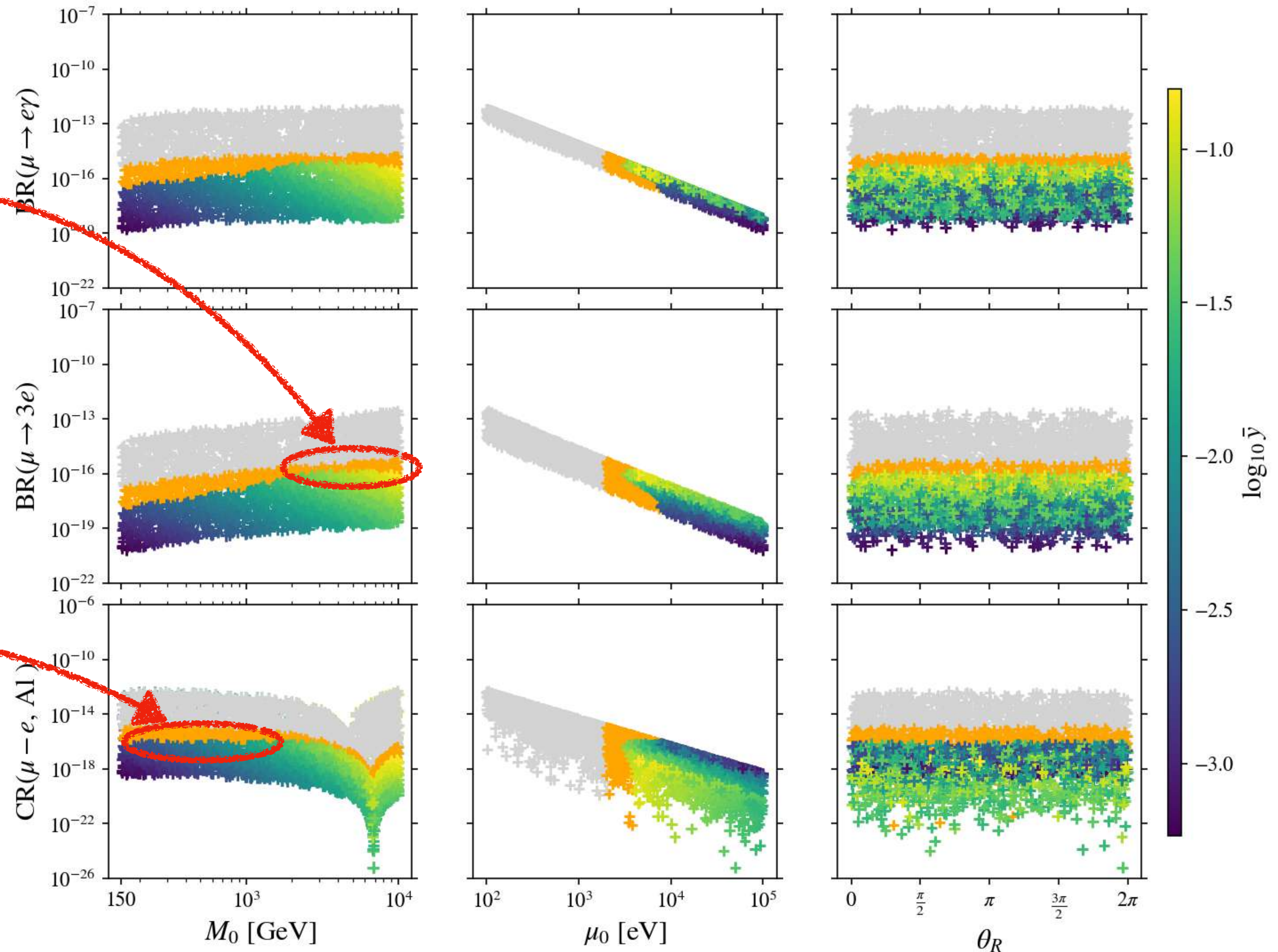
Option 2: Case 2

(FPDM, C. Hagedorn, ('24))

Case 2), $n=14, s=1, t=2 (u=0)$, NO

Mu3E Bound reached

COMET bound reached



Option 2: Case 2

(FPDM, C. Hagedorn, ('24))

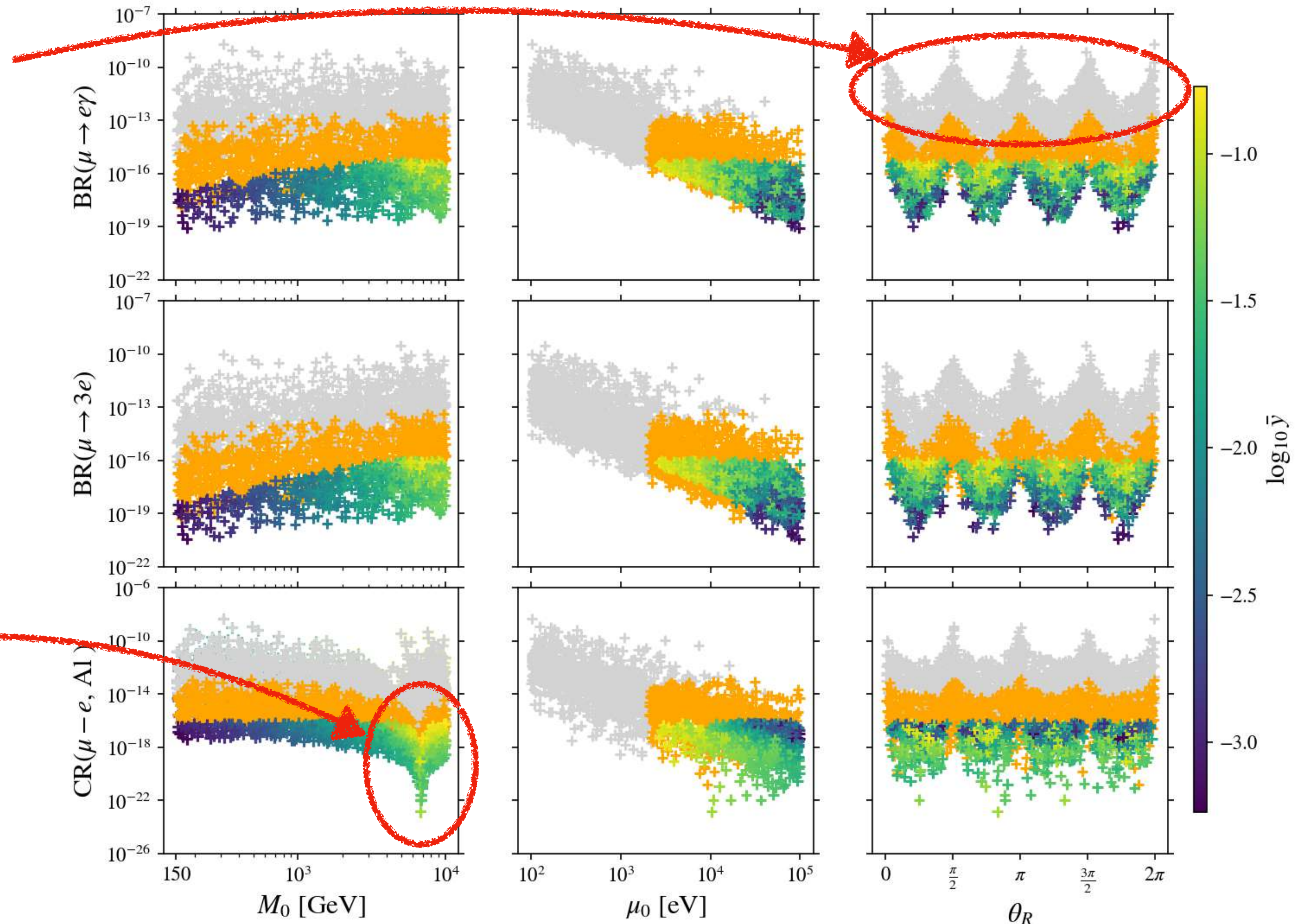
Case 2), $n=14, s=1, t=1 (u=1), \text{NO}$

Modulation in function of θ_R

Enhancement of rates for $\sin(2\theta_R) \approx 0$

Cancellation of contributions

$$x_0^{(canc)} \approx 6470 \Rightarrow M_0^{(canc)} \approx 6.5 \text{ TeV}$$



Option 2: Case 2

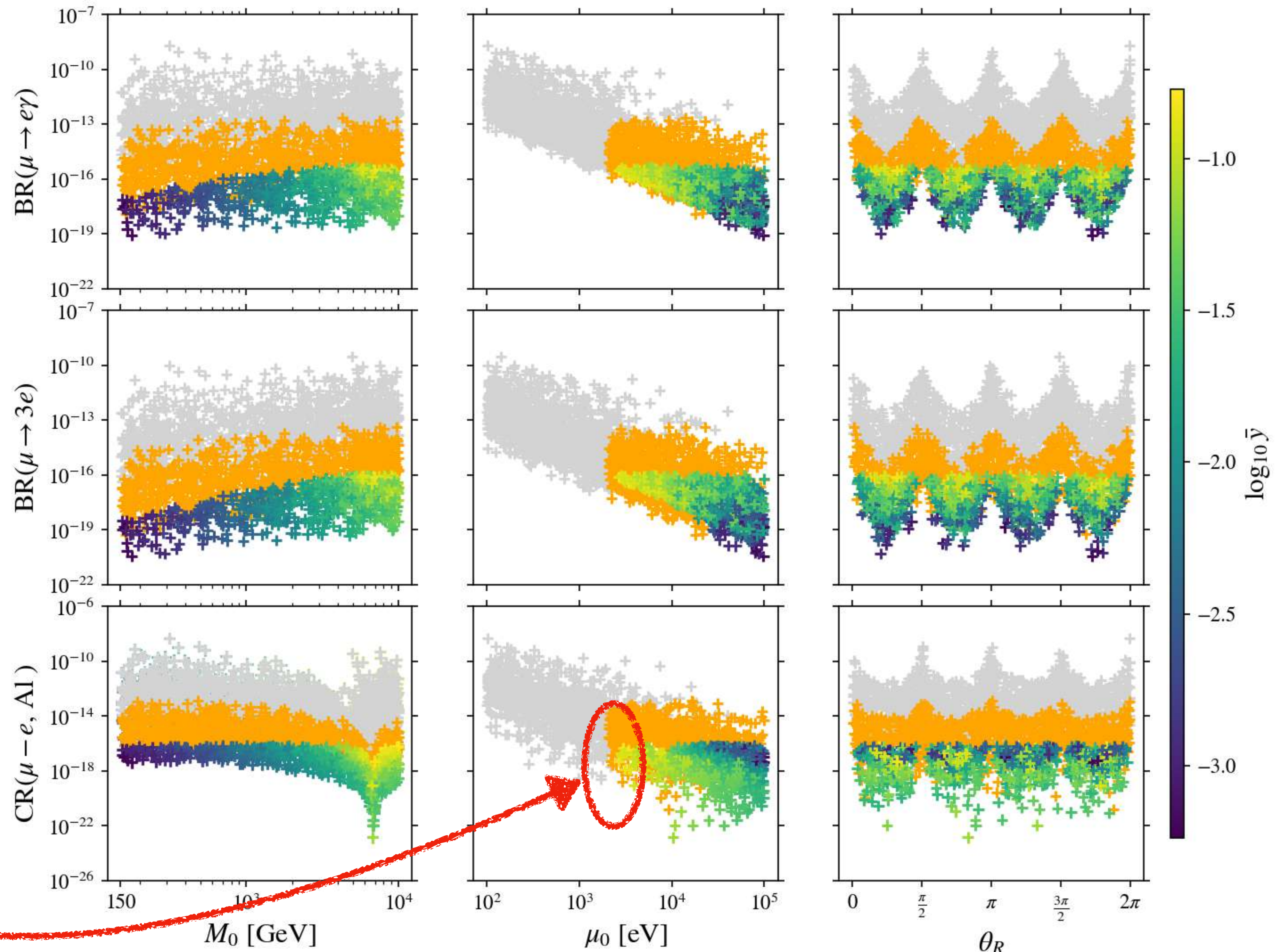
(FPDM, C. Hagedorn, ('24))

Case 2), $n = 14, s = 1, t = 1 (u = 1), \text{NO}$

Predictions are compatible with future bounds on $\mu - e$ transitions!

Lower limit for μ_0 can be extrapolated:

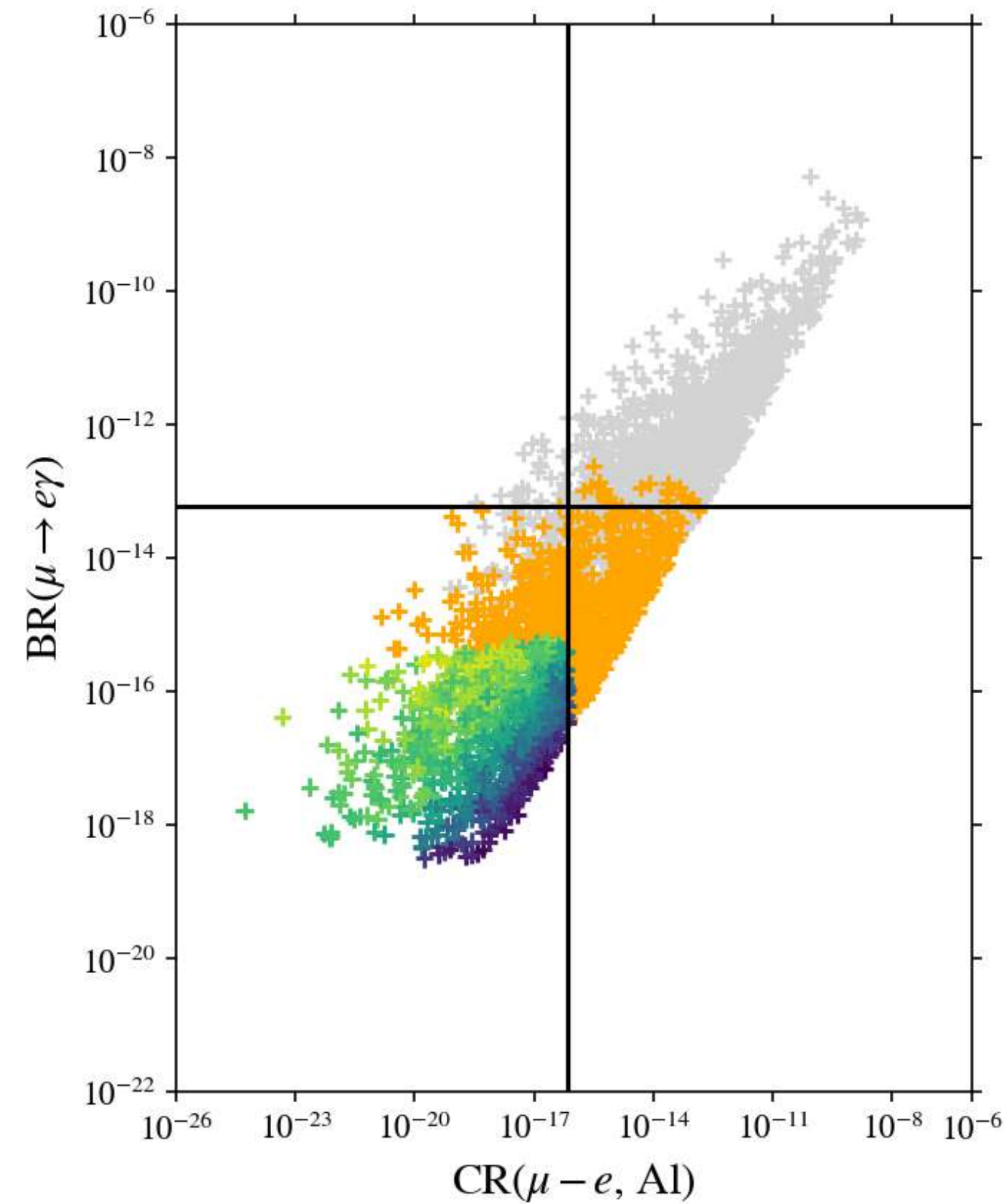
$$\mu_0 \gtrsim 2 \text{ keV}$$



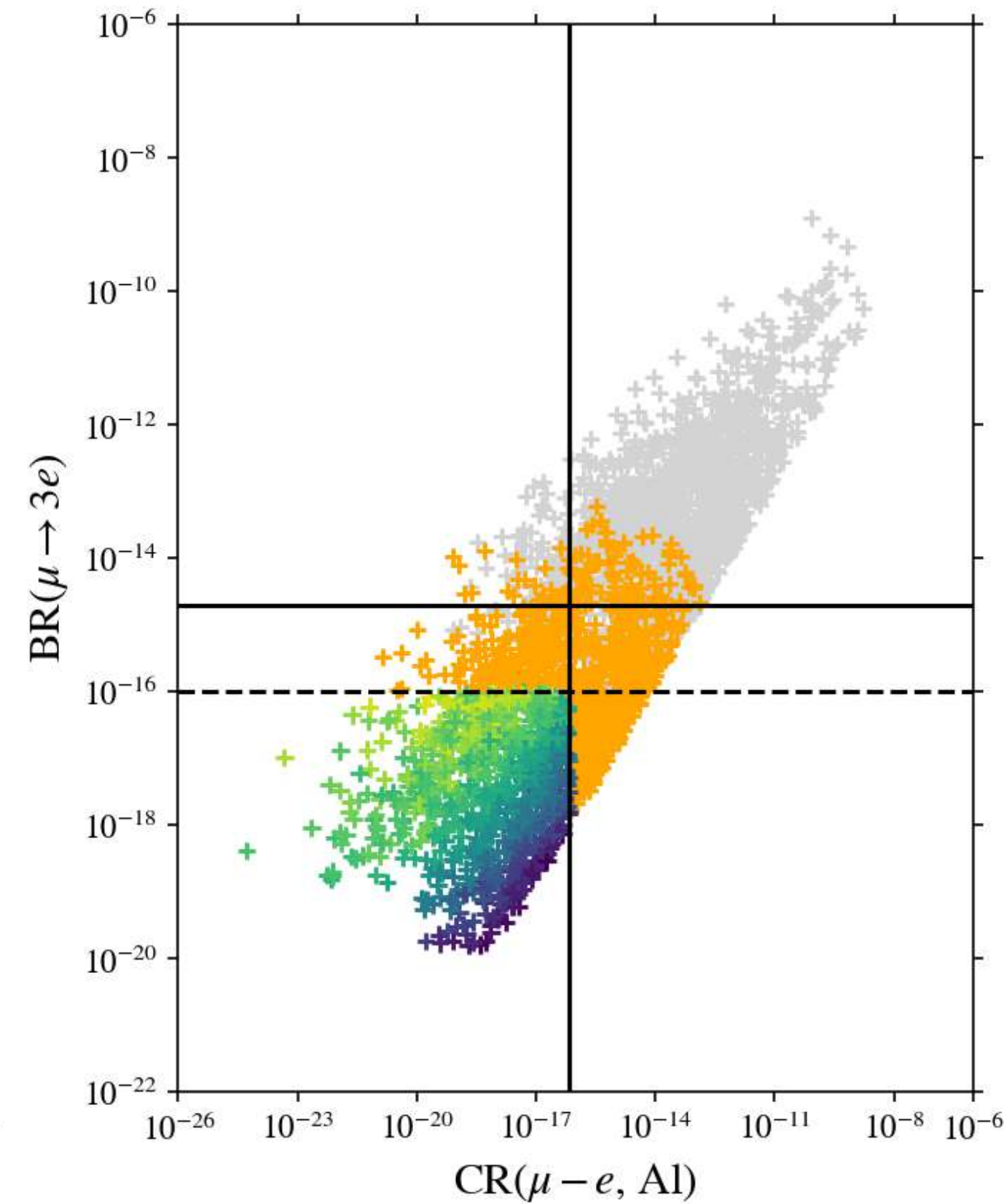
Option 2: Case 2

(FPDM, C. Hagedorn, ('24))

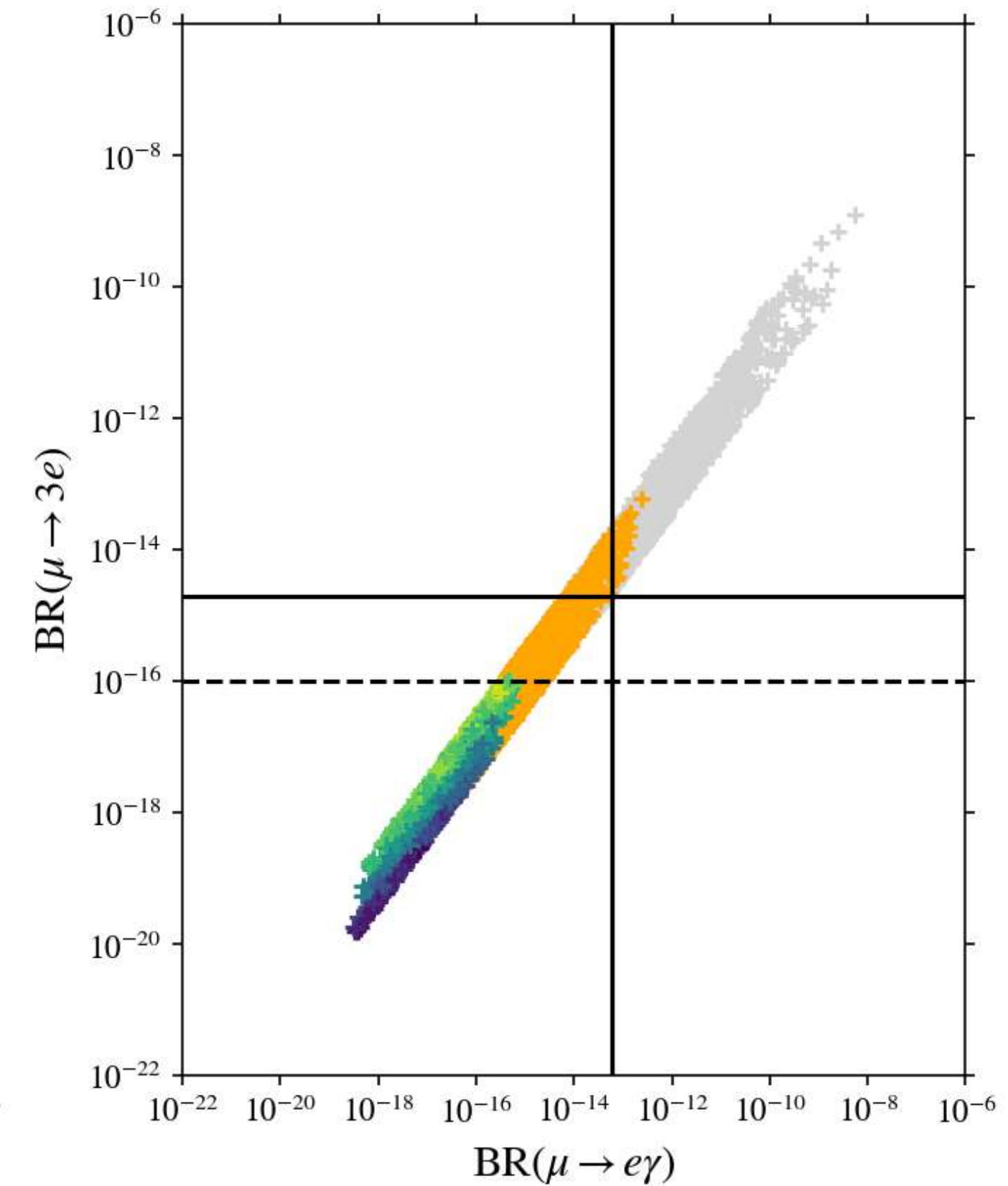
Case 2), $n = 14, s = 0, t = 1 (u = -1)$, NO



Bounds on
 $BR(\mu \rightarrow e\gamma)$ are only
mildly constraining

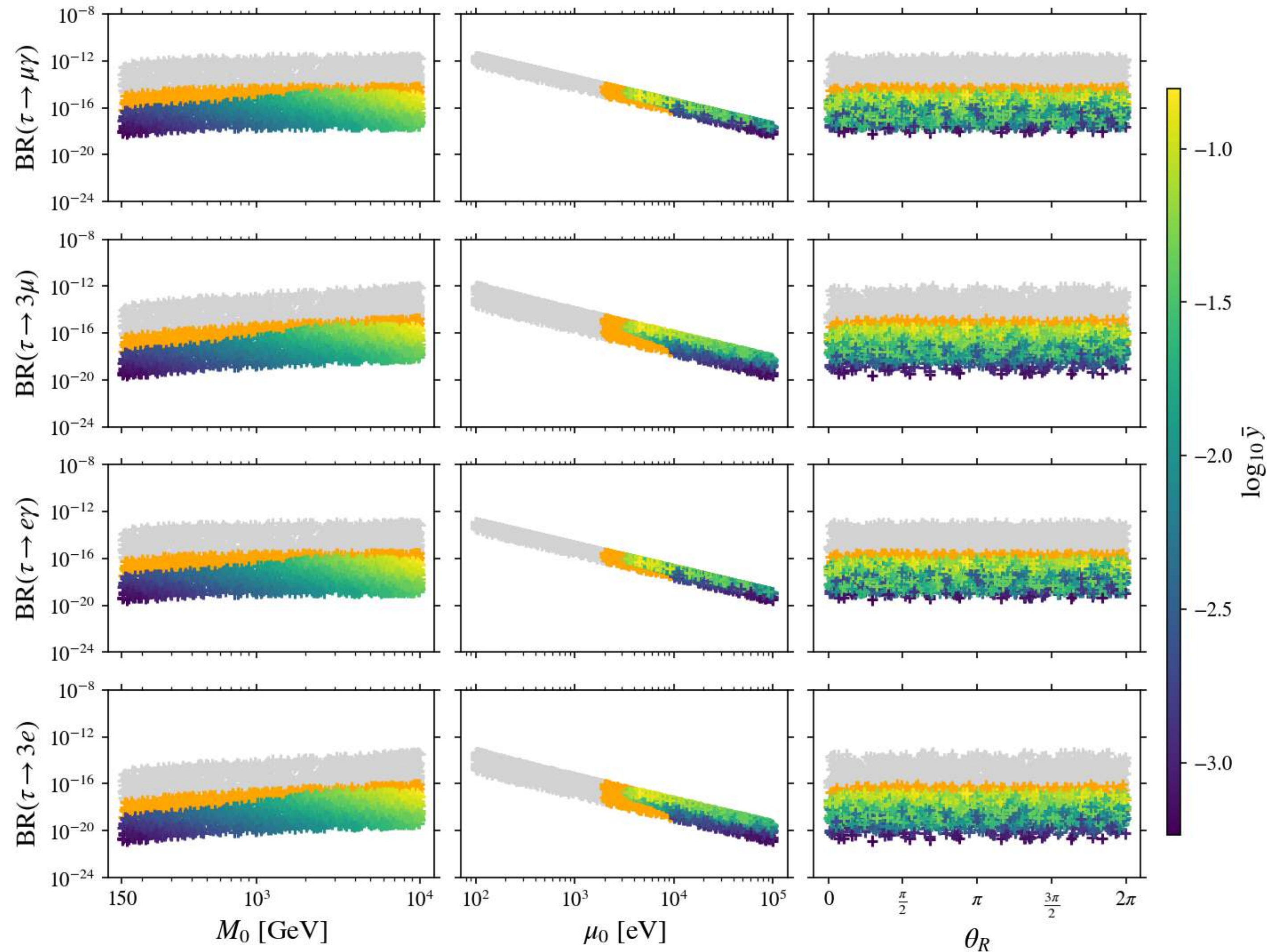


COMET and Mu2E
have big potential



Option 2: Case 2

Case 2), $n=14, s=1, t=2 (u=0)$, NO



$\tau - l$ transitions are non-constraining!

Option 2: Case 2

Summary for Option 2:

- For Option 2, all symmetry breaking information is contained in the Yukawa couplings Y_l
- Spectrum of the heavy sterile states is made of three quasi-degenerate pseudo-Dirac couples
- Mixing of heavy sterile states with light neutrinos (described by η) induces testable signals for processes violating Charged Lepton Flavour
- Future experiments could test the parameter space considered in our analysis

Option 2: Case 2

Summary for Option 2:

- For Option 2, all symmetry breaking information is contained in the Yukawa couplings Y_l
- Spectrum of the heavy sterile states is made of three quasi-degenerate pseudo-Dirac couples
- Mixing of heavy sterile states with light neutrinos (described by η) induces testable signals for processes violating Charged Lepton Flavour
- Future experiments could test the parameter space considered in our analysis

LET'S NOW MOVE ON TO OPTION 3 !

Option 3

(FPDM, C. Hagedorn, ('25, To appear))

$$Y_D = y_0 \begin{pmatrix} 1 & 0 & 0 \\ 0 & 1 & 0 \\ 0 & 0 & 1 \end{pmatrix} \quad \mu_S = \mu_0 \begin{pmatrix} 1 & 0 & 0 \\ 0 & 0 & 1 \\ 0 & 1 & 0 \end{pmatrix}$$

The flavour symmetry is broken by the M_{NS} mass term.

$$M_{NS} = U_N(\theta_N) \begin{pmatrix} M_1 & 0 & 0 \\ 0 & M_2 & 0 \\ 0 & 0 & M_3 \end{pmatrix} U_{S^\dagger}(\theta_S)$$

Option 3

(FPDM, C. Hagedorn, ('25, To appear))

$$Y_D = y_0 \begin{pmatrix} 1 & 0 & 0 \\ 0 & 1 & 0 \\ 0 & 0 & 1 \end{pmatrix} \quad \mu_S = \mu_0 \begin{pmatrix} 1 & 0 & 0 \\ 0 & 0 & 1 \\ 0 & 1 & 0 \end{pmatrix}$$

The flavour symmetry is broken by the M_{NS} mass term.

$$M_{NS} = U_N(\theta_N) \begin{pmatrix} M_1 & 0 & 0 \\ 0 & M_2 & 0 \\ 0 & 0 & M_3 \end{pmatrix} U_{S^\dagger}(\theta_S)$$

As for Option 2, the heavy neutral states mass matrix is approximately:

$$M_h \approx \begin{pmatrix} \emptyset & M_{NS} \\ M_{NS}^T & \mu_S \end{pmatrix}$$

The spectrum of heavy sterile states is:

$$\begin{aligned} m_4 &= M_1 - \frac{\mu_0}{2} & m_7 &= M_1 + \frac{\mu_0}{2} \\ m_5 &= M_2 - \frac{\mu_0}{2} & m_8 &= M_2 + \frac{\mu_0}{2} \\ m_6 &= M_3 - \frac{\mu_0}{2} & m_9 &= M_3 + \frac{\mu_0}{2} \end{aligned}$$

As per Option 2, spectrum of heavy sterile states is made of three pseudo-Dirac Couples

The main difference respect to Option 2 is the fact that heavy states are now non-degenerate!

As for Option 2, the heavy neutral states mass matrix is approximately:

$$M_h \approx \begin{pmatrix} \emptyset & M_{NS} \\ M_{NS}^T & \mu_S \end{pmatrix}$$

The spectrum of heavy sterile states is:

$$\begin{aligned} m_4 &= M_1 - \frac{\mu_0}{2} & m_7 &= M_1 + \frac{\mu_0}{2} \\ m_5 &= M_2 - \frac{\mu_0}{2} & m_8 &= M_2 + \frac{\mu_0}{2} \\ m_6 &= M_3 - \frac{\mu_0}{2} & m_9 &= M_3 + \frac{\mu_0}{2} \end{aligned}$$

As per Option 2, spectrum of heavy sterile states is made of three pseudo-Dirac Couples

The main difference respect to Option 2 is the fact that heavy states are now **non-degenerate!**

As for Option 2, the heavy neutral states mass matrix is approximately:

$$M_h \approx \begin{pmatrix} \emptyset & M_{NS} \\ M_{NS}^T & \mu_S \end{pmatrix}$$

The spectrum of heavy sterile states is:

$$\begin{aligned} m_4 &= M_1 - \frac{\mu_0}{2} & m_7 &= M_1 + \frac{\mu_0}{2} \\ m_5 &= M_2 - \frac{\mu_0}{2} & m_8 &= M_2 + \frac{\mu_0}{2} \\ m_6 &= M_3 - \frac{\mu_0}{2} & m_9 &= M_3 + \frac{\mu_0}{2} \end{aligned}$$

Mass scales M_i are set by requiring we reproduce light neutrino mass spectrum!

Option 3: Numerical Scan

y_0

- In our numerical analysis:
 $y_0 \in [10^{-4}; 1]$

Option 3: Numerical Scan

μ_0

- In our numerical analysis:

$$y_0 \in [10^{-4}; 1] \quad \mu_0 \in [0.1 \text{ keV}; 10^3 \text{ keV}]$$

Option 3: Numerical Scan

θ_S

θ_S

- In our numerical analysis:

$$y_0 \in [10^{-4}; 1] \quad \mu_0 \in [0.1 \text{ keV}; 10^3 \text{ keV}] \quad \theta_S \in [0; 2\pi]$$

Option 3: Numerical Scan

M_1
 M_2
 M_3

M_1
 M_2
 M_3

- In our numerical analysis:

$$y_0 \in [10^{-4}; 1] \quad \mu_0 \in [0.1 \text{ keV}; 10^3 \text{ keV}] \quad \theta_S \in [0; 2\pi]$$

- Fixed by fitting LO predictions of the masses to experimental values

Option 3: Numerical Scan

θ_N

θ_N

- In our numerical analysis:
 $y_0 \in [10^{-4}; 1]$ $\mu_0 \in [0.1 \text{ keV}; 10^3 \text{ keV}]$ $\theta_S \in [0; 2\pi]$
- Fixed by fitting LO predictions of the masses to experimental values
- Fixed by fitting prediction of mixing to lepton mixing data

Option 3: Numerical Scan

- In our numerical analysis:

$$y_0 \in [10^{-4}; 1] \quad \mu_0 \in [0.1 \text{ keV}; 10^3 \text{ keV}] \quad \theta_S \in [0; 2\pi]$$

- Fixed by fitting LO predictions of the masses to experimental values
- Fixed by fitting prediction of mixing to lepton mixing data
- Points of the scans are generated in a way that lightest sterile state's mass is above 150 GeV

Option 3: Case 2

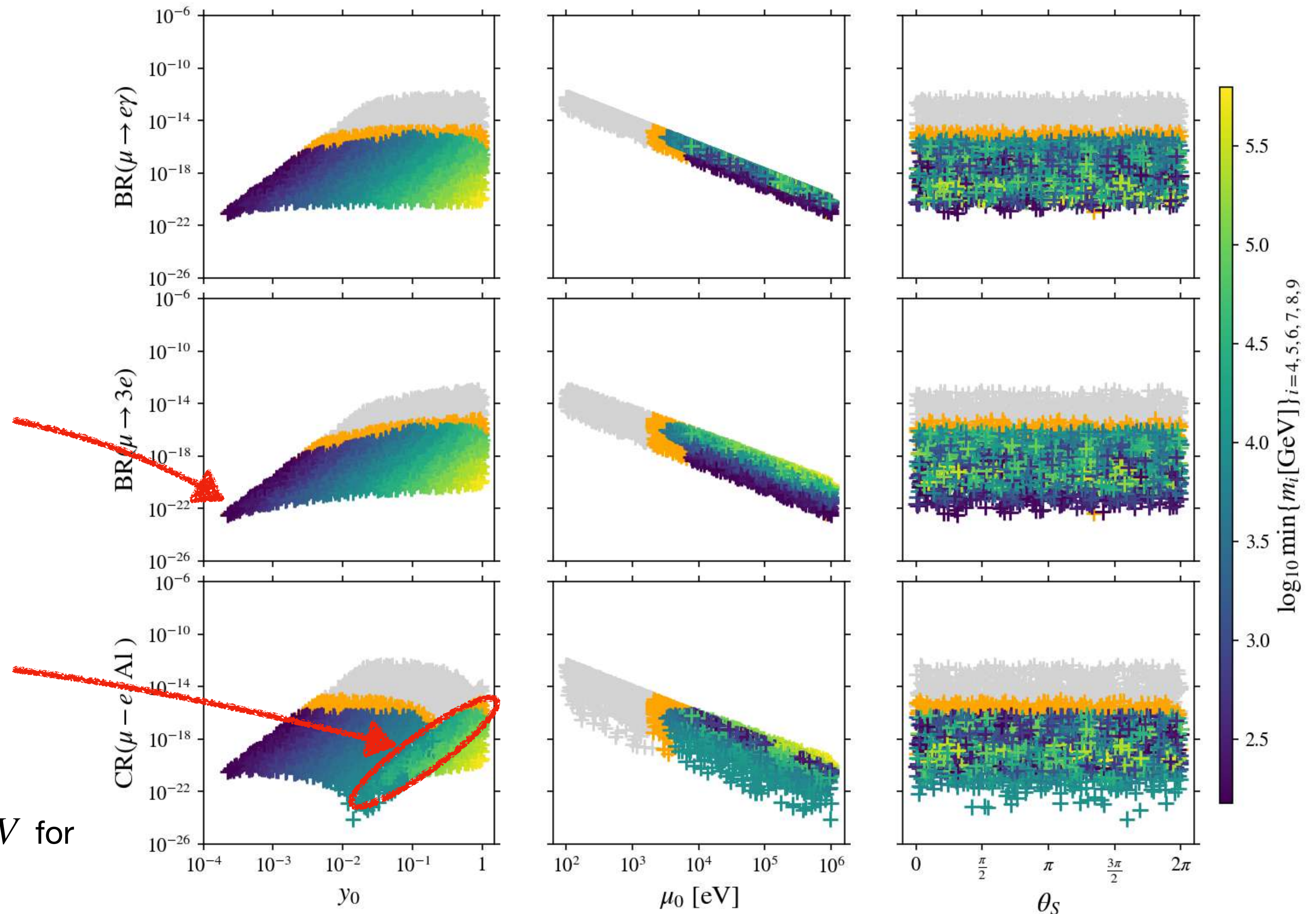
Case 2), $n=14, s=1, t=2 (u=0)$, NO

Predictions are similar to Option 2

Points converge as the mass of the lightest heavy sterile state approaches the threshold of 150 GeV

Position of the minima depends on the particular point in parameter space (in particular on μ_0)

Minima is really deep for $m_0 = 0.03(0.015) \text{ eV}$ for NO(IO)



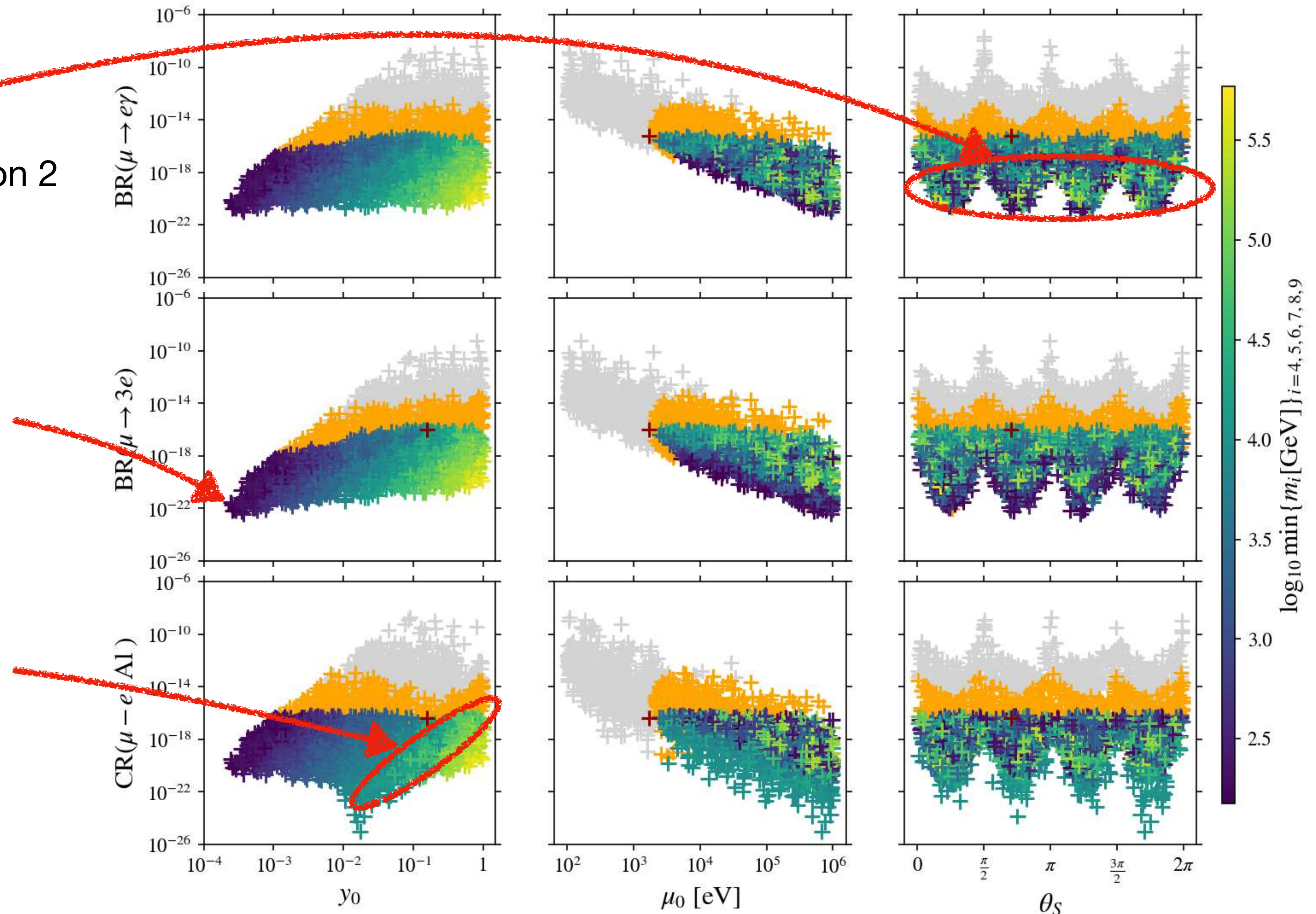
Option 3: Case 2

Case 2), $n=14, s=1, t=1 (u=1), \text{NO}$

θ_S dependence is the same as per Option 2

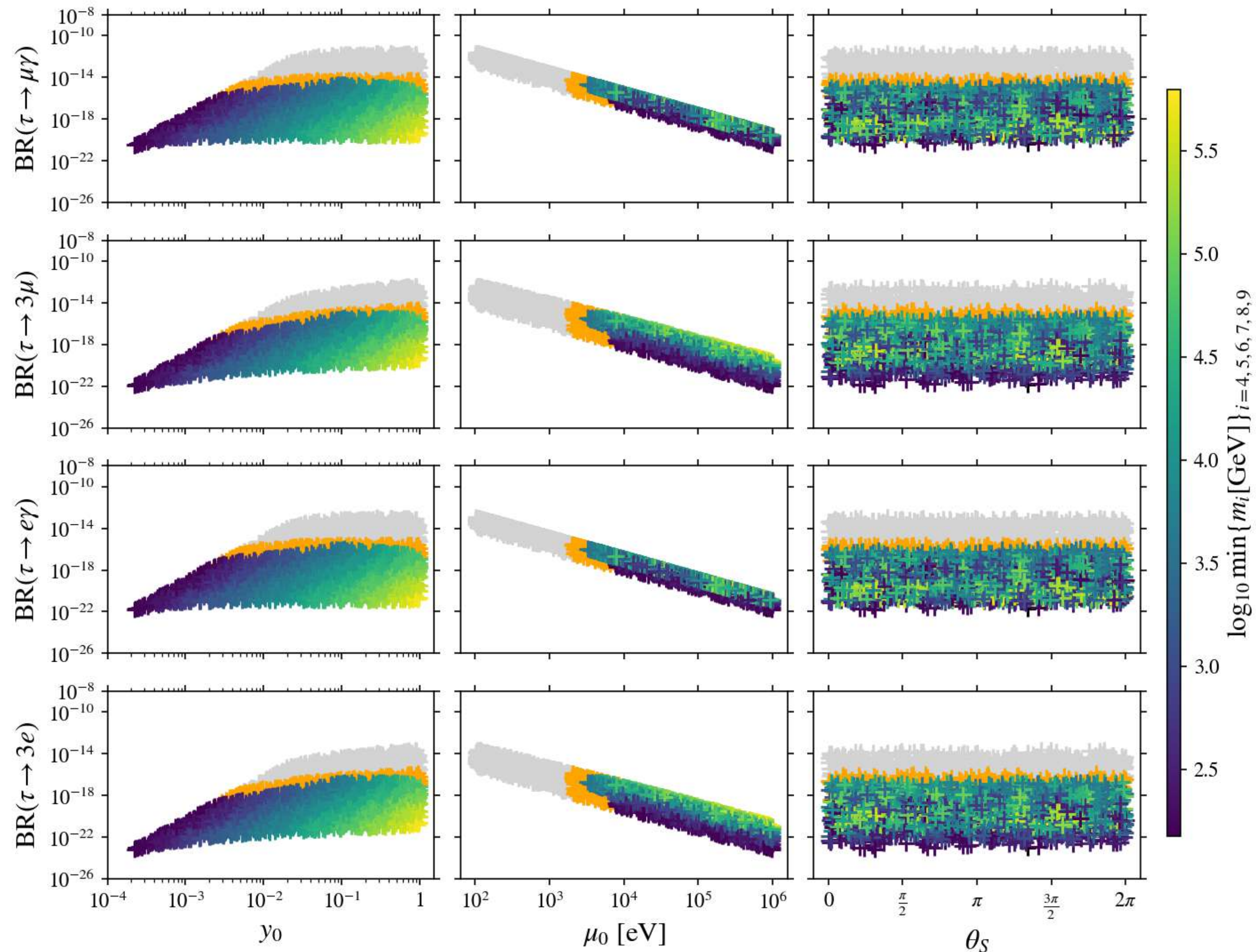
Points converge as the mass of the lightest heavy sterile state approaches the threshold of 150 GeV

Position of the minima depends on the particular point in parameter space (in particular on μ_0)



Option 3: Case 2

Case 2), $n=14, s=1, t=2 (u=0)$, NO



Again, $\tau - l$ transitions are non-constraining!

Option 2 VS. Option 3

We have discussed two Options in an ISS framework to reproduce the light neutrino mass spectrum and Mixing Data

Both solutions are equally successful in this regard

Both predict cLFV signals that could be detectable in the near future

Is there any hope to **distinguish the two options** via these?

Option 2 VS. Option 3

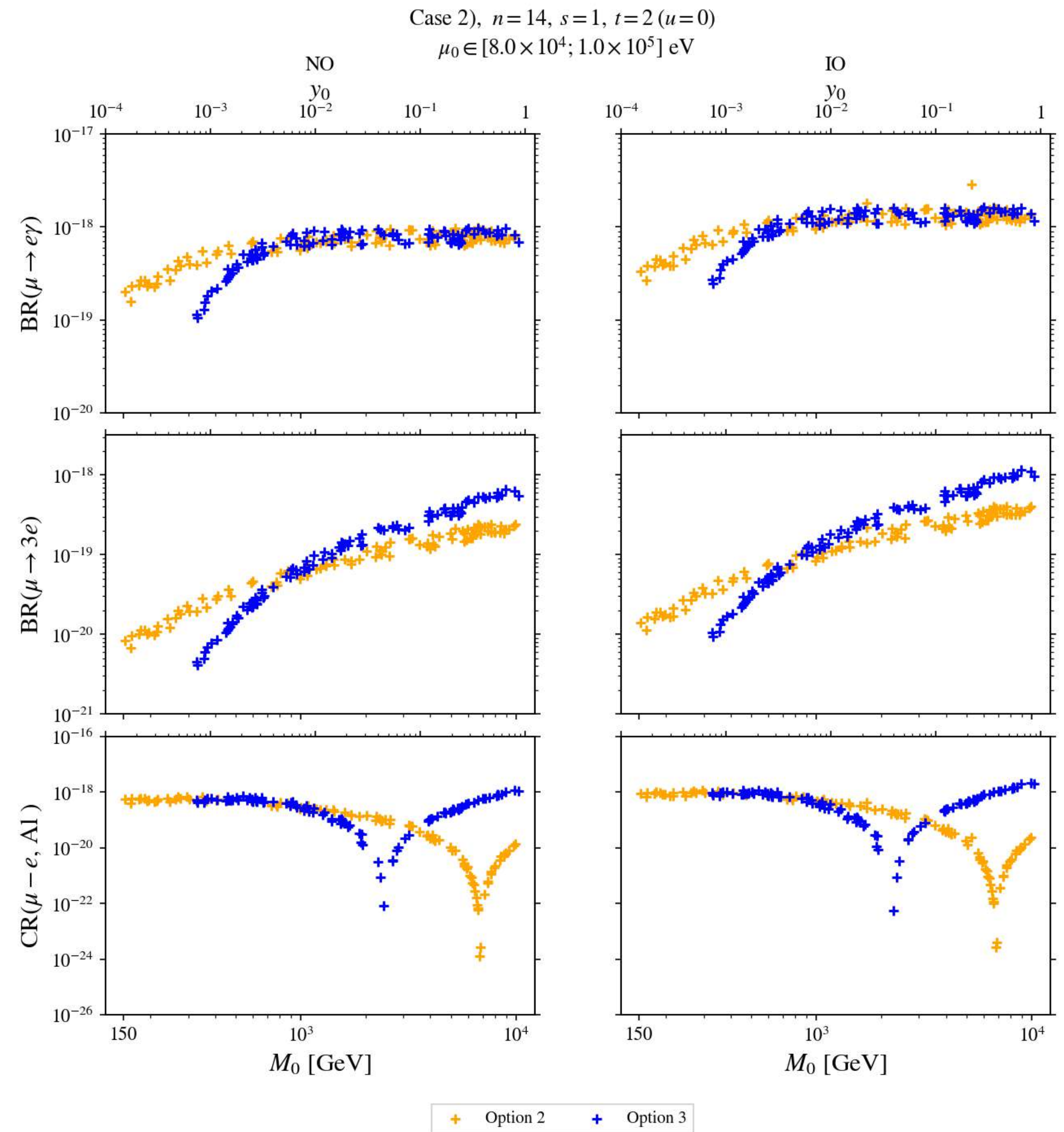
Filter points of the scan corresponding to a range of $\mu_0 \in [8 \times 10^4, 10^5] \text{ GeV}$

Upper and Lower limits predicted for the rates are comparable:

Differences are never larger than a factor $\mathcal{O}(3)$ for θ_S -independent cases,

Never larger than a factor $\mathcal{O}(6)$ for θ_S -dependent cases

No sensible difference between the two Options can be found!

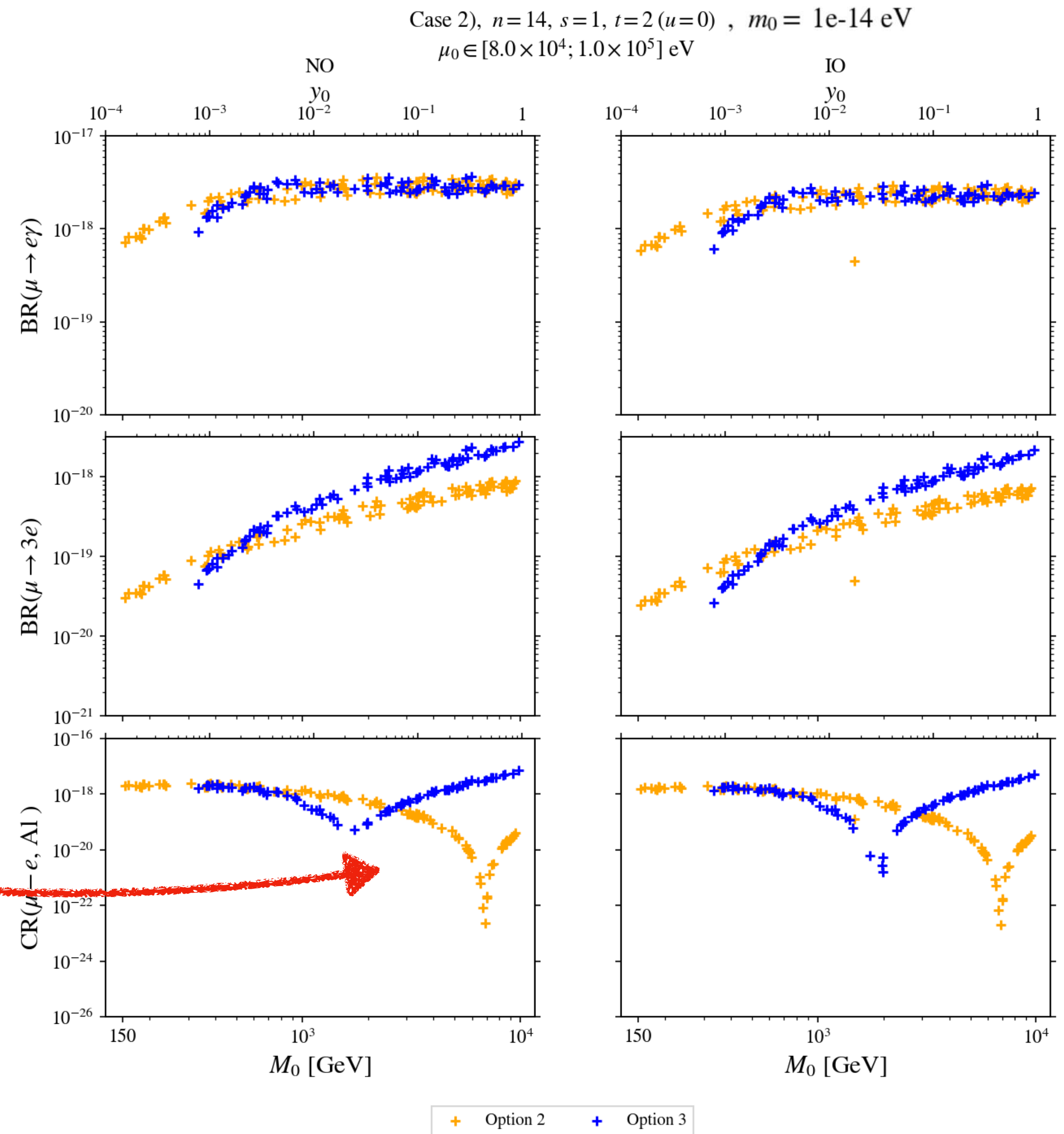


Option 2 VS. Option 3

Filter points of the scan corresponding to a range of $\mu_0 \in [8 \times 10^4, 10^5] \text{ GeV}$

In the decoupling limit, similar considerations hold

Cancellation/Local Minima of the Conversion rate is our best chance at distinguishing the two Options!



SUMMARY AND CONCLUSIONS

- We considered an ISS framework embedded with flavour and CP symmetries
- Two Options of the framework have been considered, each characterised by different representations of the fields and different spectrum of heavy states
 - Option 2 's heavy sterile states spectrum is composed of 3 almost-degenerate pseudo-Dirac couples
 - Option 3 's heavy sterile states spectrum is composed of 3 non-degenerate pseudo-Dirac couples
- Both Options predict cLFV signals which could be tested by future facilities
- Predictions for the two options are really similar, so chances of distinguishing between the two mostly comes from detection of heavy states of the spectrum

A photograph of the Pyramid of Giza at sunset. The pyramid is the central focus, showing its golden-brown stone blocks and a vertical crack running down its side. The sky is filled with soft, pinkish-purple clouds. In the foreground, a palm tree trunk is visible on the left, and a stone wall and a building with arched windows are on the right. A white text box with a black border is centered over the image, containing the text "THANKS FOR THE ATTENTION..." and "ANY QUESTIONS?".

THANKS FOR THE ATTENTION...

ANY QUESTIONS?

BACKUP SLIDES

Generalised CP Transformations

Given a set of fields ϕ , a generalised CP transformation is defined as :

$$\phi(x) \rightarrow \phi' = X \phi^*(x_{CP}) \quad x_{CP} = (x^0, -\vec{x})$$

(W. Grimus, M.N. Rebelo ('95))

(W. Grimus, G. Ecker, H. Neufeld ('84, '87, '88))

Generalised CP Transformations

Given a set of fields ϕ , a generalised CP transformation is defined as :

$$\phi(x) \rightarrow \phi' = X \phi^*(x_{CP}) \quad x_{CP} = (x^0, -\vec{x})$$

(W. Grimus, M.N. Rebelo ('95))

(W. Grimus, G. Ecker, H. Neufeld ('84, '87, '88))

CP is an involution transformation ($CP^2 = 1$), implying:

$X^*X = XX^*$ having taken X unitary, constant and symmetric.

Option 2

$$m_\nu \approx \frac{1}{M_0^2} m_D \mu_S m_D^T = \langle H \rangle \frac{\mu_0}{M_0^2} U_L^*(\theta_L) \left[\begin{pmatrix} y_1 & 0 & 0 \\ 0 & y_2 & 0 \\ 0 & 0 & y_3 \end{pmatrix} U_R^T(\theta_R) \begin{pmatrix} 1 & 0 & 0 \\ 0 & 0 & 1 \\ 0 & 1 & 0 \end{pmatrix} U_R(\theta_R) \begin{pmatrix} y_1 & 0 & 0 \\ 0 & y_2 & 0 \\ 0 & 0 & y_3 \end{pmatrix} \right] U_L^\dagger(\theta_L)$$

Heavy neutral states mass matrix:

$$M_h \approx \begin{pmatrix} \emptyset & M_{NS} \\ M_{NS}^T & \mu_S \end{pmatrix}$$

Heavy neutral states spectrum: **Three almost degenerate Pseudo-Dirac Pairs**

$$m_{(i=4,5,6)} \approx M_0 - \frac{1}{2} \mu_0 \quad m_{(i=7,8,9)} \approx M_0 + \frac{1}{2} \mu_0$$

Remember the ISS condition:

$$|\mu_0| \ll |m_D| \ll M_{NS}$$

Option 2

$$m_\nu \approx \frac{1}{M_0^2} m_D \mu_S m_D^T = \langle H \rangle \frac{\mu_0}{M_0^2} U_L^*(\theta_L) \left[\begin{pmatrix} y_1 & 0 & 0 \\ 0 & y_2 & 0 \\ 0 & 0 & y_3 \end{pmatrix} U_R^T(\theta_R) \begin{pmatrix} 1 & 0 & 0 \\ 0 & 0 & 1 \\ 0 & 1 & 0 \end{pmatrix} U_R(\theta_R) \begin{pmatrix} y_1 & 0 & 0 \\ 0 & y_2 & 0 \\ 0 & 0 & y_3 \end{pmatrix} \right] U_L^\dagger(\theta_L)$$

$$U_L(\theta_L) = \Omega(3) R_{ij}(\theta_L)$$

$$U_R(\theta_R) = \Omega(3') R_{kl}(\theta_R) \left(P_{kl}^{ij} \right)^T$$

Option 2

$$m_\nu \approx \frac{1}{M_0^2} m_D \mu_S m_D^T = \langle H \rangle \frac{\mu_0}{M_0^2} U_L^*(\theta_L) \left[\begin{array}{c} \begin{pmatrix} y_1 & 0 & 0 \\ 0 & y_2 & 0 \\ 0 & 0 & y_3 \end{pmatrix} U_R^T(\theta_R) \begin{pmatrix} 1 & 0 & 0 \\ 0 & 0 & 1 \\ 0 & 1 & 0 \end{pmatrix} U_R(\theta_R) \begin{pmatrix} y_1 & 0 & 0 \\ 0 & y_2 & 0 \\ 0 & 0 & y_3 \end{pmatrix} \end{array} \right] U_L^\dagger(\theta_L)$$

$$U_L(\theta_L) = \Omega(3) R_{ij}(\theta_L)$$

$$U_R(\theta_R) = \Omega(3') R_{kl}(\theta_R) \left(P_{kl}^{ij} \right)^T$$

$\Omega(3), \Omega(3')$ are unitary

Are determined by residual symmetry (specified by the **CASE** and n, s, t) and its embedding in G_f .

Option 2

$$m_\nu \approx \frac{1}{M_0^2} m_D \mu_S m_D^T = \langle H \rangle \frac{\mu_0}{M_0^2} U_L^*(\theta_L) \left[\begin{pmatrix} y_1 & 0 & 0 \\ 0 & y_2 & 0 \\ 0 & 0 & y_3 \end{pmatrix} U_R^T(\theta_R) \begin{pmatrix} 1 & 0 & 0 \\ 0 & 0 & 1 \\ 0 & 1 & 0 \end{pmatrix} U_R(\theta_R) \begin{pmatrix} y_1 & 0 & 0 \\ 0 & y_2 & 0 \\ 0 & 0 & y_3 \end{pmatrix} \right] U_L^\dagger(\theta_L)$$

$$U_L(\theta_L) = \Omega(3) R_{ij}(\theta_L)$$

$$U_R(\theta_R) = \Omega(3') R_{kl}(\theta_R) \left(P_{kl}^{ij} \right)^T$$

$\Omega(3), \Omega(3')$ are unitary

Are determined by residual symmetry (specified by the **CASE** and n, s, t) and its embedding in G_f .

$R_{ij}(\theta_{L,R})$ is a rotation on the ij plane

Codifies residual freedom in the choice of Ω matrices

Example: Case 2

$$Z(\mathbf{r}) = c(\mathbf{r})^{n/2} \quad X(\mathbf{r}) = c(\mathbf{r})^s d(\mathbf{r})^t X_0(\mathbf{r})$$

Same structure for all s, t :

$$\Omega(\mathbf{3})(u, v) = e^{i\frac{v\pi}{n}} U_{TB} R_{13} \left(-\frac{u\pi}{2n} \right) \begin{pmatrix} 1 & 0 & 0 \\ 0 & e^{-i\frac{v\pi}{n}} & 0 \\ 0 & 0 & -i \end{pmatrix}$$

s even, t odd:

$$\Omega(\mathbf{3}')(u, v) = e^{-i\frac{\pi}{4}} U_{TB} R_{13} \left(\frac{\pi}{4} \right) \begin{pmatrix} i & 0 & 0 \\ 0 & e^{-i\frac{\pi}{4}} & 0 \\ 0 & 0 & 1 \end{pmatrix}$$

s even, t even:

$$\Omega(\mathbf{3}')(u, v) = U_{TB} \begin{pmatrix} i & 0 & 0 \\ 0 & 1 & 0 \\ 0 & 0 & -1 \end{pmatrix}$$

s odd, t even:

$$\Omega(\mathbf{3}')(u, v) = U_{TB} \begin{pmatrix} i & 0 & 0 \\ 0 & 1 & 0 \\ 0 & 0 & 1 \end{pmatrix}$$

s odd, t odd:

$$\Omega(\mathbf{3}')(u, v) = e^{-3i\frac{\pi}{4}} U_{TB} R_{13} \left(\frac{\pi}{4} \right) \begin{pmatrix} -i & 0 & 0 \\ 0 & e^{i\frac{\pi}{4}} & 0 \\ 0 & 0 & 1 \end{pmatrix}$$

$$U_L(\theta_L) = \Omega(\mathbf{3}) R_{ij}(\theta_L)$$

$$U_R(\theta_R) = \Omega(\mathbf{3}') R_{kl}(\theta_R) \left(P_{kl}^{ij} \right)^T$$

(C. Hagedorn, E. Molinaro, A. Meroni, ('14))

Option 2

Example: Case 2

$$Z(\mathbf{r}) = c(\mathbf{r})^{n/2} \quad X(\mathbf{r}) = c(\mathbf{r})^s d(\mathbf{r})^t X_0(\mathbf{r})$$

Same structure for all s, t :
$$\Omega(\mathbf{3})(u, v) = e^{i\frac{v\pi}{n}} U_{TB} R_{13} \left(-\frac{u\pi}{2n} \right) \begin{pmatrix} 1 & 0 & 0 \\ 0 & e^{-i\frac{v\pi}{n}} & 0 \\ 0 & 0 & -i \end{pmatrix}$$

s even, t odd:
$$\Omega(\mathbf{3}')(u, v) = e^{-i\frac{\pi}{4}} U_{TB} R_{13} \left(\frac{\pi}{4} \right) \begin{pmatrix} i & 0 & 0 \\ 0 & e^{-i\frac{\pi}{4}} & 0 \\ 0 & 0 & 1 \end{pmatrix}$$

s even, t even:
$$\Omega(\mathbf{3}')(u, v) = U_{TB} \begin{pmatrix} i & 0 & 0 \\ 0 & 1 & 0 \\ 0 & 0 & -1 \end{pmatrix}$$

s odd, t even:
$$\Omega(\mathbf{3}')(u, v) = U_{TB} \begin{pmatrix} i & 0 & 0 \\ 0 & 1 & 0 \\ 0 & 0 & 1 \end{pmatrix}$$

s odd, t odd:
$$\Omega(\mathbf{3}')(u, v) = e^{-3i\frac{\pi}{4}} U_{TB} R_{13} \left(\frac{\pi}{4} \right) \begin{pmatrix} -i & 0 & 0 \\ 0 & e^{i\frac{\pi}{4}} & 0 \\ 0 & 0 & 1 \end{pmatrix}$$

$$U_L(\theta_L) = \Omega(\mathbf{3}) R_{ij}(\theta_L)$$

$$U_R(\theta_R) = \Omega(\mathbf{3}') R_{kl}(\theta_R) \left(P_{kl}^{ij} \right)^T$$

(C. Hagedorn, E. Molinaro, A. Meroni, ('14))

Option 2

Example: Case 2

$$Z(\mathbf{r}) = c(\mathbf{r})^{n/2} \quad X(\mathbf{r}) = c(\mathbf{r})^s d(\mathbf{r})^t X_0(\mathbf{r})$$

Same structure for all s, t : $\Omega(\mathbf{3})(u, v) = e^{i\frac{v\pi}{n}} U_{TB} R_{13} \begin{pmatrix} -\frac{u\pi}{2n} \\ \\ \end{pmatrix} \begin{pmatrix} 1 & 0 & 0 \\ 0 & e^{-i\frac{v\pi}{n}} & 0 \\ 0 & 0 & -i \end{pmatrix}$

s even, t odd: $\Omega(\mathbf{3}')(u, v) = e^{-i\frac{\pi}{4}} U_{TB} R_{13} \begin{pmatrix} \frac{\pi}{4} \\ \\ \end{pmatrix} \begin{pmatrix} i & 0 & 0 \\ 0 & e^{-i\frac{\pi}{4}} & 0 \\ 0 & 0 & 1 \end{pmatrix}$

s even, t even: $\Omega(\mathbf{3}')(u, v) = U_{TB} \begin{pmatrix} i & 0 & 0 \\ 0 & 1 & 0 \\ 0 & 0 & -1 \end{pmatrix}$

s odd, t even: $\Omega(\mathbf{3}')(u, v) = U_{TB} \begin{pmatrix} i & 0 & 0 \\ 0 & 1 & 0 \\ 0 & 0 & 1 \end{pmatrix}$

s odd, t odd: $\Omega(\mathbf{3}')(u, v) = e^{-3i\frac{\pi}{4}} U_{TB} R_{13} \begin{pmatrix} \frac{\pi}{4} \\ \\ \end{pmatrix} \begin{pmatrix} -i & 0 & 0 \\ 0 & e^{i\frac{\pi}{4}} & 0 \\ 0 & 0 & 1 \end{pmatrix}$

$$U_L(\theta_L) = \Omega(\mathbf{3}) R_{ij}(\theta_L)$$

$$U_R(\theta_R) = \Omega(\mathbf{3}') R_{kl}(\theta_R) \left(P_{kl}^{ij} \right)^T$$

In the basis in which $U_l = 1$:

$$U_{PMNS} = U_L(\theta_L) = \Omega(\mathbf{3}) R_{ij}(\theta_L)$$

(C. Hagedorn, E. Molinaro, A. Meroni, ('14))

Example: Case 2

$$U_L(\theta_L) = \Omega(3)R_{ij}(\theta_L)$$

$$U_R(\theta_R) = \Omega(3')R_{kl}(\theta_R)\left(P_{kl}^{ij}\right)^T$$

In the basis in which $U_l = 1$:

$$U_{PMNS} = U_L(\theta_L) = \Omega(3) R_{ij}(\theta_L)$$

The predictions for mixing angles and CP invariants:

$$\sin^2 \theta_{13} = \frac{1}{3}(1 - \cos \phi_u \cos(2\theta_L))$$

$$\sin^2 \theta_{12} = \frac{1}{2 + \cos \phi_u \cos(2\theta_L)}$$

$$\sin^2 \theta_{23} = \frac{1}{2} \left(1 + \frac{\sqrt{3} \sin \phi_u \cos(2\theta_L)}{2 + \cos \phi_u \cos(2\theta_L)} \right)$$

$$J_{CP} = -\frac{\sin(2\theta_L)}{6\sqrt{3}}$$

$$I_1 = \frac{1}{9} \left([\cos \phi_u + \cos(2\theta_L)] \sin \phi_v - \sin \phi_u \cos \phi_v \sin(2\theta_L) \right)$$

$$I_2 = \frac{1}{9} \sin(2\phi_u) \sin(2\theta_L)$$

Example: Case 2

$$U_L(\theta_L) = \Omega(3)R_{ij}(\theta_L)$$

$$U_R(\theta_R) = \Omega(3')R_{kl}(\theta_R)\left(P_{kl}^{ij}\right)^T$$

In the basis in which $U_l = 1$:

$$U_{PMNS} = U_L(\theta_L) = \Omega(3) R_{ij}(\theta_L)$$

The predictions for mixing angles and CP invariants:

$$\sin^2 \theta_{13} = \frac{1}{3}(1 - \cos \phi_u \cos(2\theta_L))$$

$$\sin^2 \theta_{12} = \frac{1}{2 + \cos \phi_u \cos(2\theta_L)}$$

$$\sin^2 \theta_{23} = \frac{1}{2} \left(1 + \frac{\sqrt{3} \sin \phi_u \cos(2\theta_L)}{2 + \cos \phi_u \cos(2\theta_L)} \right)$$

$$J_{CP} = -\frac{\sin(2\theta_L)}{6\sqrt{3}}$$

$$I_1 = \frac{1}{9} \left([\cos \phi_u + \cos(2\theta_L)] \sin \phi_v - \sin \phi_u \cos \phi_v \sin(2\theta_L) \right)$$

$$I_2 = \frac{1}{9} \sin(2\phi_u) \sin(2\theta_L)$$

Predictions of mixing only depend on $\Omega(3)$!!

Generalised CP Transformations

Given a set of fields ϕ , a generalised CP transformation is defined as :

$$\phi(x) \rightarrow \phi' = X \phi^*(x_{CP}) \quad x_{CP} = (x^0, -\vec{x})$$

(W. Grimus, M.N. Rebelo ('95))

(W. Grimus, G. Ecker, H. Neufeld ('84, '87, '88))

CP is an involution transformation ($CP^2 = 1$), implying:

$X^*X = XX^*$ having taken X unitary, constant and symmetric.

When combined with Flavour Symmetries, a **consistency**

condition is required:

$$X^{-1} \rho(g) X = \rho(g')^* \quad g, g' \in G_f$$

(M. Holthausen, M. Lindner, M.A. Schmidt ('14))

Generalised CP Transformations

Given a set of fields ϕ , a generalised CP transformation is defined as :

$$\phi(x) \rightarrow \phi' = X \phi^*(x_{CP}) \quad x_{CP} = (x^0, -\vec{x})$$

(W. Grimus, M.N. Rebelo ('95))

(W. Grimus, G. Ecker, H. Neufeld ('84, '87, '88))

CP is an involution transformation ($CP^2 = 1$), implying:

$X^*X = XX^*$ having taken X unitary, constant and symmetric.

When combined with Flavour Symmetries, a **consistency condition** is required:

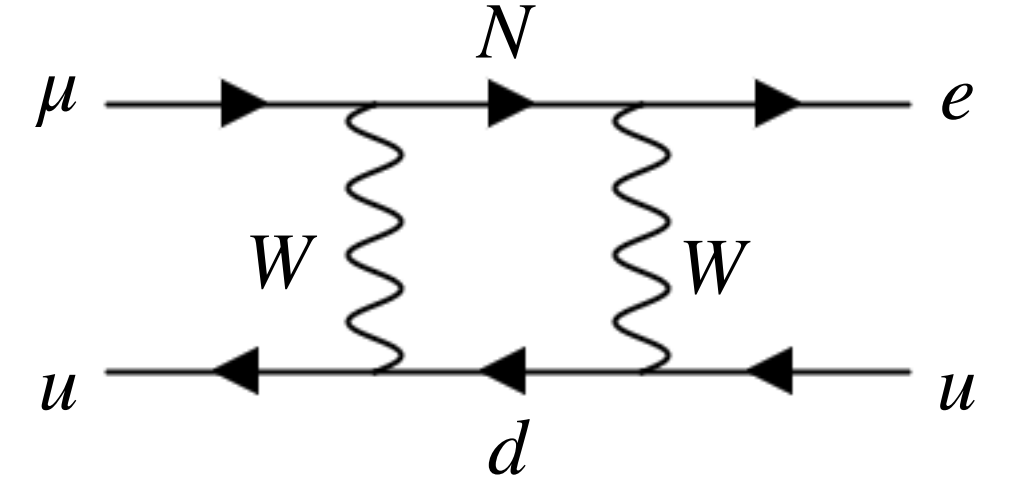
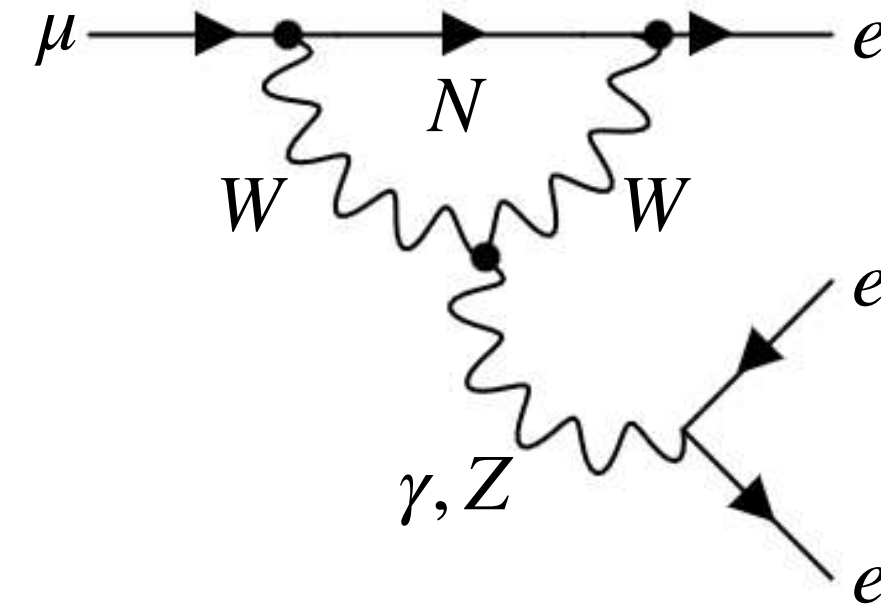
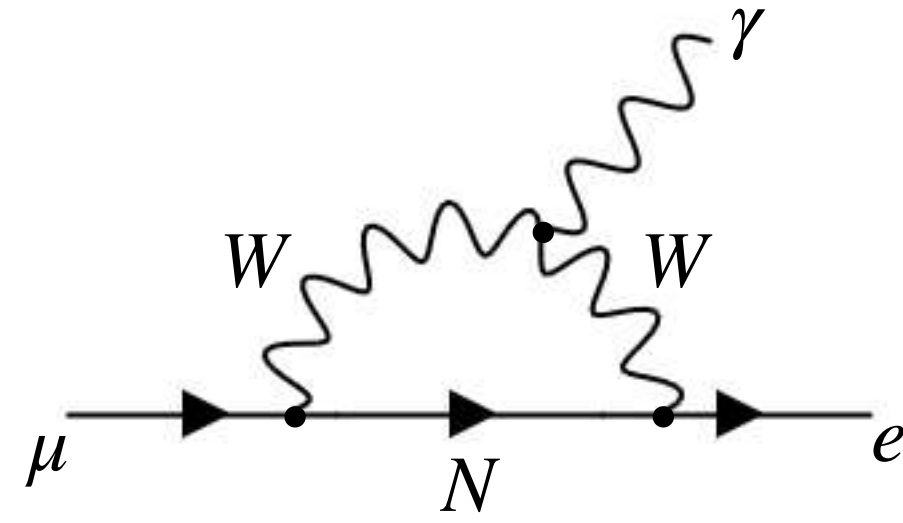
$$X^{-1} \rho(g) X = \rho(g')^* \quad g, g' \in G_f$$

(M. Holthausen, M. Lindner, M.A. Schmidt ('14))

CP has to be an **AUTOMORPHISM** of the flavour group

Option 2

cLFV in the ISS



Relevant (approximated) loop functions for Option 2:

$$G_{\gamma}^{\beta\alpha} \approx \eta_{\alpha\beta} + \mathcal{O}\left(\frac{Y\mu_0}{M_0}, \frac{\mu_0}{M_0}\right)$$

$$F_{\gamma}^{\beta\alpha} \approx -2 \left(\frac{7}{12} + \frac{1}{6} \log x_0 \right) \eta_{\alpha\beta} + \mathcal{O}\left(\frac{Y\mu_0}{M_0}, \frac{m\mu_0}{M_0}\right)$$

$$F_Z^{\beta\alpha} \approx \eta_{\alpha\beta} (5 - 3 \log x_0) + \mathcal{O}\left(\frac{Y\mu_0}{M_0}, \frac{\mu_0}{M_0}\right)$$

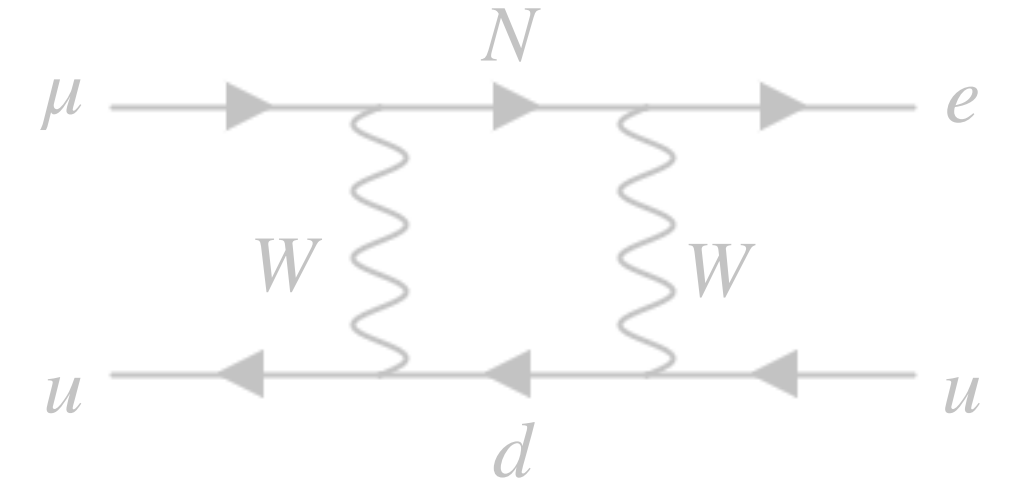
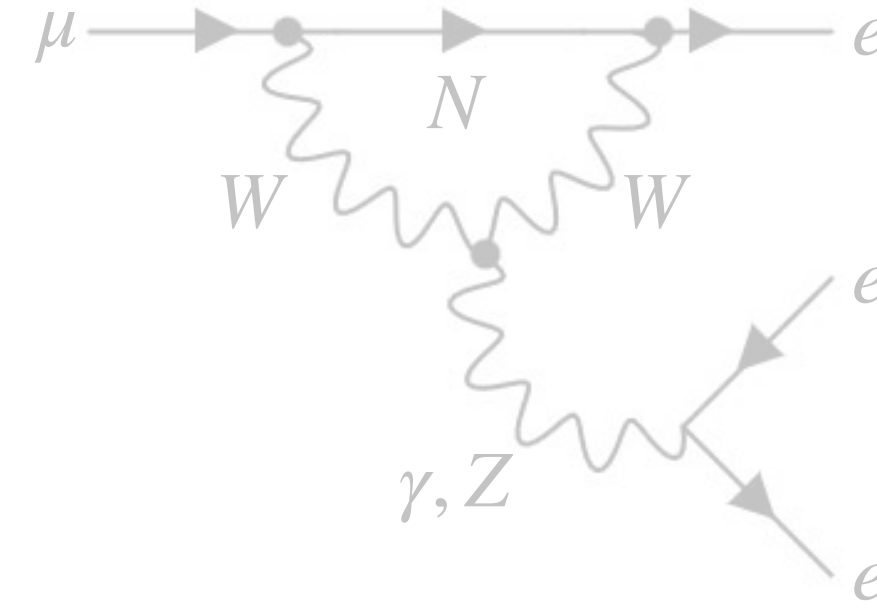
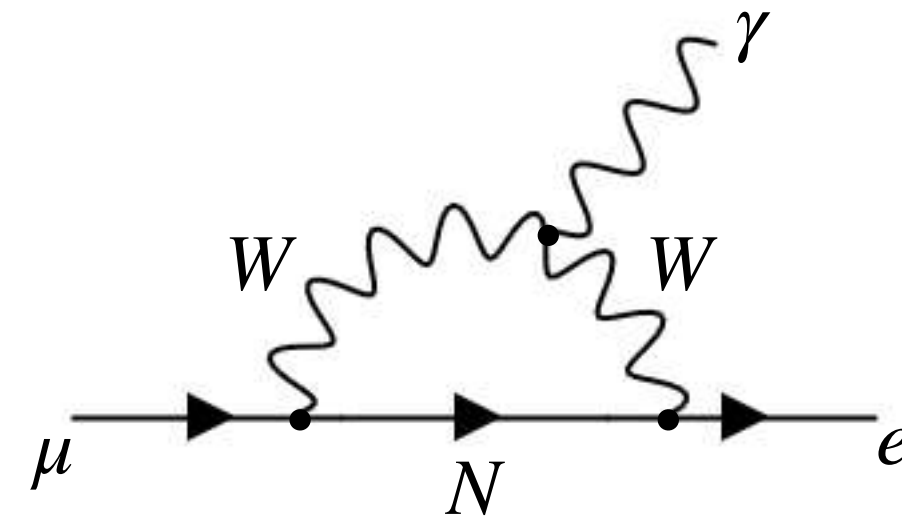
$$F_{box}^{\beta3\alpha} \approx -2\eta_{\alpha\beta} + \mathcal{O}\left(\frac{Y^2\mu_0}{M_0}, \frac{\mu_0^2}{M_0^2}\right)$$

$$F_{box}^{\mu e u u} = 2\eta_{e\mu} \left[-4 - |V_{ub}|^2 (F_{box}(0, x_b) - F_{box}(x_0, x_b) - 4) \right]$$

$$F_{box}^{\mu e d d} = 2\eta_{e\mu} \left[1 - |V_{td}|^2 (F_{Xbox}(0, x_t) - F_{Xbox}(x_0, x_t) + 1) \right]$$

Option 2

cLFV in the ISS



Relevant (approximated) loop functions for Option 2:

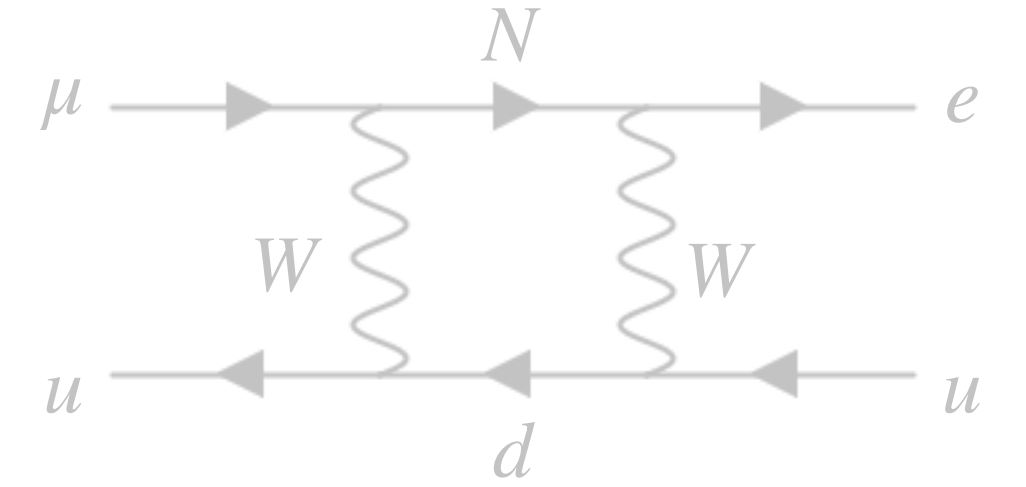
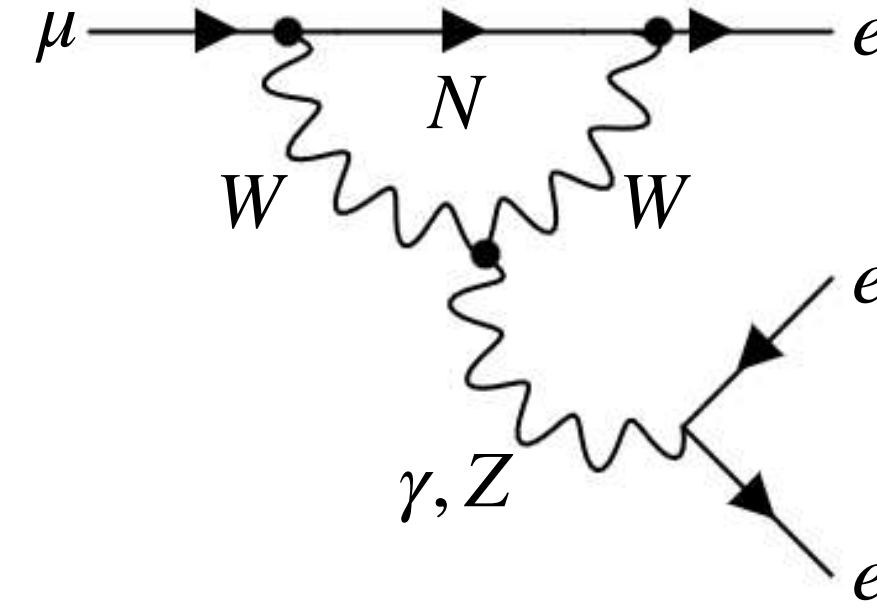
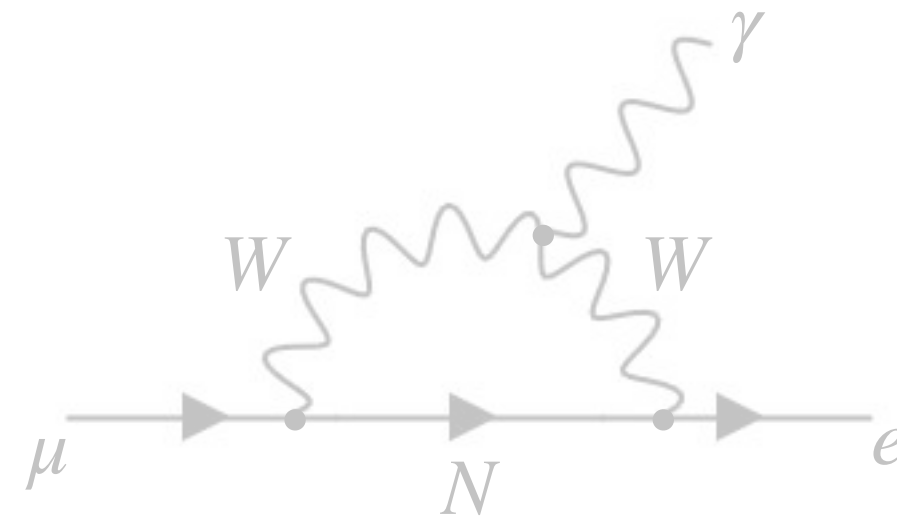
$$\left. \begin{aligned}
 G_{\gamma}^{\beta\alpha} &\approx \eta_{\alpha\beta} + \mathcal{O}\left(\frac{Y\mu_0}{M_0}, \frac{\mu_0}{M_0}\right) \\
 F_{\gamma}^{\beta\alpha} &\approx -2 \left(\frac{7}{12} + \frac{1}{6} \log x_0 \right) \eta_{\alpha\beta} + \mathcal{O}\left(\frac{Y\mu_0}{M_0}, \frac{m\mu_0}{M_0}\right) \\
 F_Z^{\beta\alpha} &\approx \eta_{\alpha\beta} (5 - 3 \log x_0) + \mathcal{O}\left(\frac{Y\mu_0}{M_0}, \frac{\mu_0}{M_0}\right) \\
 F_{box}^{\beta 3\alpha} &\approx -2\eta_{\alpha\beta} + \mathcal{O}\left(\frac{Y^2\mu_0}{M_0}, \frac{\mu_0^2}{M_0^2}\right)
 \end{aligned} \right\} \text{Photon Penguins}$$

$$F_{box}^{\mu e u u} = 2\eta_{e\mu} \left[-4 - |V_{ub}|^2 (F_{box}(0, x_b) - F_{box}(x_0, x_b) - 4) \right]$$

$$F_{box}^{\mu e d d} = 2\eta_{e\mu} \left[1 - |V_{td}|^2 (F_{Xbox}(0, x_t) - F_{Xbox}(x_0, x_t) + 1) \right]$$

Option 2

cLFV in the ISS



Relevant (approximated) loop functions for Option 2:

$$\left. \begin{aligned}
 G_{\gamma}^{\beta\alpha} &\approx \eta_{\alpha\beta} + \mathcal{O}\left(\frac{Y\mu_0}{M_0}, \frac{\mu_0}{M_0}\right) \\
 F_{\gamma}^{\beta\alpha} &\approx -2 \left(\frac{7}{12} + \frac{1}{6} \log x_0 \right) \eta_{\alpha\beta} + \mathcal{O}\left(\frac{Y\mu_0}{M_0}, \frac{m\mu_0}{M_0}\right) \\
 F_Z^{\beta\alpha} &\approx \eta_{\alpha\beta} (5 - 3 \log x_0) + \mathcal{O}\left(\frac{Y\mu_0}{M_0}, \frac{\mu_0}{M_0}\right)
 \end{aligned} \right\} \text{Z Penguin}$$

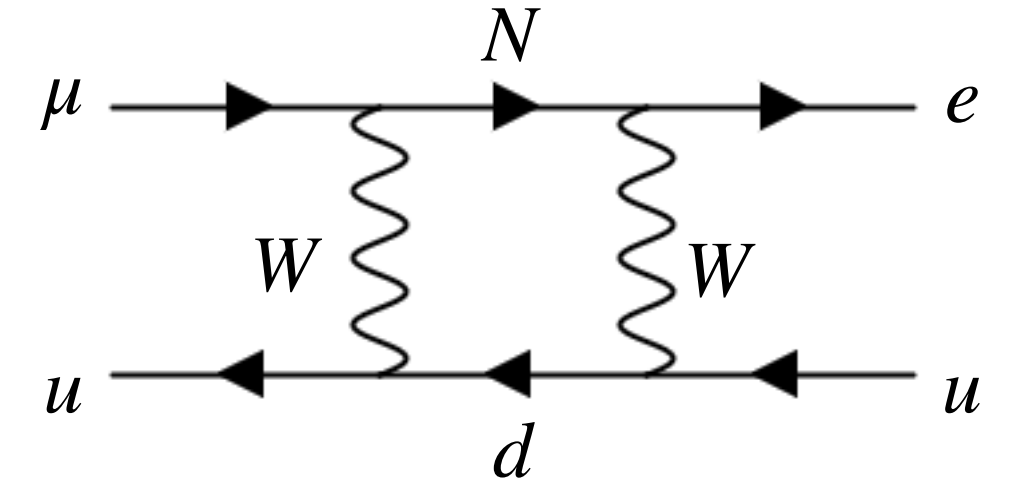
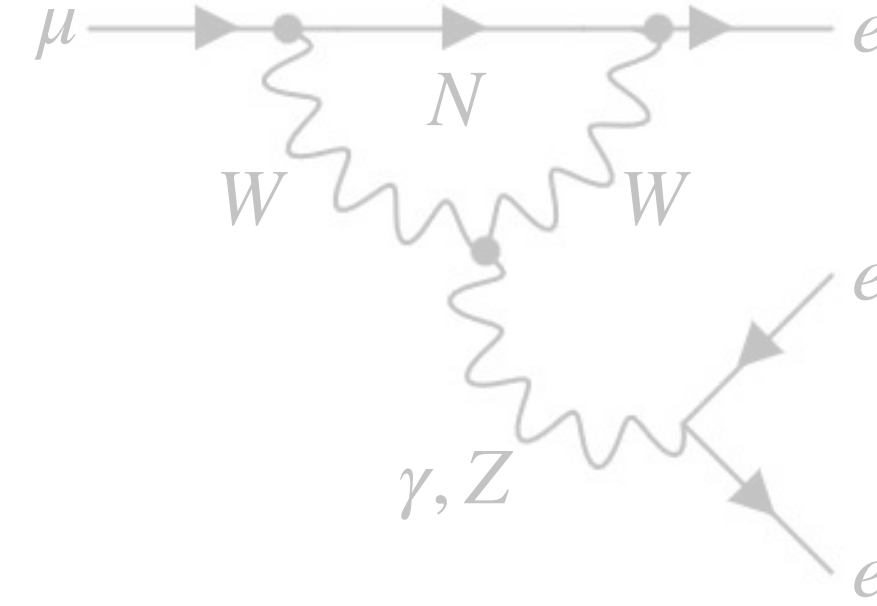
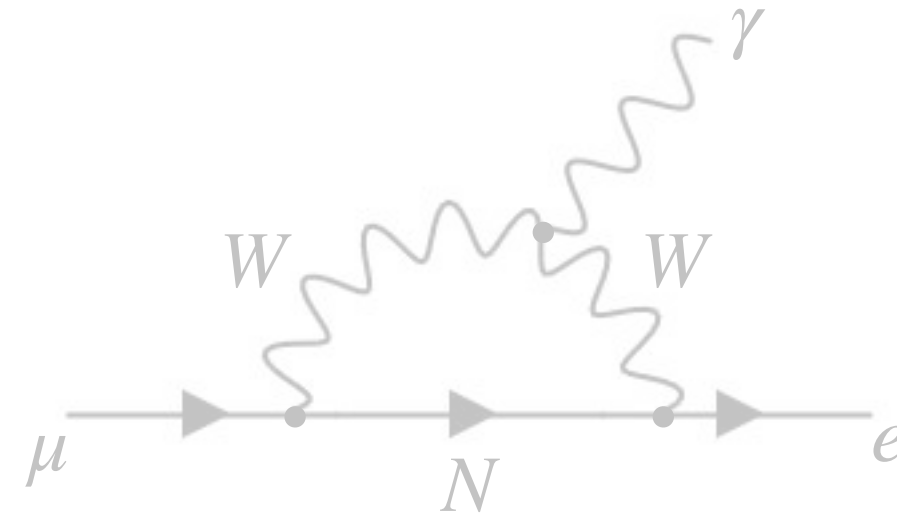
$$F_{box}^{\beta3\alpha} \approx -2\eta_{\alpha\beta} + \mathcal{O}\left(\frac{Y^2\mu_0}{M_0}, \frac{\mu_0^2}{M_0^2}\right)$$

$$F_{box}^{\mu e u u} = 2\eta_{e\mu} \left[-4 - |V_{ub}|^2 (F_{box}(0, x_b) - F_{box}(x_0, x_b) - 4) \right]$$

$$F_{box}^{\mu e d d} = 2\eta_{e\mu} \left[1 - |V_{td}|^2 (F_{Xbox}(0, x_t) - F_{Xbox}(x_0, x_t) + 1) \right]$$

Option 2

cLFV in the ISS



Relevant (approximated) loop functions for Option 2:

$$G_{\gamma}^{\beta\alpha} \approx \eta_{\alpha\beta} + \mathcal{O}\left(\frac{Y\mu_0}{M_0}, \frac{\mu_0}{M_0}\right)$$

$$F_{\gamma}^{\beta\alpha} \approx -2 \left(\frac{7}{12} + \frac{1}{6} \log x_0 \right) \eta_{\alpha\beta} + \mathcal{O}\left(\frac{Y\mu_0}{M_0}, \frac{m\mu_0}{M_0}\right)$$

$$F_Z^{\beta\alpha} \approx \eta_{\alpha\beta} (5 - 3 \log x_0) + \mathcal{O}\left(\frac{Y\mu_0}{M_0}, \frac{\mu_0}{M_0}\right)$$

$$F_{box}^{\beta3\alpha} \approx -2\eta_{\alpha\beta} + \mathcal{O}\left(\frac{Y^2\mu_0}{M_0}, \frac{\mu_0^2}{M_0^2}\right)$$

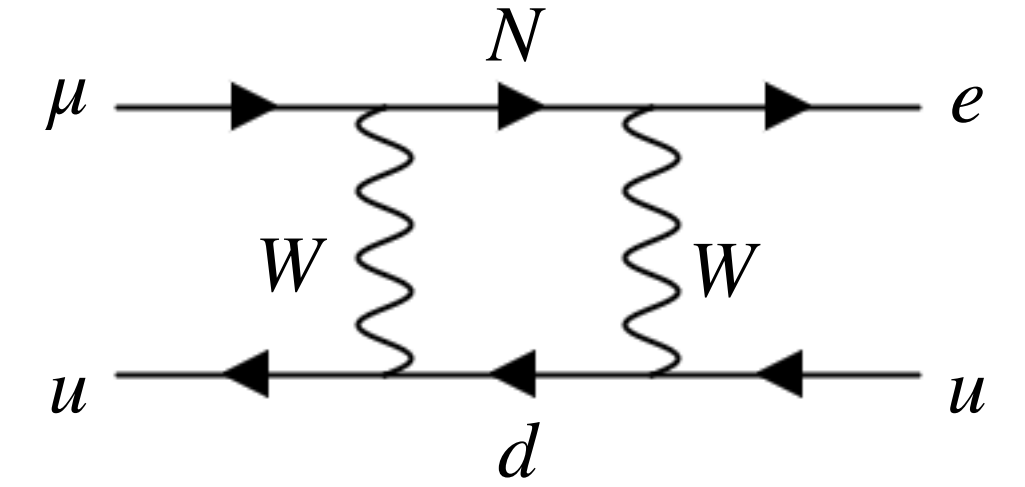
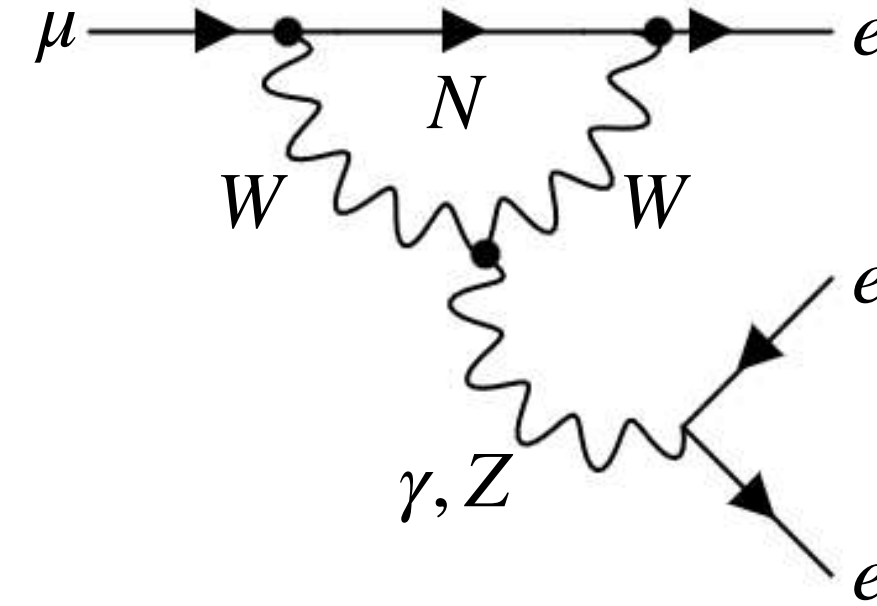
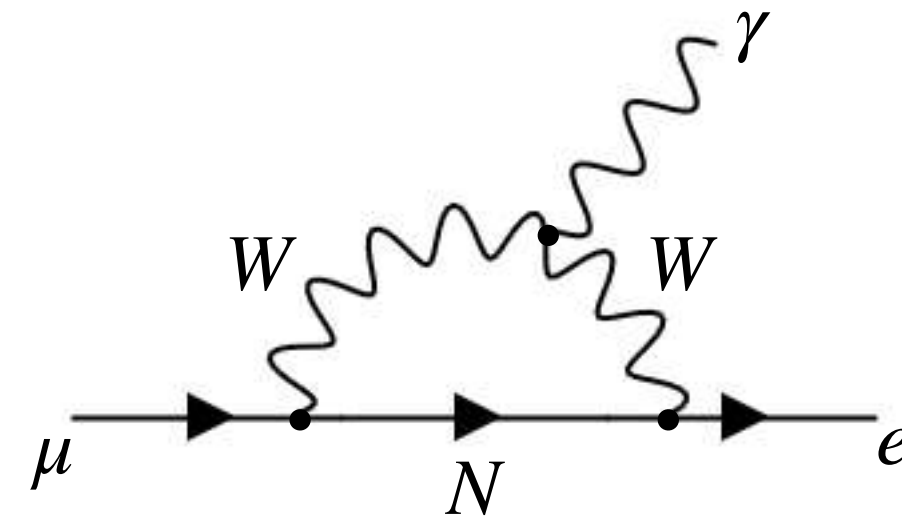
$$F_{box}^{\mu e u u} = 2\eta_{e\mu} \left[-4 - |V_{ub}|^2 (F_{box}(0, x_b) - F_{box}(x_0, x_b) - 4) \right]$$

$$F_{box}^{\mu e d d} = 2\eta_{e\mu} \left[1 - |V_{td}|^2 (F_{Xbox}(0, x_t) - F_{Xbox}(x_0, x_t) + 1) \right]$$

Box Diagrams

Option 2

cLFV in the ISS



Relevant (approximated) loop functions for Option 2:

$$\eta_{\alpha\beta}$$

$$\eta_{\alpha\beta}$$

$$\eta_{\alpha\beta}$$

$$\eta_{\alpha\beta}$$

$$\eta_{e\mu}$$

$$\eta_{e\mu}$$

Rates of the processes are proportional to η at LO for Option 2!

$$\eta = \frac{v^2}{4M_0^2} U_L(\theta_L) \text{diag}(y_1^2, y_2^2, y_3^2) U_L(\theta_L)^\dagger$$

Option 2



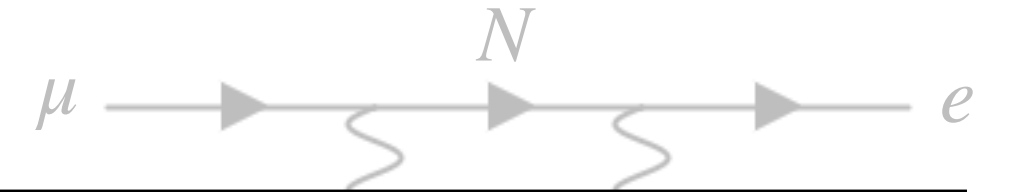
The form of the η matrix elements depends on the particular case:

$$\text{Case 1) } \eta_{e\mu} = \frac{1}{6}\eta'_0 \left[2\Delta y_{21}^2 + \Delta y_{31}^2 \left(-1 + \cos(2\theta_L) - \sqrt{3} \sin(2\theta_L) \right) \right]$$

$$\text{Case 2) } \eta_{\mu e} = \frac{1}{6}\eta'_0 \left[2\Delta y_{21}^2 - \Delta y_{31}^2 \left(1 - \cos(2\theta_L) \cos \phi_u + \sqrt{3} \left(\cos(2\theta_L) \sin \phi_u - i \sin(2\theta_L) \right) \right) \right]$$

$$\text{Case 3) } \eta_{e\mu} = \frac{1}{24}\eta'_0 \left\{ 2(1 + i\sqrt{3})(\Delta y_{21}^2 - 2\Delta y_{31}^2) \sin^2(\phi_m) \xi_2(\pi - \phi_m) + \right. \\ \left. + \Delta y_{21}^2 \left[\cos(2\theta_L)(1 + i\sqrt{3})\xi_1(2\phi_m) + \sqrt{2} \sin(2\theta_L) \left(2\xi_2(\phi_m - 3\phi_s) + i(i + \sqrt{3})\xi_2(\phi_m + 3\phi_s) \right) \right] \right\}$$

Option 2



The form of the η matrix elements depends on the particular case:

$$\text{Case 1)} \quad \eta_{e\mu} = \frac{1}{6}\eta'_0 \left[2\Delta y_{21}^2 + \Delta y_{31}^2 \left(-1 + \cos(2\theta_L) - \sqrt{3} \sin(2\theta_L) \right) \right]$$

$$\text{Case 2)} \quad \eta_{\mu e} = \frac{1}{6}\eta'_0 \left[2\Delta y_{21}^2 - \Delta y_{31}^2 \left(1 - \cos(2\theta_L) \cos \phi_u + \sqrt{3} \left(\cos(2\theta_L) \sin \phi_u - i \sin(2\theta_L) \right) \right) \right]$$

$$\left(\phi_u = \frac{2\pi(2s - t)}{n} \right)$$

$$\text{Case 3)} \quad \eta_{e\mu} = \frac{1}{24}\eta'_0 \left\{ 2(1 + i\sqrt{3})(\Delta y_{21}^2 - 2\Delta y_{31}^2) \sin^2(\phi_m) \xi_2(\pi - \phi_m) + \right. \\ \left. + \Delta y_{21}^2 \left[\cos(2\theta_L)(1 + i\sqrt{3})\xi_1(2\phi_m) + \sqrt{2} \sin(2\theta_L) \left(2\xi_2(\phi_m - 3\phi_s) + i(i + \sqrt{3})\xi_2(\phi_m + 3\phi_s) \right) \right] \right\}$$

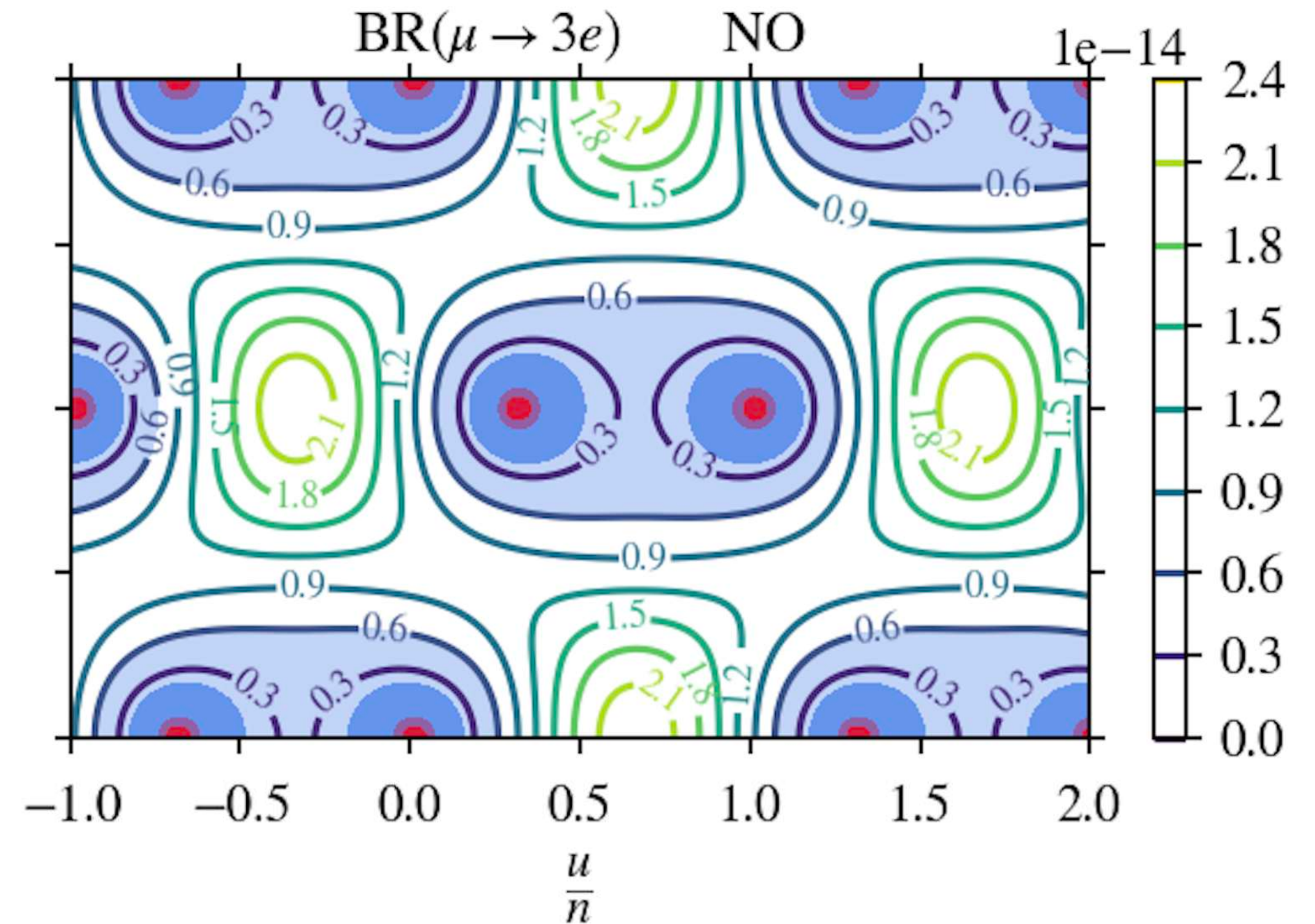
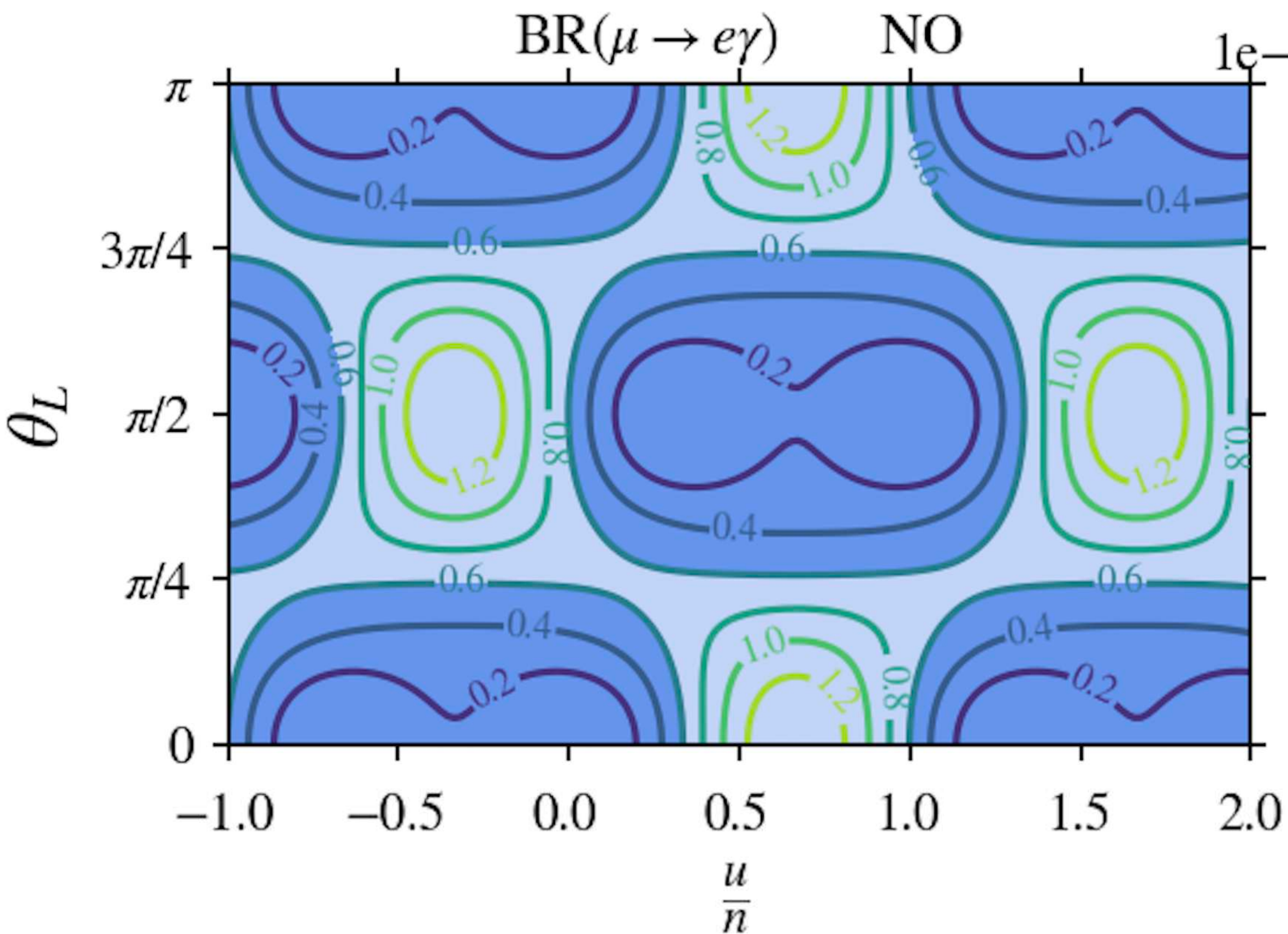
We show some results for Case 2...

Option 2: Case 2

$$M_0 = 3 \text{ TeV}$$

$$\mu_0 = 1 \text{ keV}$$

t even



$$BR(\mu \rightarrow e\gamma) \lesssim 6 \times 10^{-14} \quad \text{Meg-II}$$

$$BR(\mu \rightarrow 3e) \lesssim 20(1) \times 10^{-16} \quad \text{Mu3E Phase-I (II)}$$

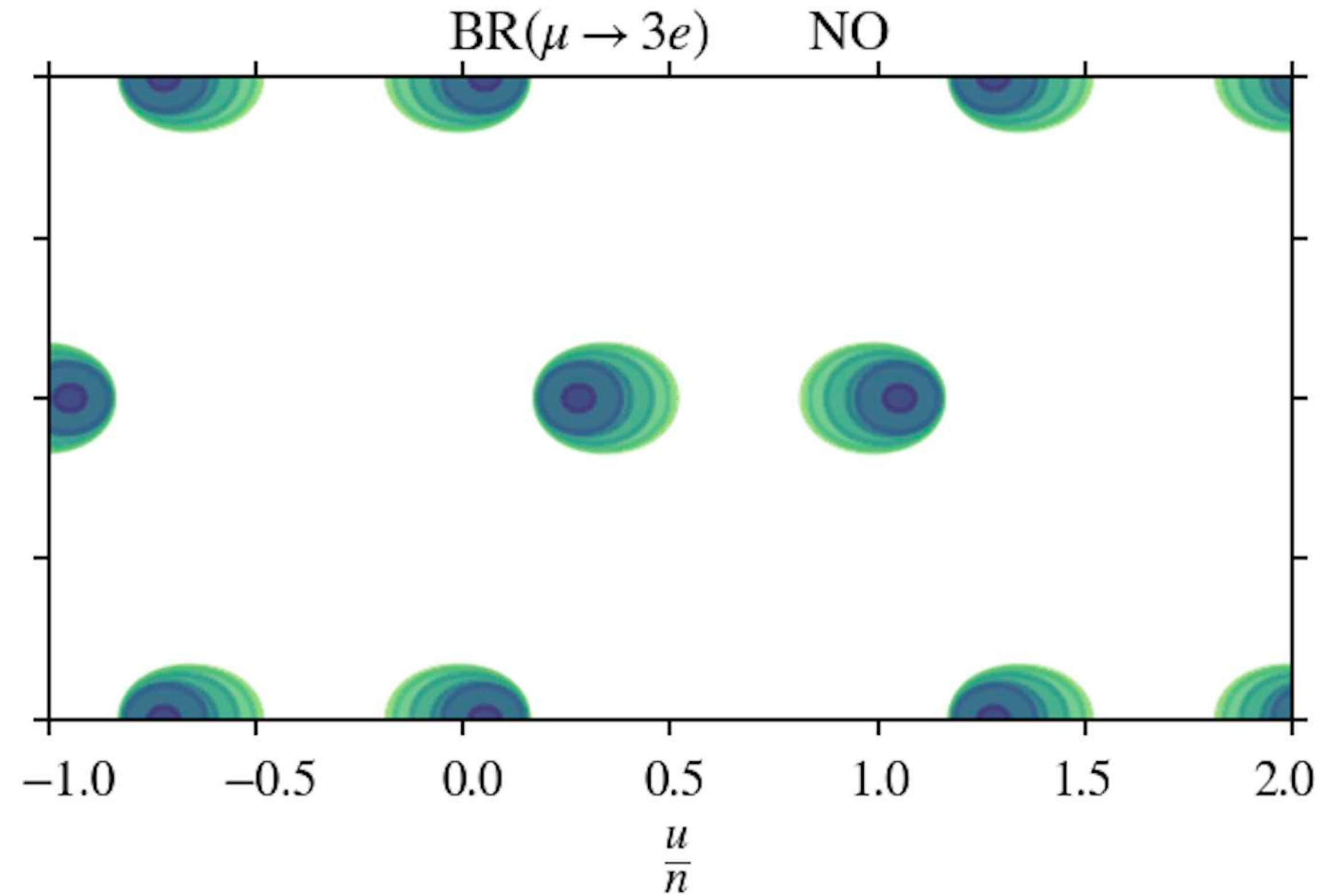
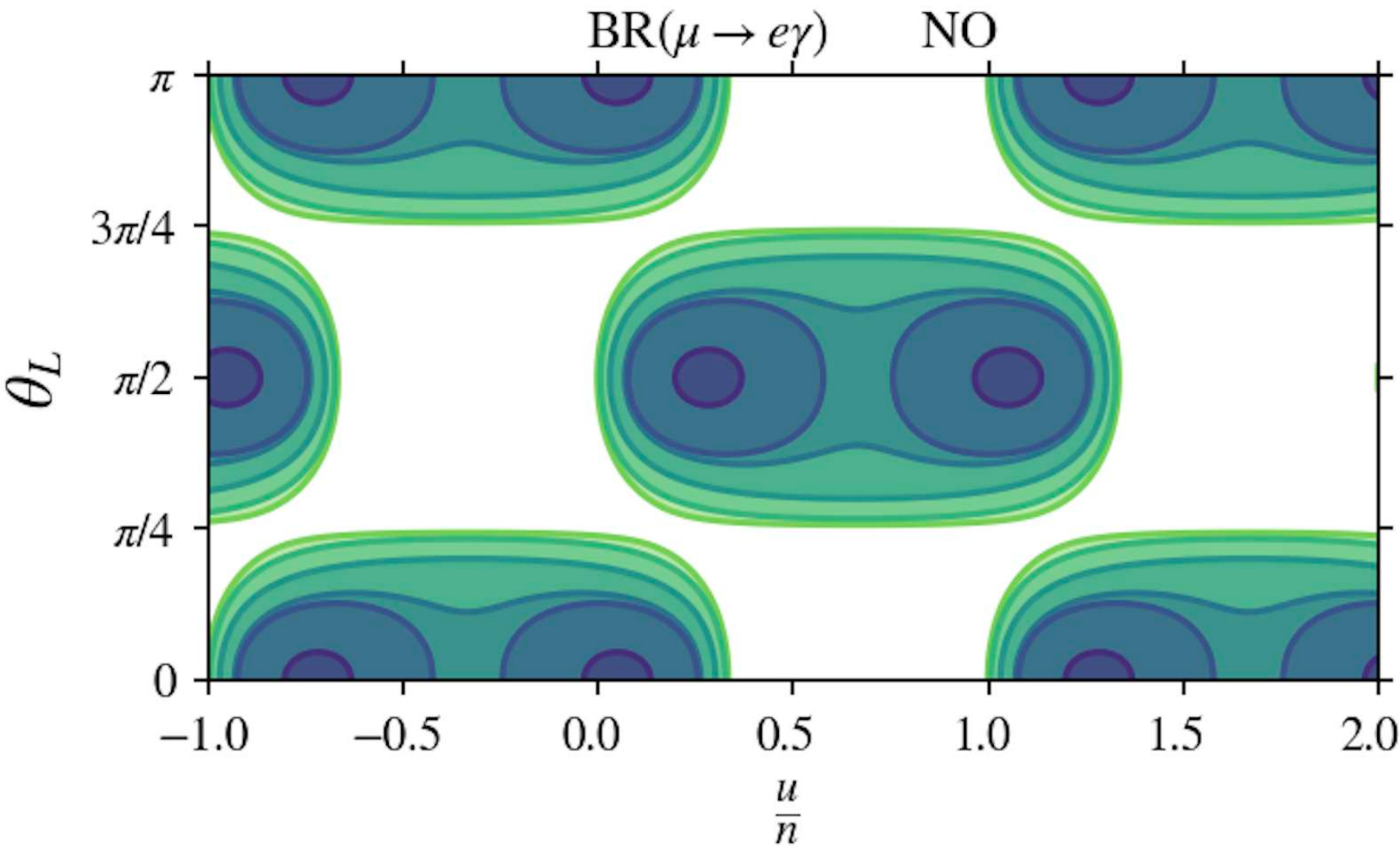
(FPDM, C. Hagedorn, ('24))

Option 2: Case 2

- $\theta_R = 0.785$
- $\theta_R = 0.654$
- $\theta_R = 0.524$
- $\theta_R = 0.393$
- $\theta_R = 0.262$
- $\theta_R = 0.131$

$M_0 = 3 \text{ TeV}$
 $\mu_0 = 1 \text{ keV}$

t odd



$BR(\mu \rightarrow e\gamma) \lesssim 6 \times 10^{-14}$ **Meg-II**

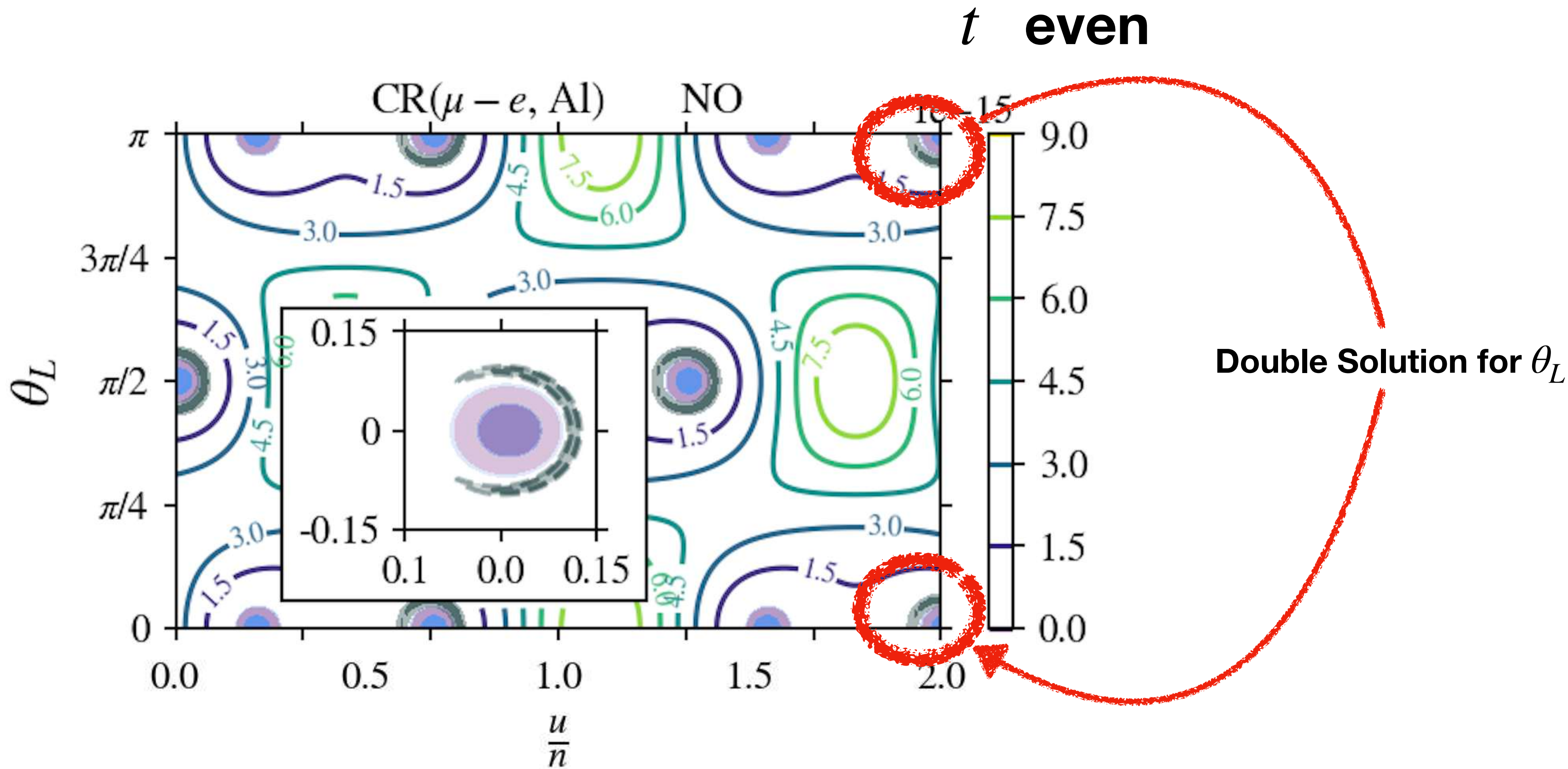
$BR(\mu \rightarrow 3e) \lesssim 20 \times 10^{-16}$ **Mu3E Phase-I (II)**

(FPDM, C. Hagedorn, ('24))

Option 2: Case 2

$$M_0 = 3 \text{ TeV}$$

$$\mu_0 = 1 \text{ keV}$$



$$CR(\mu - e, Al) \lesssim 7.0(8.0) \times 10^{-17} \quad \text{COMET Phase-II (Mu2E)}$$

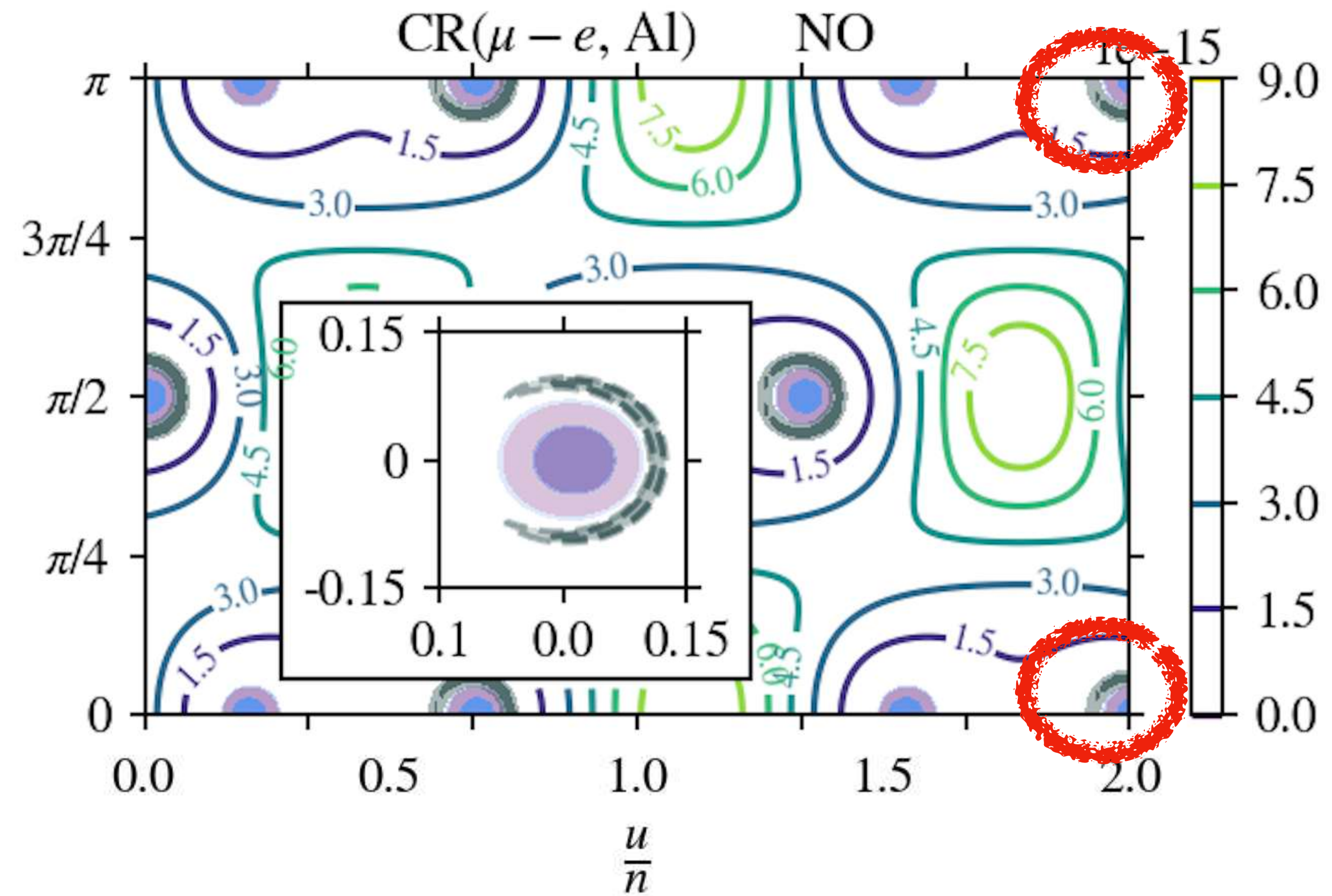
(FPDM, C. Hagedorn, ('24))

Option 2: Case 2

$$M_0 = 3 \text{ TeV}$$

$$\mu_0 = 1 \text{ keV}$$

t even



	$\sin^2 \theta_{12}$	$\sin^2 \theta_{13}$	$\sin^2 \theta_{23}$
$n = 14; s = t = 1$	0.34	0.021(0.022)	0.559(0.561)
$n = 14; s = t = 0$	0.341	0.022	0.5
$n = 14; s = 0; t = 1$	0.34	0.022	0.436
$n = 14; s = 1; t = 2$	0.341	0.022	0.5

$$\tilde{\theta}_L \approx 0.183 \text{ (2.959)}$$

Best fit results: ($\chi_{mix}^2 \leq 12$)

$CR(\mu - e, Al) \lesssim 7.0(8.0) \times 10^{-17}$ **COMET Phase-II (Mu2E)**

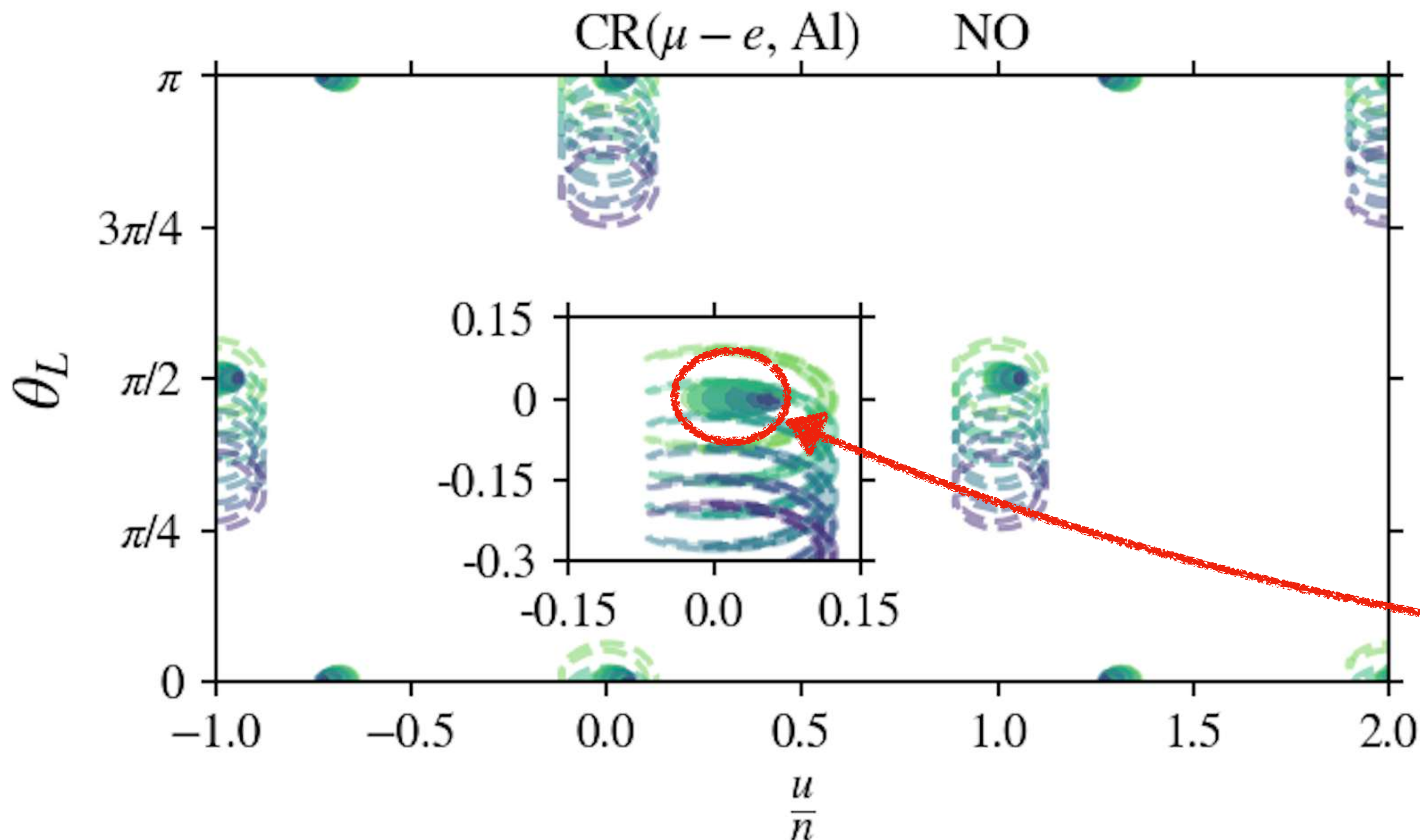
(FPDM, C. Hagedorn, ('24))

Option 2: Case 2

$$M_0 = 3 \text{ TeV}$$

$$\mu_0 = 1 \text{ keV}$$

t odd



θ_R Shifts best-fit regions upward:

$$\tan(\delta_\theta) = - \frac{y_i y_j \cot(2\theta_R)}{y_i^2 + y_j^2}$$

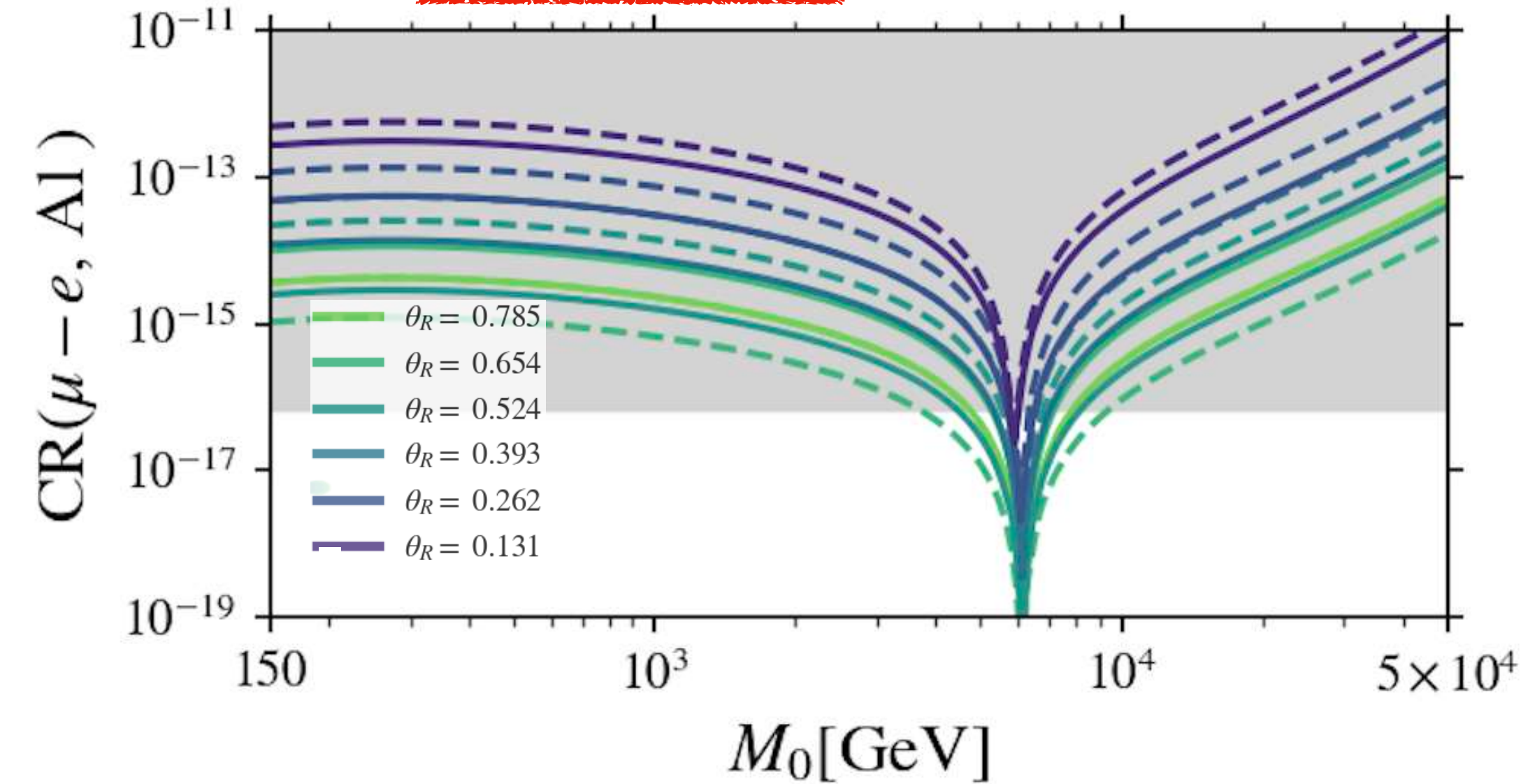
Different choices of θ_R give different predictions for cLFV

$$CR(\mu - e, Al) \lesssim 7.0 \times 10^{-17} \quad \text{COMET Phase-II}$$

(FPDM, C. Hagedorn, ('24))

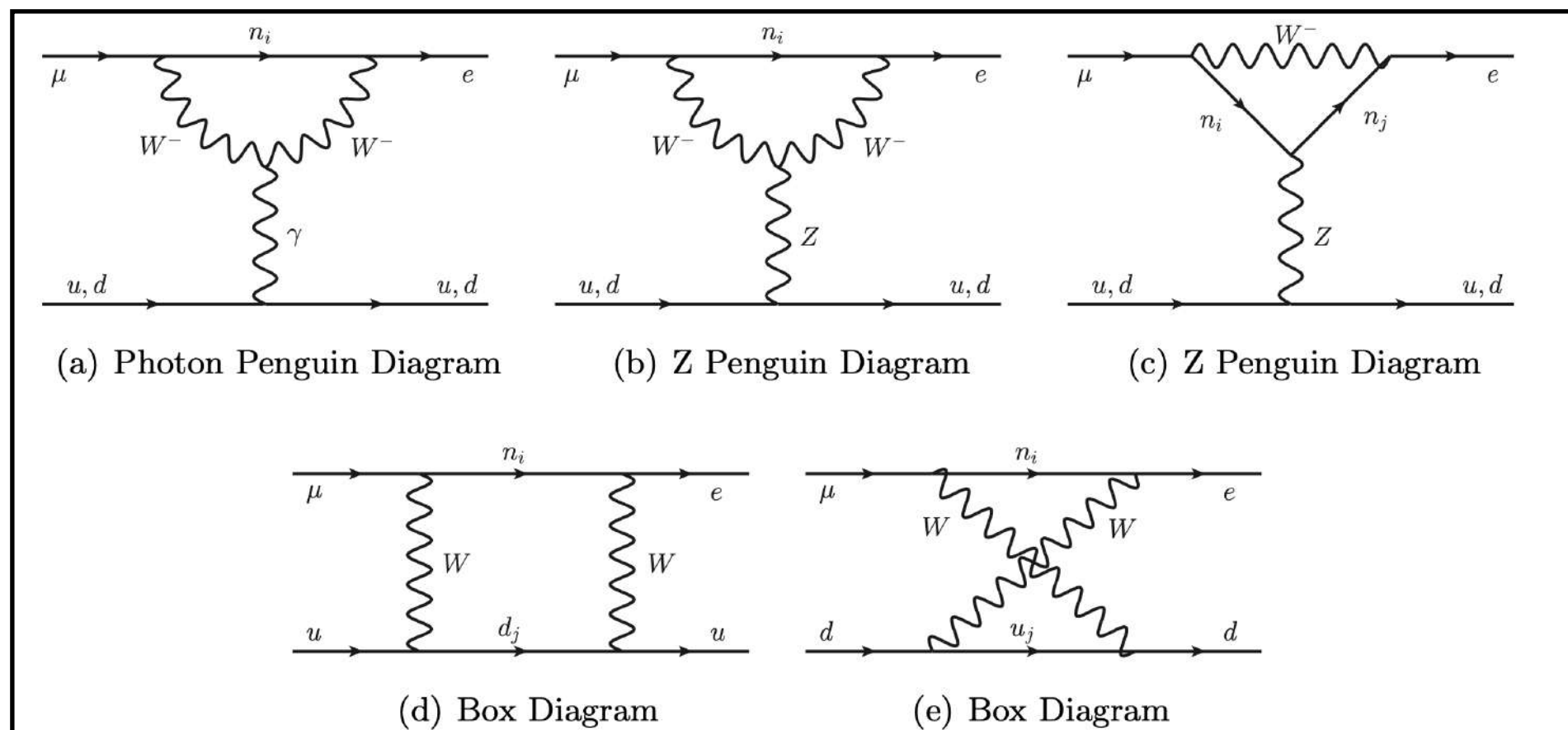
Option 2: Case 2

$$\mu_0 = 1 \text{ keV}$$



Conversion Rate has some interesting properties:

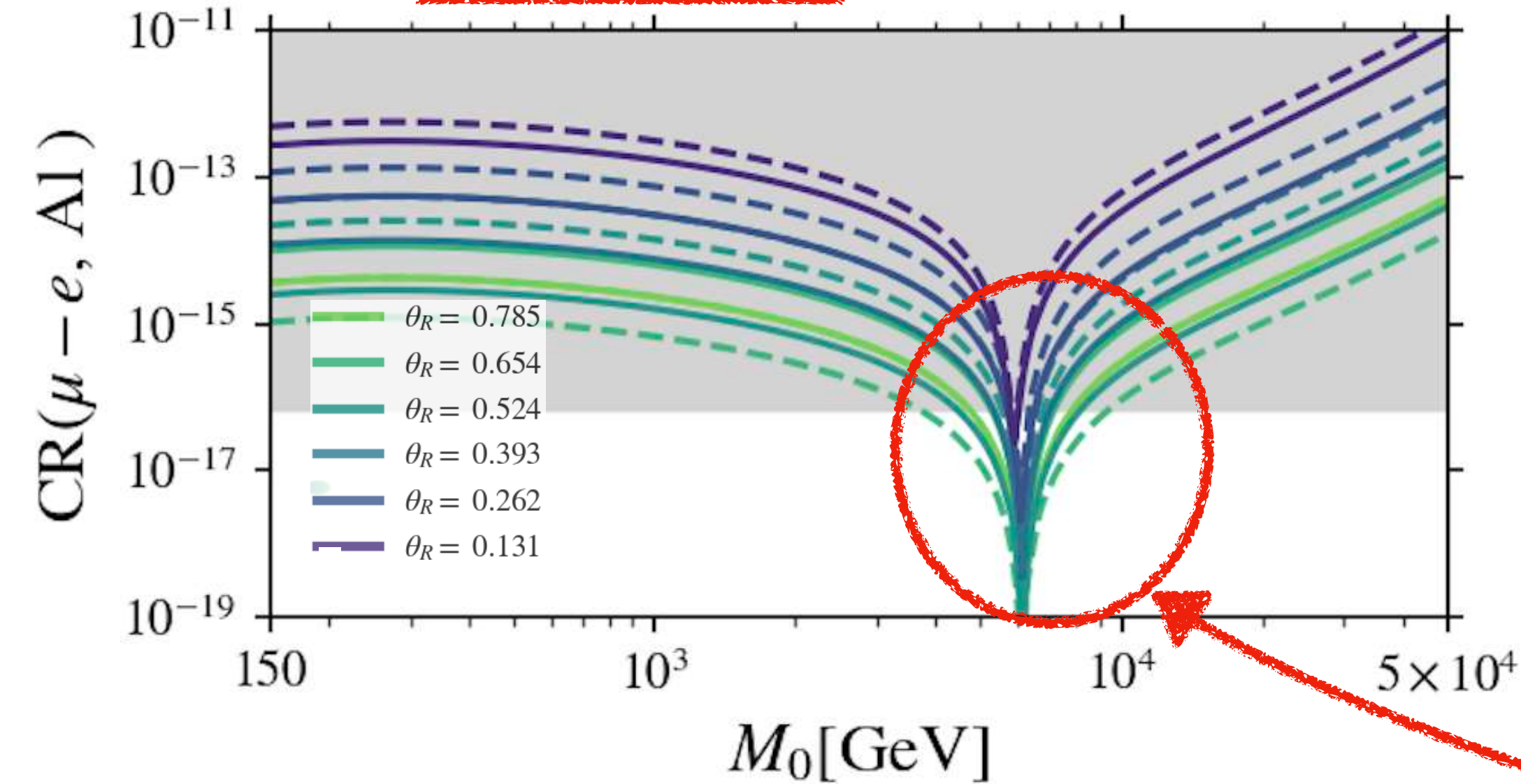
$$CR(\mu - e, Al) = \frac{2G_F^2 \alpha_w^2 m_\mu^5}{(4\pi)^2 \Gamma_{capt}} \left| 4V^{(p)} \left(2\tilde{F}_u^{\mu e} + \tilde{F}_d^{\mu e} \right) + 4V^{(n)} \left(\tilde{F}_u^{\mu e} + 2\tilde{F}_d^{\mu e} \right) + s_w^2 \frac{G_\gamma^{\mu e} D}{2e} \right|^2$$



(R. Alonso, M. Dhen, M. B. Gavela, T. Hambye ('12))

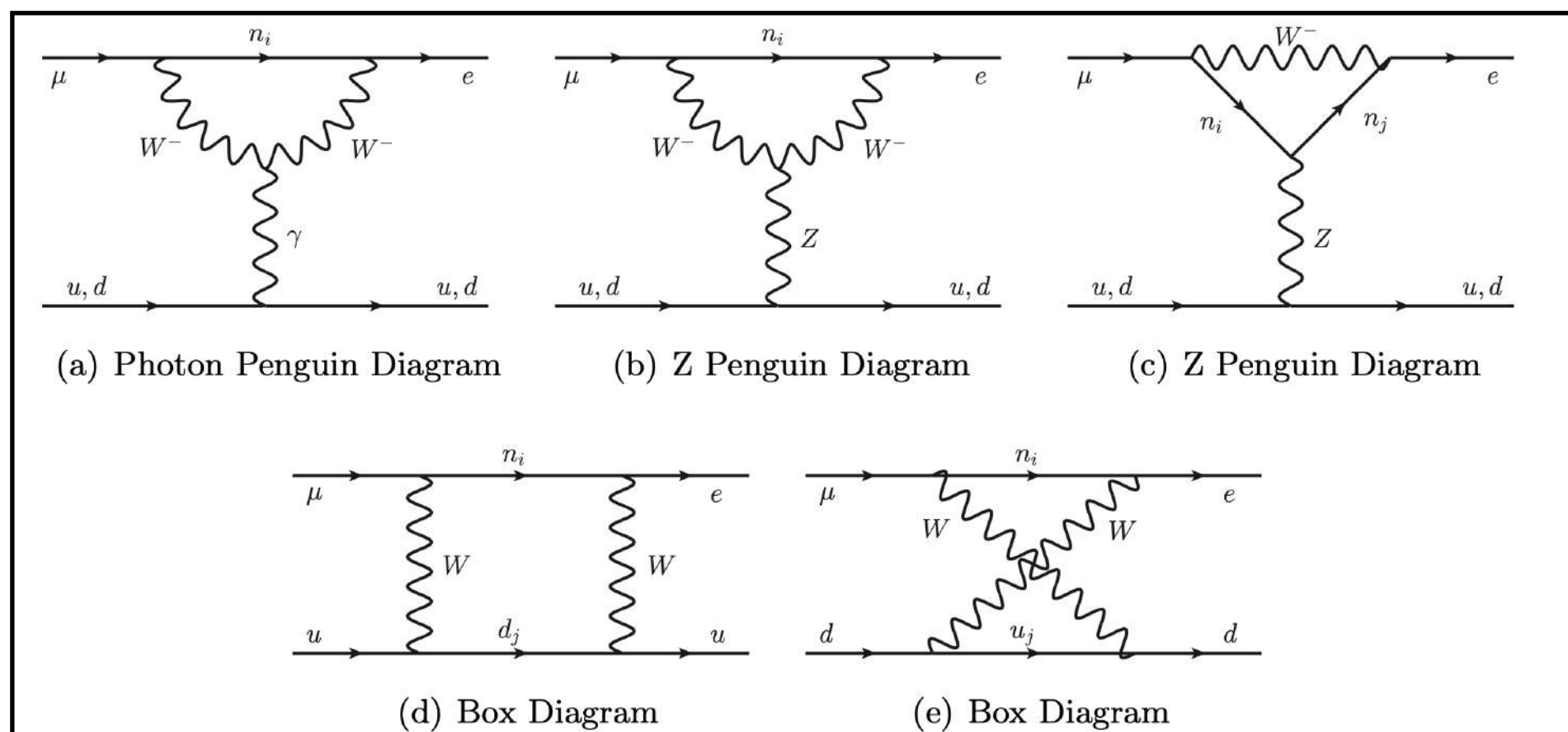
Option 2: Case 2

$$\mu_0 = 1 \text{ keV}$$



Conversion Rate has some interesting properties:

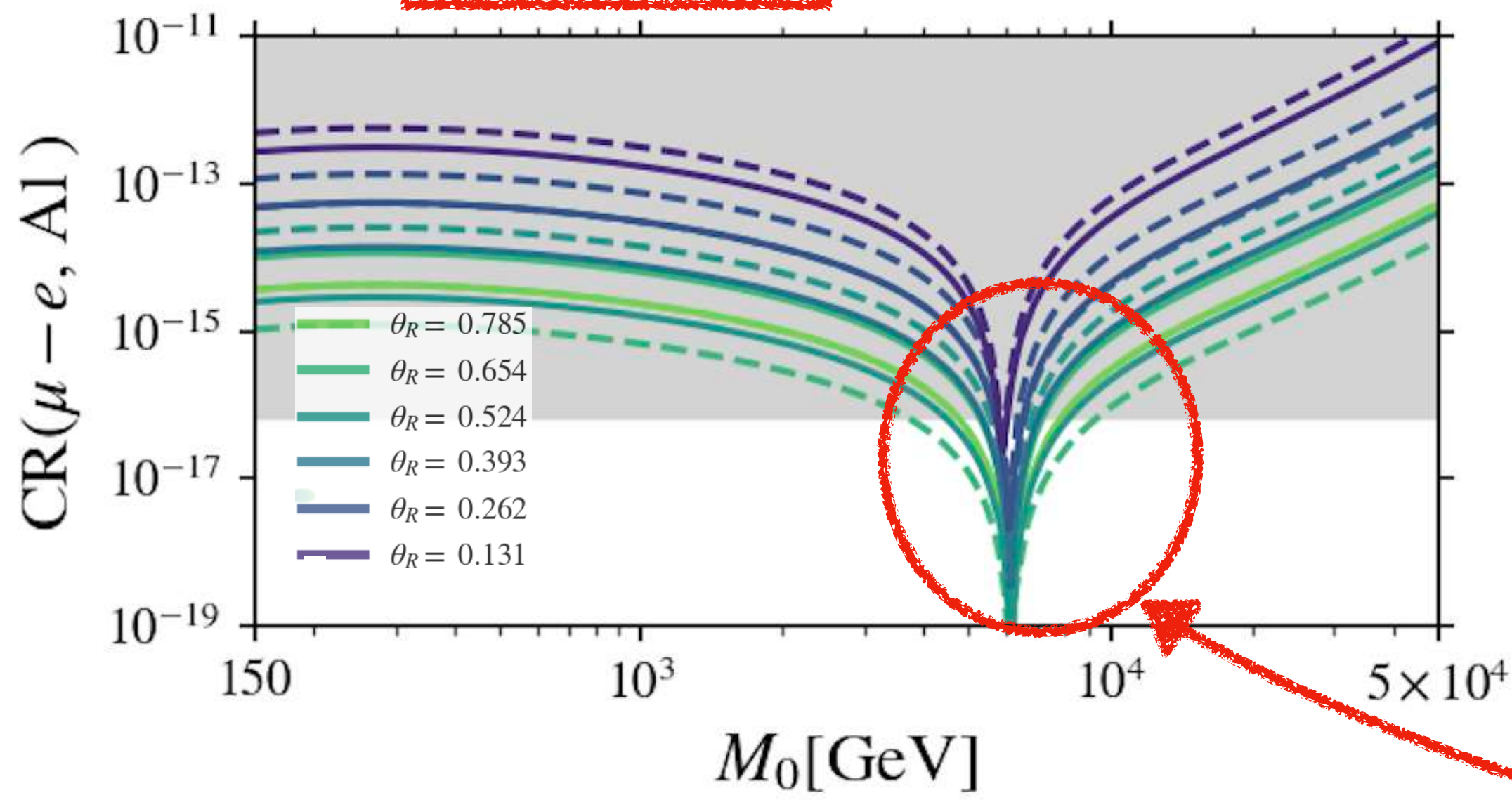
$$CR(\mu - e, Al) = \frac{2G_F^2 \alpha_w^2 m_\mu^5}{(4\pi)^2 \Gamma_{capt}} \left| 4V^{(p)} \left(2\tilde{F}_u^{\mu e} + \tilde{F}_d^{\mu e} \right) + 4V^{(n)} \left(\tilde{F}_u^{\mu e} + 2\tilde{F}_d^{\mu e} \right) + s_w^2 \frac{G_\gamma^{\mu e} D}{2e} \right|^2$$



**Cancellation of the rate:
Doesn't depend on θ_R of μ_0 !**

Option 2: Case 2

$\mu_0 = 1 \text{ keV}$

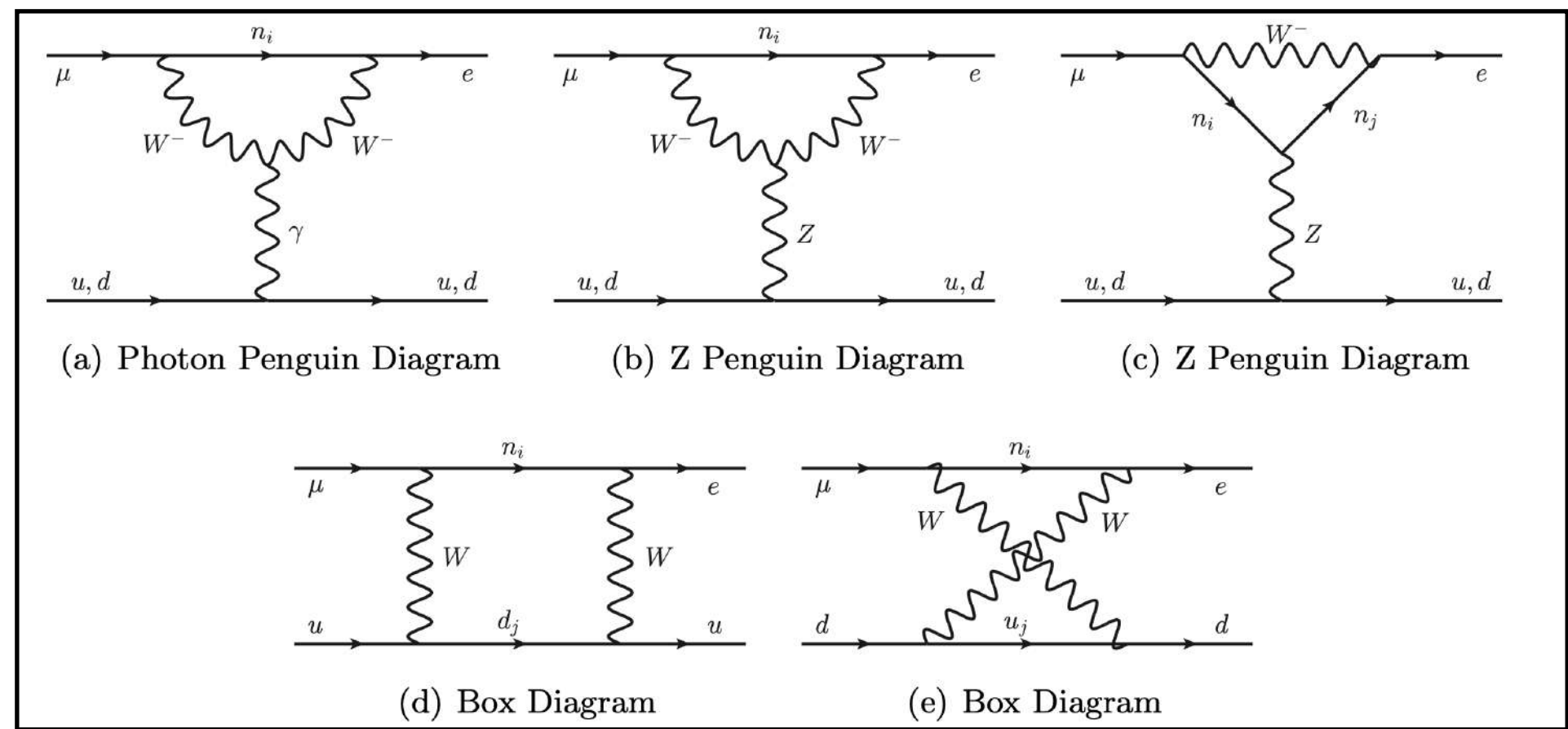


Conversion Rate has some interesting properties:

$$CR(\mu - e, Al) = \frac{2G_F^2 \alpha_w^2 m_\mu^5}{(4\pi)^2 \Gamma_{capt}} \left| 4V^{(p)} \left(2\tilde{F}_u^{\mu e} + \tilde{F}_d^{\mu e} \right) + 4V^{(n)} \left(\tilde{F}_u^{\mu e} + 2\tilde{F}_d^{\mu e} \right) + s_w^2 \frac{G_\gamma^{\mu e} D}{2e} \right|^2$$

Up and down quark contributions have different sign due to different charge and weak isospin

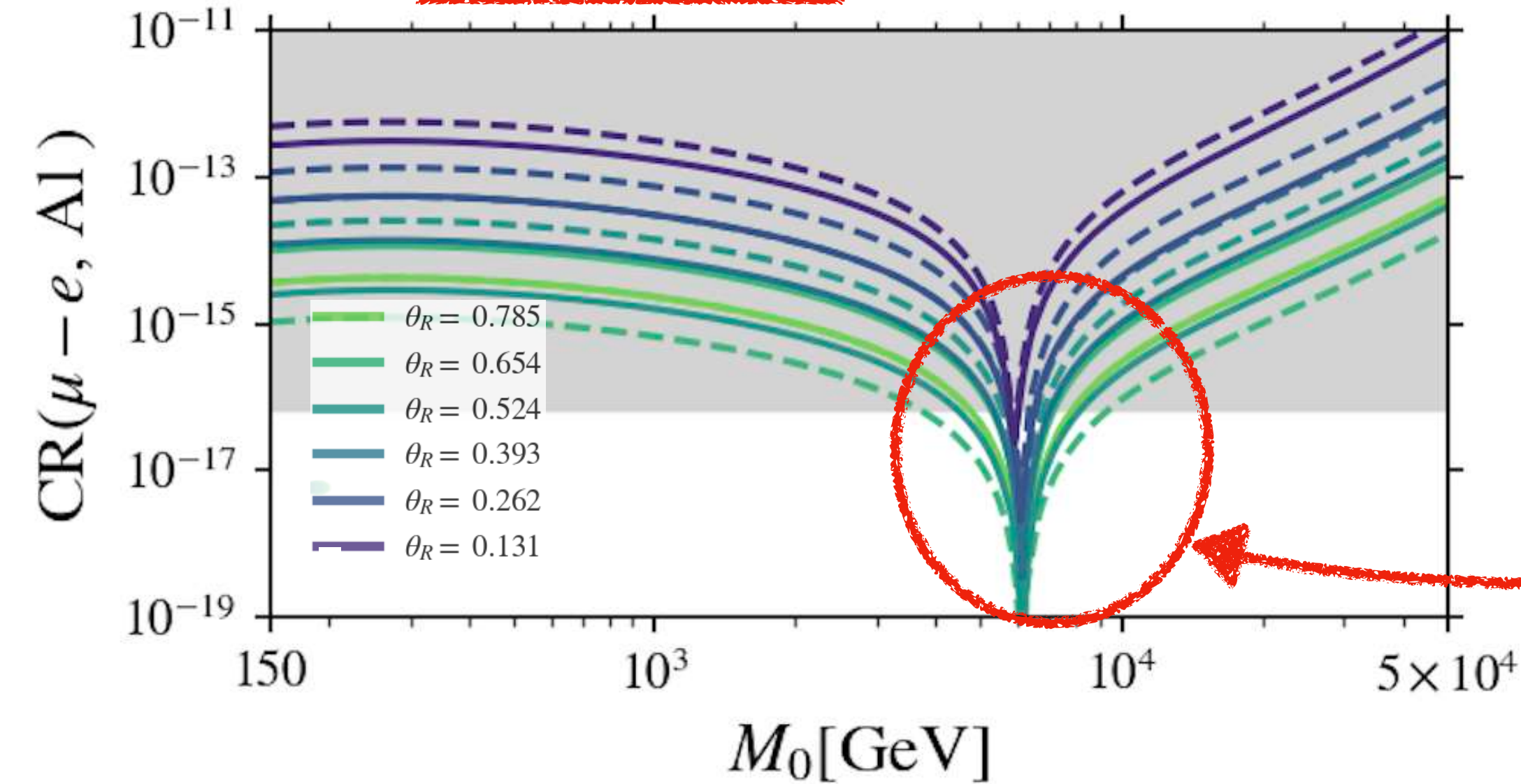
**Cancellation of the rate:
Doesn't depend on θ_R of μ_0 !**



(R. Alonso, M. Dhen, M. B. Gavela, T. Hambye ('12))

Option 2: Case 2

$$\mu_0 = 1 \text{ keV}$$



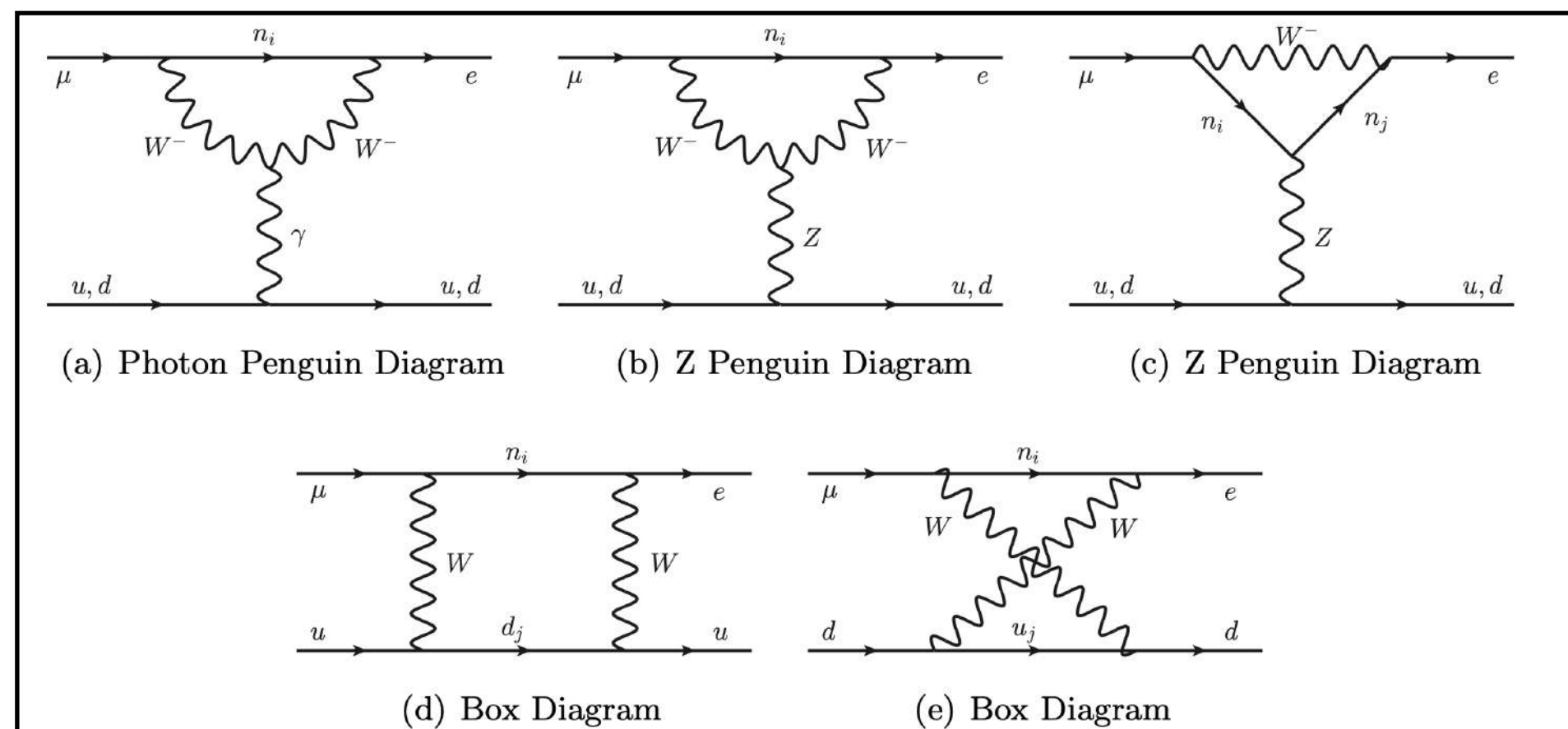
Conversion Rate has some interesting properties:

$$CR(\mu - e, Al) = \frac{2G_F^2 \alpha_w^2 m_\mu^5}{(4\pi)^2 \Gamma_{capt}} \left| 4V^{(p)} \left(2\tilde{F}_u^{\mu e} + \tilde{F}_d^{\mu e} \right) + 4V^{(n)} \left(\tilde{F}_u^{\mu e} + 2\tilde{F}_d^{\mu e} \right) + s_w^2 \frac{G_\gamma^{\mu e} D}{2e} \right|^2$$

$$M_0^2 = \exp \left(\frac{\frac{9}{8} V^{(n)} + \left(\frac{9}{8} + \frac{37}{12} s_w^2 \right) V^{(p)} - \frac{s_w^2}{16e} D}{\frac{3}{8} V^{(n)} + \left(\frac{4s_w^2}{3} - \frac{3}{8} \right) V^{(p)}} \right) M_W^2$$

Due to factorisation of $\eta_{e\mu}$, cancellation of the rate is also independent of the particular case!!

$$x_0^{(canc)} \approx 6470 \Rightarrow M_0^{(canc)} \approx 6.5 \text{ TeV}$$



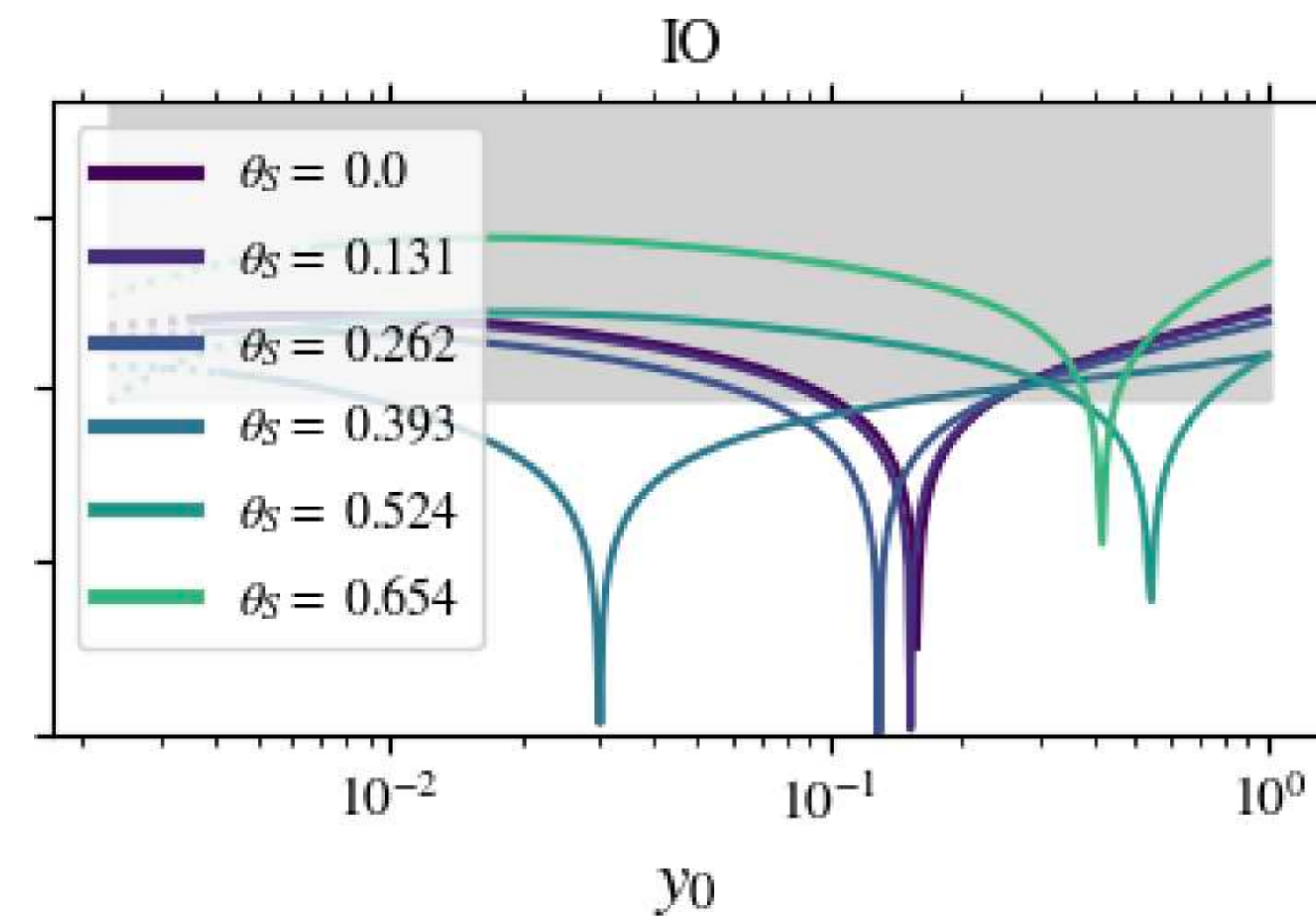
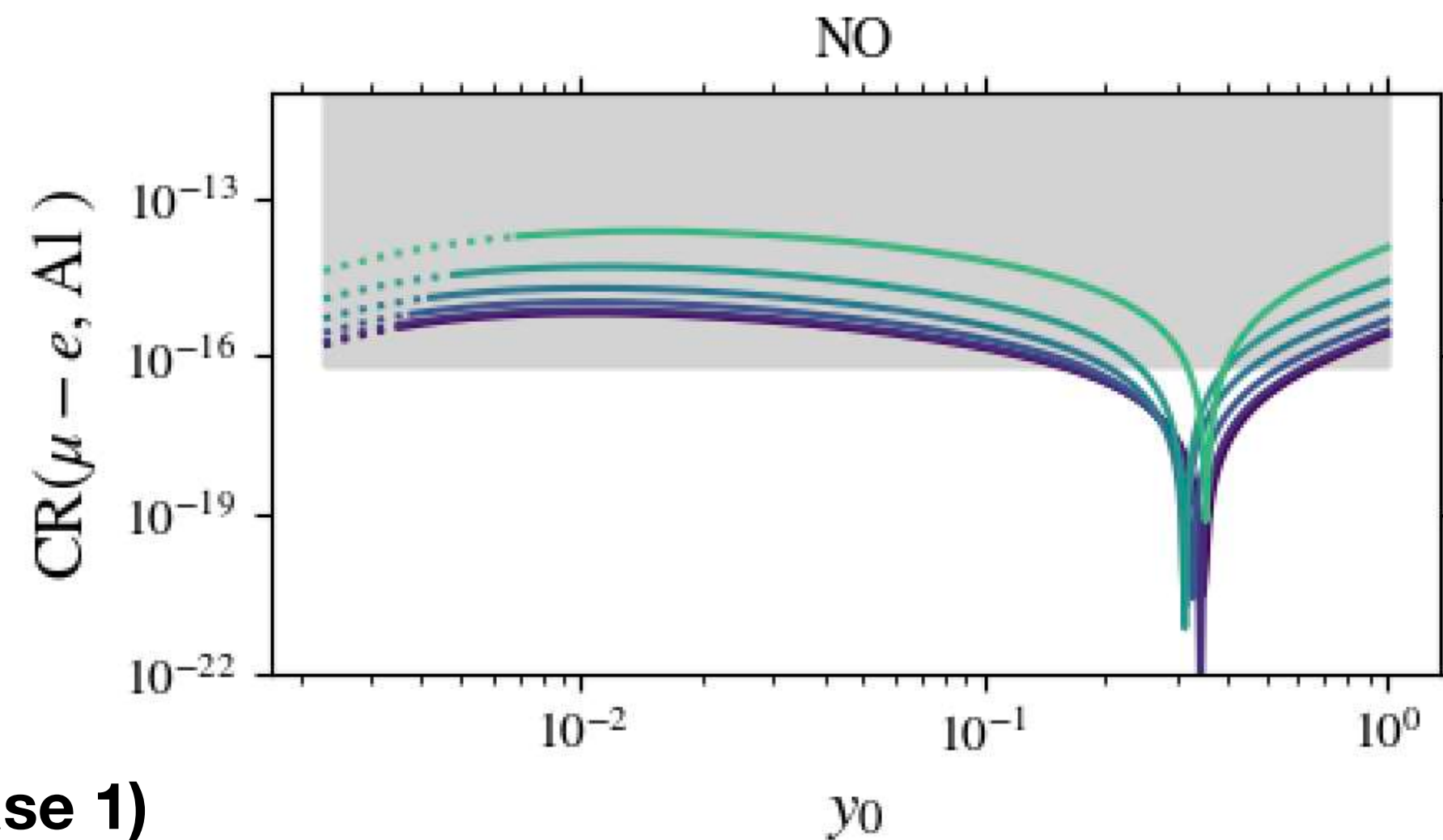
(R. Alonso, M. Dhen, M. B. Gavela, T. Hambye ('12))

Option 3: Decoupling Limit Predictions

In the decoupling limit, we will have $m_1 \rightarrow 0$, $m_3 \rightarrow 0$ for NO and IO.

$$\bar{\chi}^{(NO)} = \exp \left(\frac{\frac{9}{8}V^{(n)} + \left(\frac{9}{8} + \frac{37}{12}s_w^2\right)V^{(p)} - \frac{s_w^2}{16e}D}{\frac{3}{8}V^{(n)} + \left(\frac{4s_w^2}{3} - \frac{3}{8}\right)V^{(p)}} - \frac{r \log \frac{m_2}{m_3}}{r + \frac{m_2}{m_1^2}} \right) \quad \bar{\chi}^{(IO)} = \exp \left(\frac{\frac{9}{8}V^{(n)} + \left(\frac{9}{8} + \frac{37}{12}s_w^2\right)V^{(p)} - \frac{s_w^2}{16e}D}{\frac{3}{8}V^{(n)} + \left(\frac{4s_w^2}{3} - \frac{3}{8}\right)V^{(p)}} + \frac{\frac{m_2}{m_1} \log \frac{m_2}{m_1}}{1 + r - \frac{m_2}{m_1}} \right)$$

Case 1), $n=26, s=1$, ($m_0 \rightarrow 0$)



($\mu_0 = 3 \text{ keV}$)

Case 1)

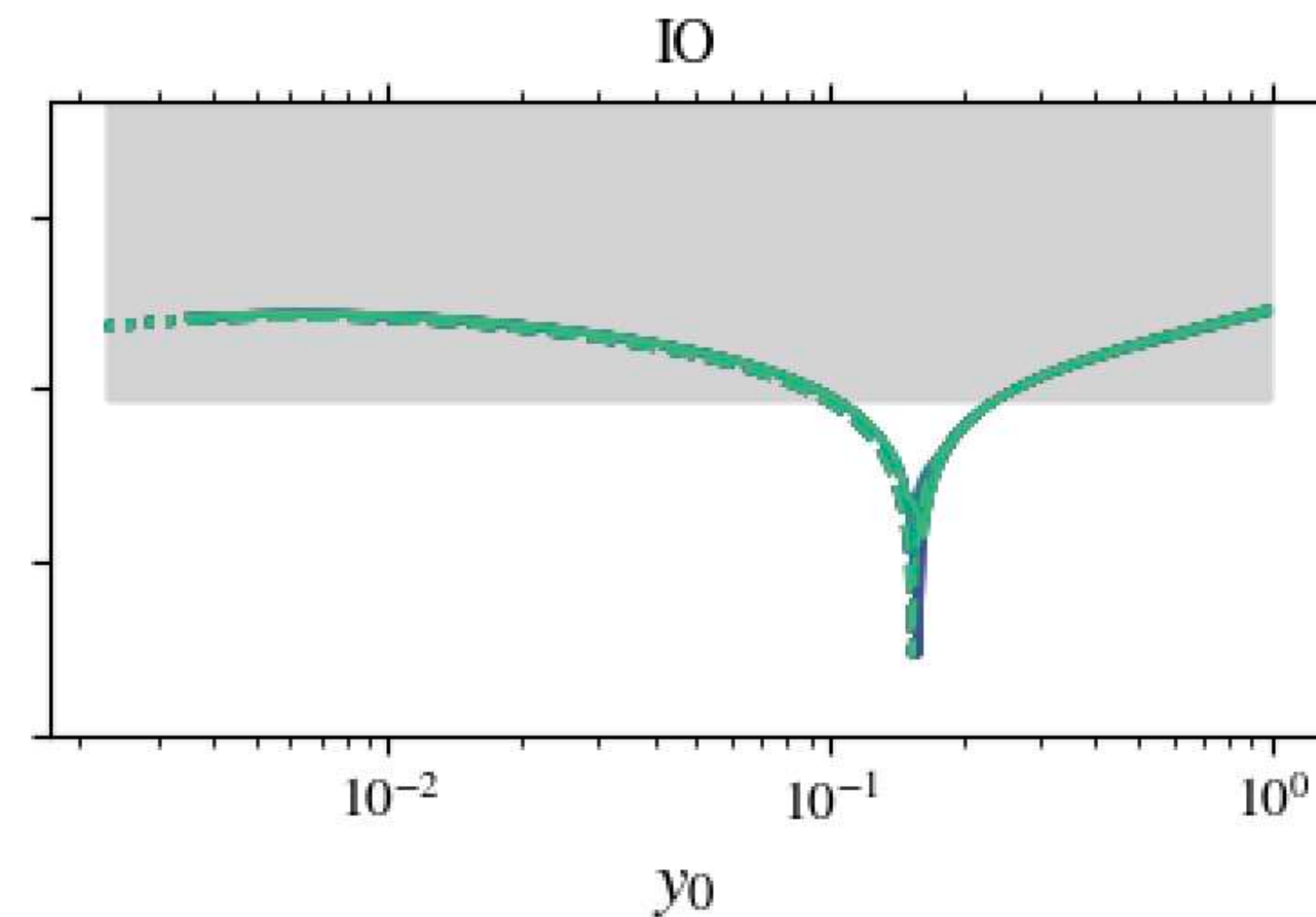
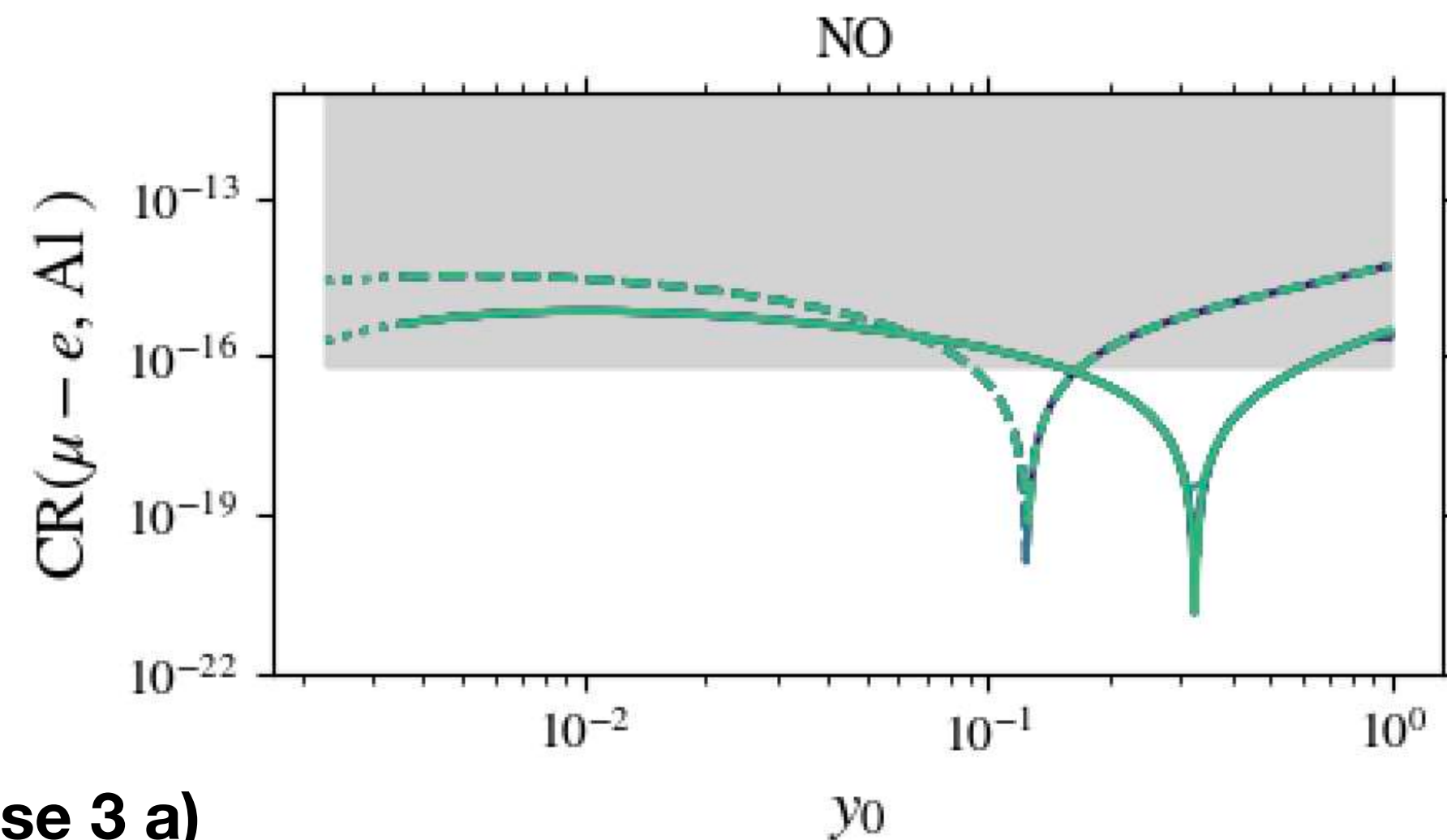
- Stronger dependence on the different values of θ_s than for non-decoupling limit
- Single solution for θ_N

Option 3: Decoupling Limit Predictions

In the decoupling limit, we will have $m_1 \rightarrow 0$, $m_3 \rightarrow 0$ for NO and IO.

$$\bar{\chi}^{(NO)} = \exp \left(\frac{\frac{9}{8}V^{(n)} + \left(\frac{9}{8} + \frac{37}{12}s_w^2\right)V^{(p)} - \frac{s_w^2}{16e}D}{\frac{3}{8}V^{(n)} + \left(\frac{4s_w^2}{3} - \frac{3}{8}\right)V^{(p)}} - \frac{r \log \frac{m_2}{m_3}}{r + \frac{m_2}{m_1^2}} \right) \quad \bar{\chi}^{(IO)} = \exp \left(\frac{\frac{9}{8}V^{(n)} + \left(\frac{9}{8} + \frac{37}{12}s_w^2\right)V^{(p)} - \frac{s_w^2}{16e}D}{\frac{3}{8}V^{(n)} + \left(\frac{4s_w^2}{3} - \frac{3}{8}\right)V^{(p)}} + \frac{\frac{m_2}{m_1} \log \frac{m_2}{m_1}}{1 + r - \frac{m_2}{m_1}} \right)$$

Case 3 a), $n = 34, m = 2, s = 0$, ($m_0 \rightarrow 0$)



($\mu_0 = 3 \text{ keV}$)

Case 3 a)

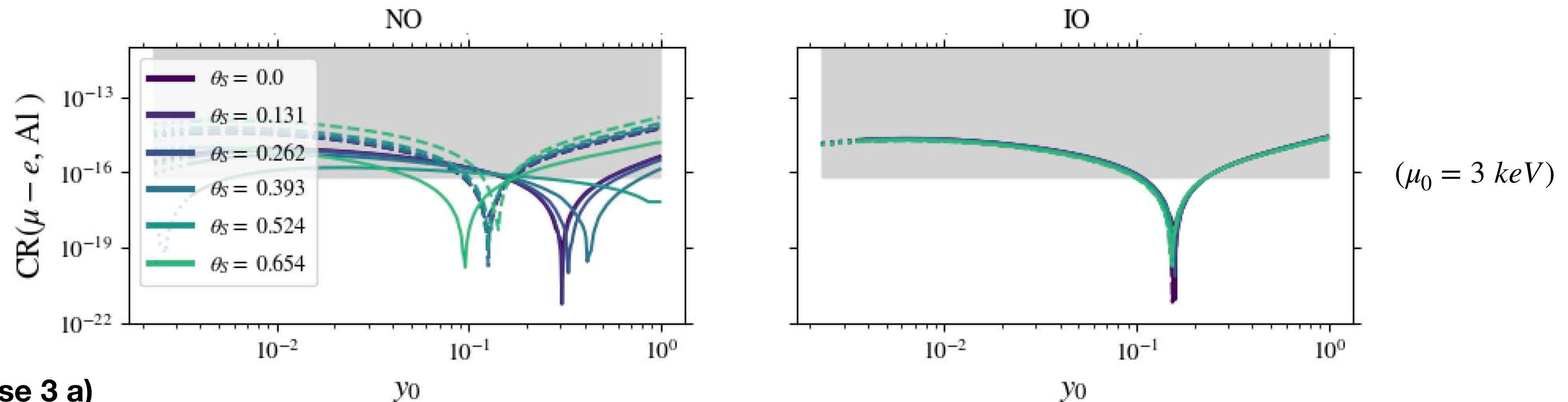
- Double solution for θ_N results in different values of r
- Effect is strongly visible in the decoupling limit, and only for NO.

Option 3: Decoupling Limit Predictions

In the decoupling limit, we will have $m_1 \rightarrow 0$, $m_3 \rightarrow 0$ for NO and IO.

$$\bar{\chi}^{(NO)} = \exp \left(\frac{\frac{9}{8}V^{(n)} + \left(\frac{9}{8} + \frac{37}{12}s_w^2\right)V^{(p)} - \frac{s_w^2}{16e}D}{\frac{3}{8}V^{(n)} + \left(\frac{4s_w^2}{3} - \frac{3}{8}\right)V^{(p)}} - \frac{r \log \frac{m_2}{m_3}}{r + \frac{m_2}{m_1^2}} \right) \quad \bar{\chi}^{(IO)} = \exp \left(\frac{\frac{9}{8}V^{(n)} + \left(\frac{9}{8} + \frac{37}{12}s_w^2\right)V^{(p)} - \frac{s_w^2}{16e}D}{\frac{3}{8}V^{(n)} + \left(\frac{4s_w^2}{3} - \frac{3}{8}\right)V^{(p)}} + \frac{\frac{m_2}{m_1} \log \frac{m_2}{m_1}}{1 + r - \frac{m_2}{m_1}} \right)$$

Case 3 a), $n = 16, m = 1, s = 0$, ($m_0 \rightarrow 0$)



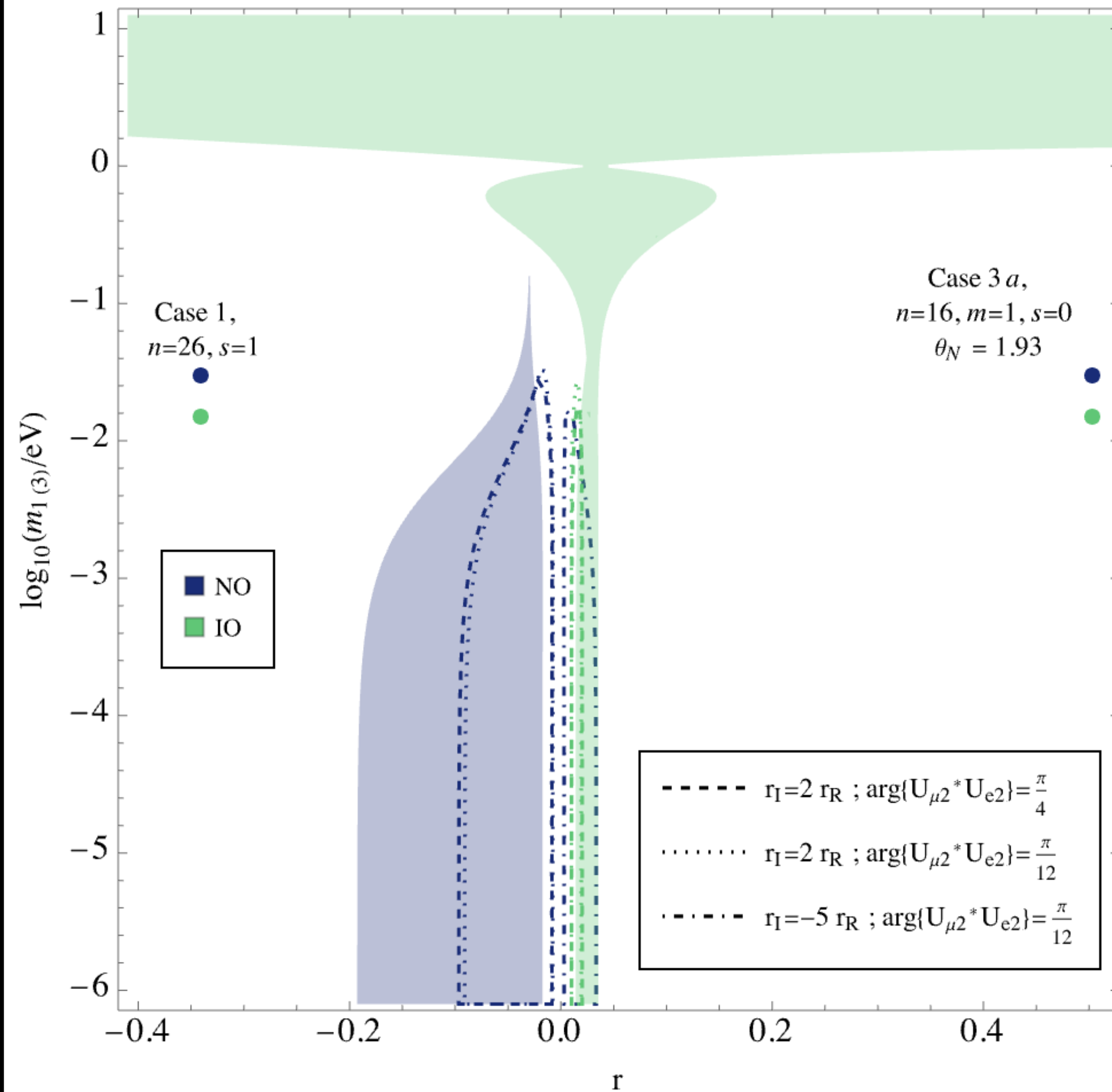
Case 3 a)

- Double solution for θ_N results in different values of r , and dependence on θ_S
- Effect is strongly visible in the decoupling limit, and only for NO.

$$\frac{\operatorname{Re} \left\{ U_{\mu 3}^* U_{e 3} \right\}}{\operatorname{Re} \left\{ U_{\mu 2}^* U_{e 2} \right\}} = \frac{\operatorname{Im} \left\{ U_{\mu 3}^* U_{e 3} \right\}}{\operatorname{Im} \left\{ U_{\mu 2}^* U_{e 2} \right\}}, \quad U = U_N(\theta_N)$$

It can be proven that, when a cancellation is not possible, this is replaced by a **local minimum**

Regions in which \bar{X} exists



$$\frac{\operatorname{Re} \left\{ U_{\mu 3}^* U_{e 3} \right\}}{\operatorname{Re} \left\{ U_{\mu 2}^* U_{e 2} \right\}} = \frac{\operatorname{Im} \left\{ U_{\mu 3}^* U_{e 3} \right\}}{\operatorname{Im} \left\{ U_{\mu 2}^* U_{e 2} \right\}}, \quad U = U_N(\theta_N)$$

It can be proven that, when a cancellation is not possible, this is replaced by a **local minimum**

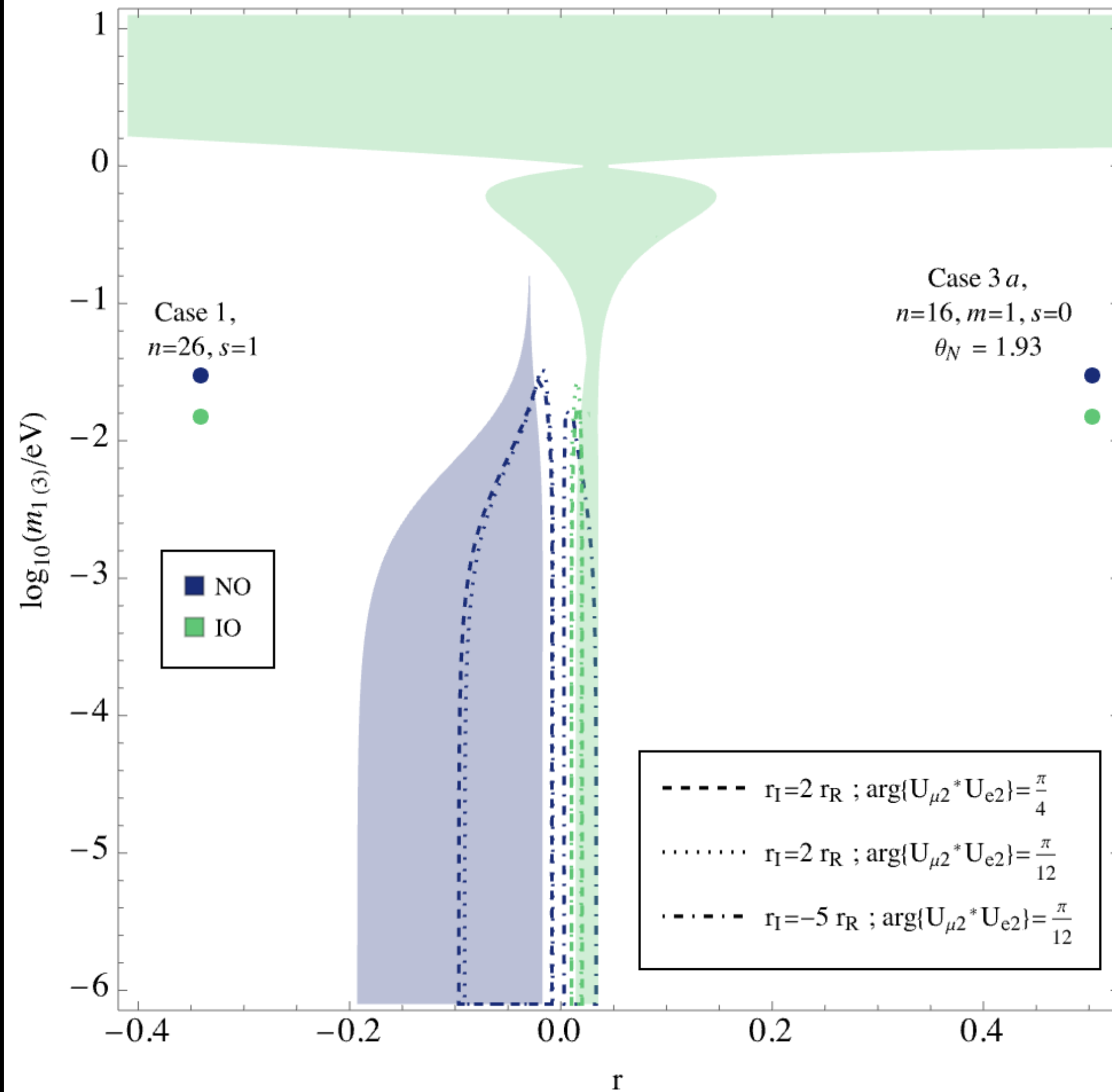
For $BR(\mu \rightarrow e\gamma)$, the cancellation happens for :

$$\bar{X} = -3 \frac{-1 + w_2^2 + r(-1 + w_3^2)}{-1 + w_2 + r(-1 + w_3)}$$

$$\cdot W \left(-e^{\frac{11}{6}} \frac{-1 + w_2 + r(-1 + w_3)}{3(-1 + w_2^2 + r(-1 + w_3^2))} w_2^{-\frac{w_2^2}{-1 + w_2^2 + r(-1 + w_3^2)}} w_3^{-\frac{r w_3^2}{-1 + w_2^2 + r(-1 + w_3^2)}} \right)$$

$$w_2 = \frac{m_2}{m_1} \quad w_3 = \frac{m_3}{m_1}$$

Regions in which \bar{X} exists



$$\frac{\operatorname{Re} \left\{ U_{\mu 3}^* U_{e 3} \right\}}{\operatorname{Re} \left\{ U_{\mu 2}^* U_{e 2} \right\}} = \frac{\operatorname{Im} \left\{ U_{\mu 3}^* U_{e 3} \right\}}{\operatorname{Im} \left\{ U_{\mu 2}^* U_{e 2} \right\}}, \quad U = U_N(\theta_N)$$

It can be proven that, when a cancellation is not possible, this is replaced by a **local minimum**

For $BR(\mu \rightarrow e\gamma)$, the cancellation happens for :

$$\bar{X} = -3 \frac{-1 + w_2^2 + r(-1 + w_3^2)}{-1 + w_2 + r(-1 + w_3)}$$

$$\cdot W \left(-e^{\frac{11}{6}} \frac{-1 + w_2 + r(-1 + w_3)}{3(-1 + w_2^2 + r(-1 + w_3^2))} w_2^{-\frac{w_2^2}{-1 + w_2^2 + r(-1 + w_3^2)}} w_3^{-\frac{r w_3^2}{-1 + w_2^2 + r(-1 + w_3^2)}} \right)$$

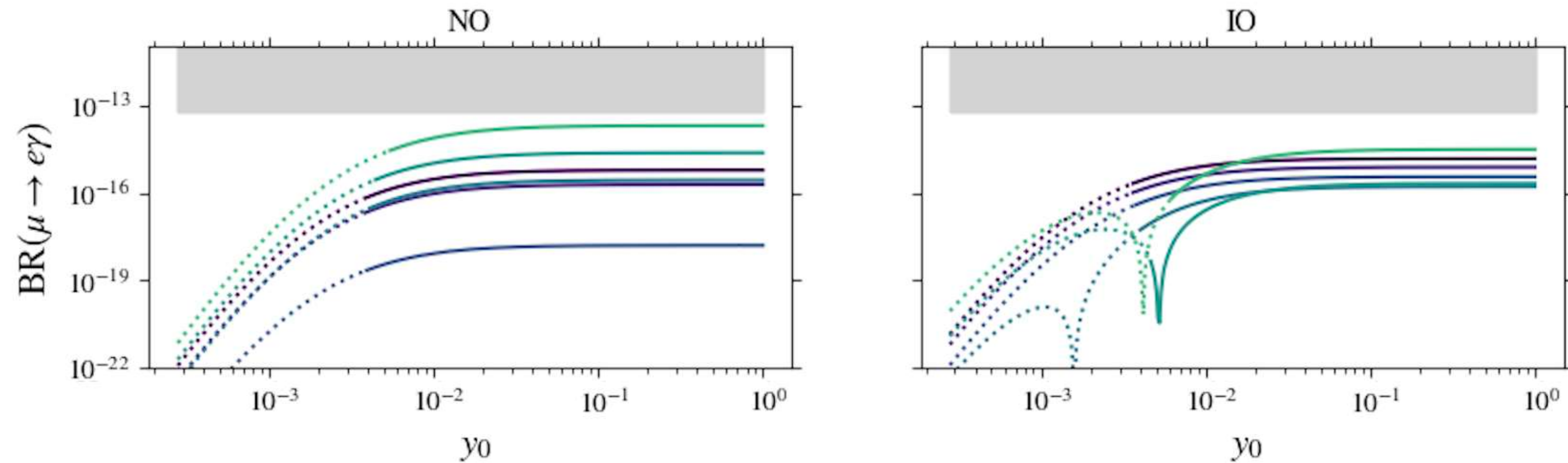
$$w_2 = \frac{m_2}{m_1} \quad w_3 = \frac{m_3}{m_1}$$

Expression of the Location of the local minima is similar but way more involved...

Regions in which \bar{X} exists

$$\frac{\text{Re} \left\{ U_{\mu 3}^* U_{e 3} \right\}}{\text{Re} \left\{ U_{\mu 2}^* U_{e 2} \right\}} = \frac{\text{Im} \left\{ U_{\mu 3}^* U_{e 3} \right\}}{\text{Im} \left\{ U_{\mu 2}^* U_{e 2} \right\}}, \quad U = U_N(\theta_N)$$

Case 3 b.1), $n = 20, m = 11, s = 0$



$(\mu_0 = 3 \text{ keV})$

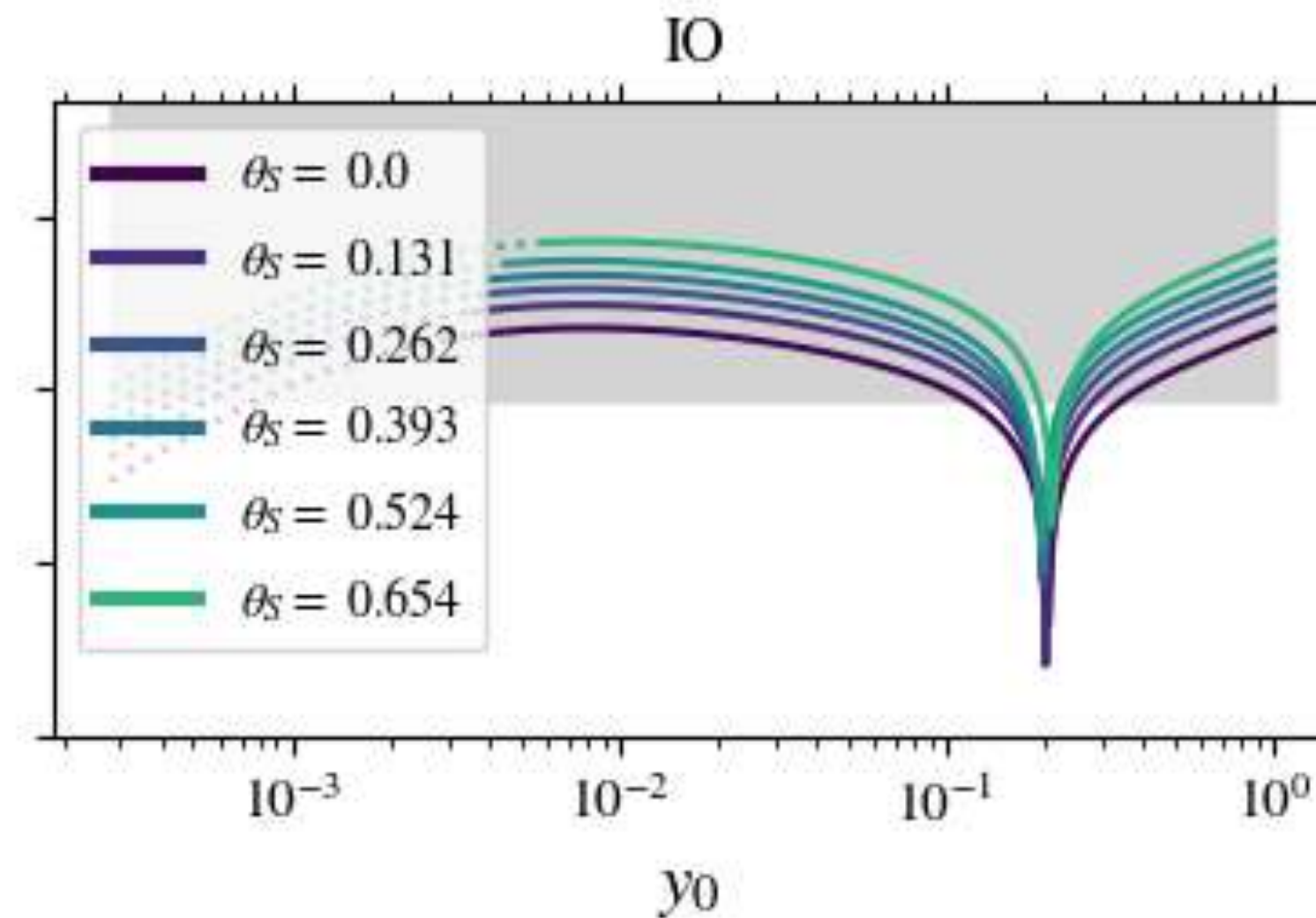
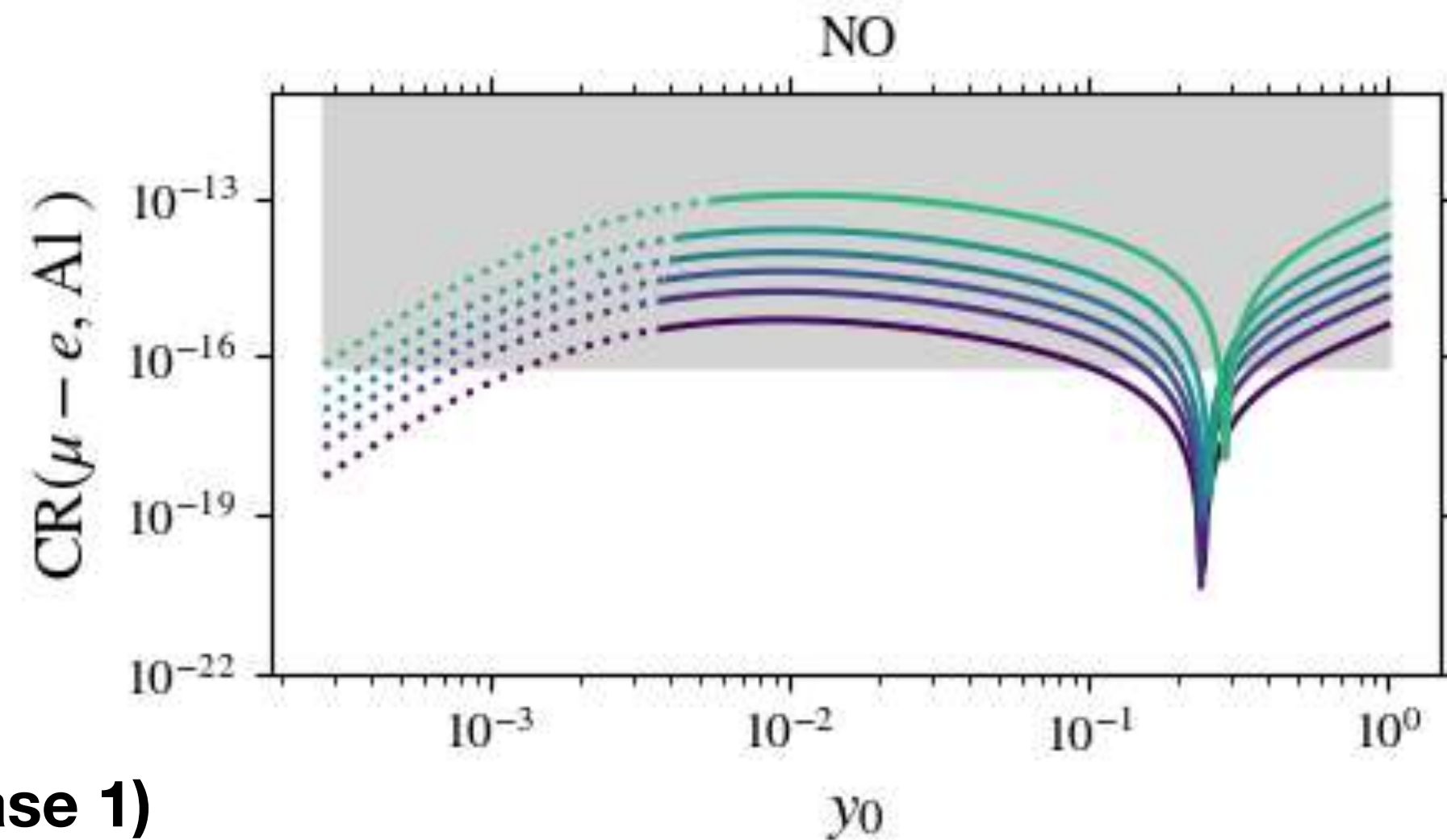
Cancellations of $BR(\mu \rightarrow e\gamma)$ can generally happen for values of the lightest sterile state mass close to 150 GeV

Differently from Option 2, cancellation depends upon the particular CASE (expression of r and spectrum)

The Conversion rate also shows a cancellation for:

$$\bar{x} = \exp \left(\frac{\frac{9}{8}V(n) + \left(\frac{9}{8} + \frac{37}{12}s_w^2\right)V(p) - \frac{s_w^2}{16e}D}{\frac{3}{8}V(n) + \left(\frac{4s_w^2}{3} - \frac{3}{8}\right)V(p)} + \frac{\frac{m_2}{m_1} \log \frac{m_2}{m_1} + r \frac{m_3}{m_1} \log \frac{m_3}{m_1}}{\frac{m_2}{m_1} - 1 + r \left(\frac{m_3}{m_1} - 1\right)} \right)$$

Case 1), $n=26, s=1$



($\mu_0 = 3 \text{ keV}$)

Case 1)

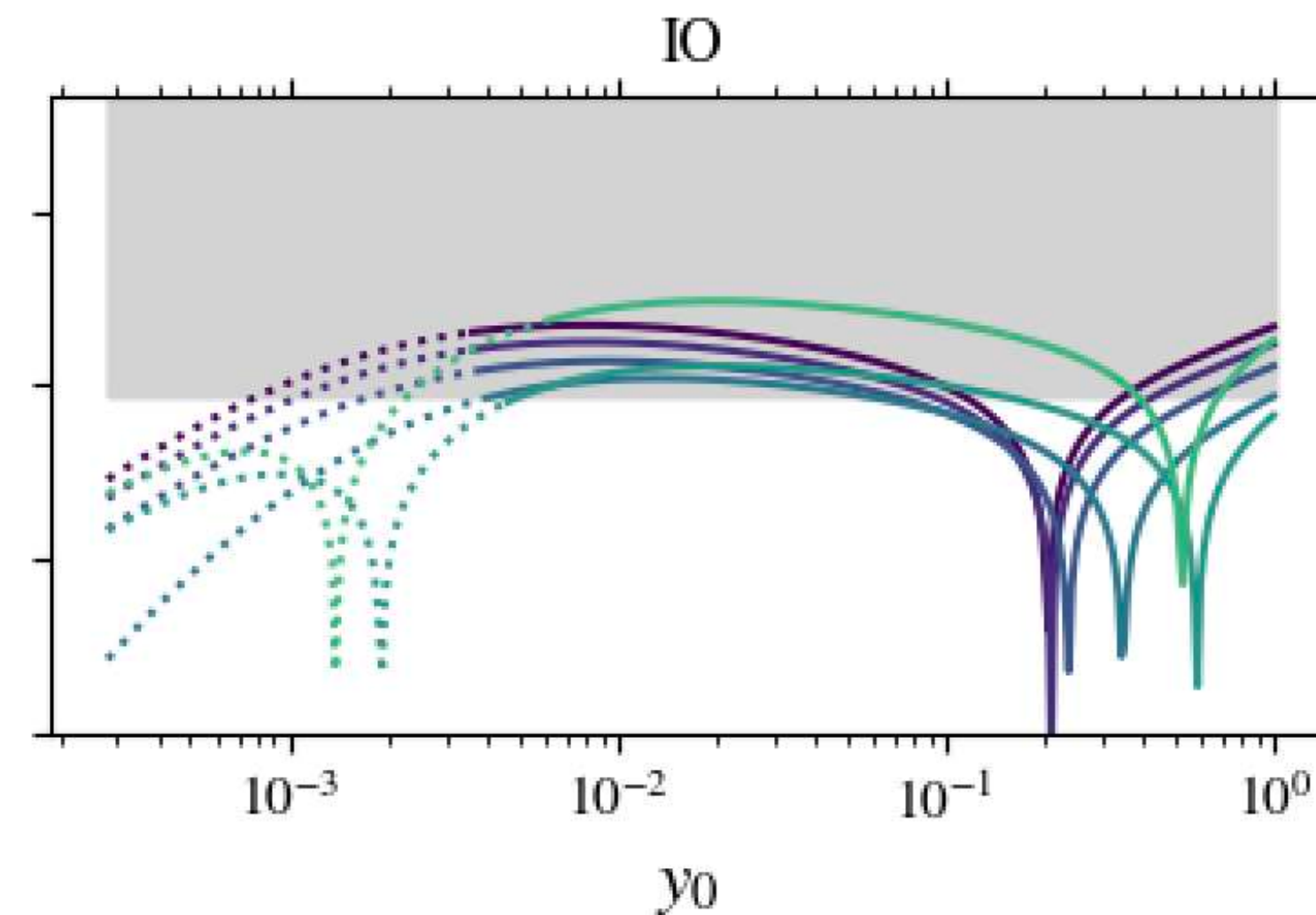
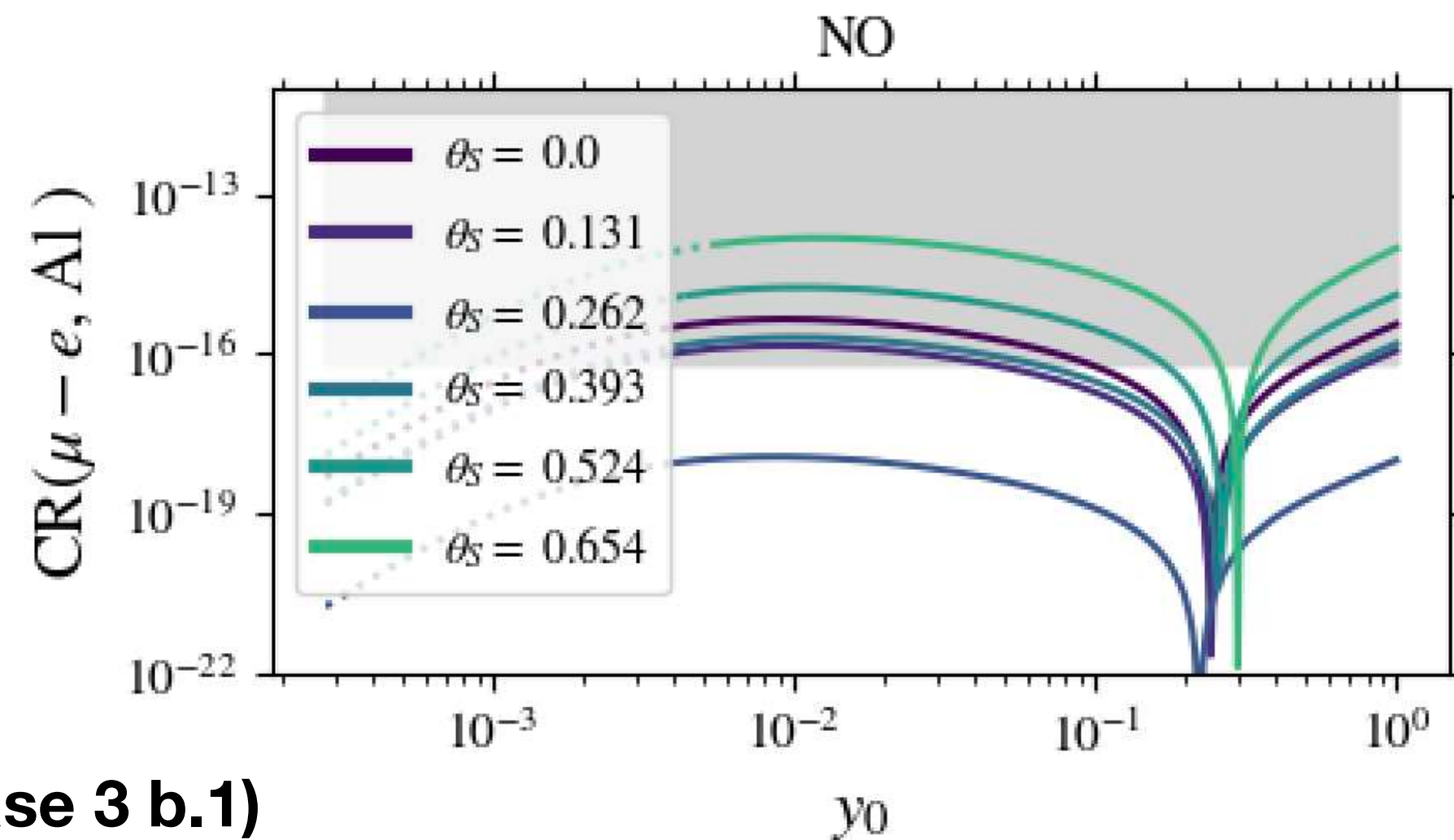
- Weak dependence on the different values of θ_S
- Single solution for θ_N

Differently from Option 2, cancellation depends upon the particular CASE (expression of r and spectrum)

The Conversion rate also shows a cancellation for:

$$\bar{x} = \exp \left(\frac{\frac{9}{8}V(n) + \left(\frac{9}{8} + \frac{37}{12}s_w^2\right)V(p) - \frac{s_w^2}{16e}D}{\frac{3}{8}V(n) + \left(\frac{4s_w^2}{3} - \frac{3}{8}\right)V(p)} + \frac{\frac{m_2}{m_1} \log \frac{m_2}{m_1} + r \frac{m_3}{m_1} \log \frac{m_3}{m_1}}{\frac{m_2}{m_1} - 1 + r \left(\frac{m_3}{m_1} - 1\right)} \right)$$

Case 3 b.1), $n = 20, m = 11, s = 0$



($\mu_0 = 3 \text{ keV}$)

Case 3 b.1)

- Stronger dependence on the different values of θ_S
- Single solution for θ_N

When no cancellation happens, we find a local minima:

$$r_R = \frac{\operatorname{Re} \left\{ U_{\mu 3}^* U_{e 3} \right\}}{\operatorname{Re} \left\{ U_{\mu 2}^* U_{e 2} \right\}} \quad ; \quad r_I = \frac{\operatorname{Im} \left\{ U_{\mu 3}^* U_{e 3} \right\}}{\operatorname{Im} \left\{ U_{\mu 2}^* U_{e 2} \right\}} \quad \text{with} \quad r_R \neq r_I$$

$$y_0^{(min)} = \sqrt{\frac{2m_{(1,3)}}{\mu_0 v^2} M_W^2} \exp \left(\frac{1 - \mathcal{K}_R - \mathcal{K}_I \phi^2}{2 - \mathcal{K}_R^2 - \mathcal{K}_I^2 \phi^2} \right)$$

$$\mathcal{K}_{R,I} = - \left[\frac{\frac{9}{8} V^{(n)} + \left(\frac{9}{8} + \frac{37}{12} s_w^2 \right) V^{(p)} - \frac{s_w^2}{16e} D}{\frac{3}{8} V^{(n)} + \left(\frac{4s_w^2}{3} - \frac{3}{8} \right) V^{(p)}} + \frac{\frac{m_2}{m_1} \log \frac{m_2}{m_1} + r \frac{m_3}{m_1} \log \frac{m_3}{m_1}}{\frac{m_2}{m_1} - 1 + r \left(\frac{m_3}{m_1} - 1 \right)} \right]^{-1}$$

With:

$$\phi = \left| \arg \left\{ U_{\mu 2}^* U_{e 2} \right\} \frac{-54e(V^{(n)} + V^{(p)}) + s_w^2(3D - 148eV^{(p)}) \left(-1 + \frac{m_2}{m_1} + r_R \left(-1 + \frac{m_3}{m_1} \right) \right) - 2e(9V^{(n)} + (-9 + 32s_w^2)V^{(p)}) \left(\frac{m_2}{m_1} \log \frac{m_2}{m_1} + r_I \frac{m_3}{m_1} \log \frac{m_3}{m_1} \right)}{-54e(V^{(n)} + V^{(p)}) + s_w^2(3D - 148eV^{(p)}) \left(-1 + \frac{m_2}{m_1} + r_I \left(-1 + \frac{m_3}{m_1} \right) \right) - 2e(9V^{(n)} + (-9 + 32s_w^2)V^{(p)}) \left(\frac{m_2}{m_1} \log \frac{m_2}{m_1} + r_R \frac{m_3}{m_1} \log \frac{m_3}{m_1} \right)} \right|^2$$

When no cancellation happens, we find a local minima:

$$r_R = \frac{\operatorname{Re} \left\{ U_{\mu 3}^* U_{e 3} \right\}}{\operatorname{Re} \left\{ U_{\mu 2}^* U_{e 2} \right\}} \quad ; \quad r_I = \frac{\operatorname{Im} \left\{ U_{\mu 3}^* U_{e 3} \right\}}{\operatorname{Im} \left\{ U_{\mu 2}^* U_{e 2} \right\}} \quad \text{with} \quad r_R \neq r_I$$

$$y_0^{(min)} = \sqrt{\frac{2m_{(1,3)}}{\mu_0 v^2} M_W^2} \exp \left(\frac{1 - \mathcal{K}_R - \mathcal{K}_I \phi^2}{2 - \mathcal{K}_R^2 - \mathcal{K}_I^2 \phi^2} \right) \quad \mathcal{K}_{R,I} = - \left[\frac{\frac{9}{8} V^{(n)} + \left(\frac{9}{8} + \frac{37}{12} s_w^2 \right) V^{(p)} - \frac{s_w^2}{16e} D}{\frac{3}{8} V^{(n)} + \left(\frac{4s_w^2}{3} - \frac{3}{8} \right) V^{(p)}} + \frac{\frac{m_2}{m_1} \log \frac{m_2}{m_1} + r \frac{m_3}{m_1} \log \frac{m_3}{m_1}}{\frac{m_2}{m_1} - 1 + r \left(\frac{m_3}{m_1} - 1 \right)} \right]^{-1}$$

With:

$$\phi = \left| \arg \left\{ U_{\mu 2}^* U_{e 2} \right\} \frac{-54e(V^{(n)} + V^{(p)}) + s_w^2(3D - 148eV^{(p)}) \left(-1 + \frac{m_2}{m_1} + r_R \left(-1 + \frac{m_3}{m_1} \right) \right) - 2e(9V^{(n)} + (-9 + 32s_w^2)V^{(p)}) \left(\frac{m_2}{m_1} \log \frac{m_2}{m_1} + r_I \frac{m_3}{m_1} \log \frac{m_3}{m_1} \right)}{-54e(V^{(n)} + V^{(p)}) + s_w^2(3D - 148eV^{(p)}) \left(-1 + \frac{m_2}{m_1} + r_I \left(-1 + \frac{m_3}{m_1} \right) \right) - 2e(9V^{(n)} + (-9 + 32s_w^2)V^{(p)}) \left(\frac{m_2}{m_1} \log \frac{m_2}{m_1} + r_R \frac{m_3}{m_1} \log \frac{m_3}{m_1} \right)} \right|^2$$

Way too complicated... What does this mean???



When no cancellation happens, we find a local minima:

$$r_R = \frac{\mathbf{Re} \left\{ U_{\mu 3}^* U_{e3} \right\}}{\mathbf{Re} \left\{ U_{\mu 2}^* U_{e2} \right\}} \quad ; \quad r_I = \frac{\mathbf{Im} \left\{ U_{\mu 3}^* U_{e3} \right\}}{\mathbf{Im} \left\{ U_{\mu 2}^* U_{e2} \right\}} \quad \text{with} \quad r_R \neq r_I$$

$$y_0^{(min)} = \sqrt{\frac{2m_{(1,3)}}{\mu_0 v^2} M_W^2} \exp \left(\frac{1 - \mathcal{K}_R - \mathcal{K}_I \phi^2}{2 - \mathcal{K}_R^2 - \mathcal{K}_I^2 \phi^2} \right)$$

$$\mathcal{K}_{R,I} = - \left[\frac{\frac{9}{8} V^{(n)} + \left(\frac{9}{8} + \frac{37}{12} s_w^2 \right) V^{(p)} - \frac{s_w^2}{16e} D}{\frac{3}{8} V^{(n)} + \left(\frac{4s_w^2}{3} - \frac{3}{8} \right) V^{(p)}} + \frac{\frac{m_2}{m_1} \log \frac{m_2}{m_1} + r \frac{m_3}{m_1} \log \frac{m_3}{m_1}}{\frac{m_2}{m_1} - 1 + r \left(\frac{m_3}{m_1} - 1 \right)} \right]^{-1}$$

General structure of the rate is $\mathcal{R} \propto \mathbf{Re} \{ \bar{\mathcal{L}} \}^2 + \mathbf{Im} \{ \bar{\mathcal{L}} \}^2$

When no cancellation happens, we find a local minima:

$$r_R = \frac{\operatorname{Re} \left\{ U_{\mu 3}^* U_{e 3} \right\}}{\operatorname{Re} \left\{ U_{\mu 2}^* U_{e 2} \right\}} \quad ; \quad r_I = \frac{\operatorname{Im} \left\{ U_{\mu 3}^* U_{e 3} \right\}}{\operatorname{Im} \left\{ U_{\mu 2}^* U_{e 2} \right\}} \quad \text{with} \quad r_R \neq r_I$$

$$y_0^{(\min)} = \sqrt{\frac{2m_{(1,3)}}{\mu_0 v^2} M_W^2} \exp \left(\frac{1 - \mathcal{K}_R - \mathcal{K}_I \phi^2}{2 - \mathcal{K}_R^2 - \mathcal{K}_I^2 \phi^2} \right)$$

$$\mathcal{K}_{R,I} = - \left[\frac{\frac{9}{8} V^{(n)} + \left(\frac{9}{8} + \frac{37}{12} s_w^2 \right) V^{(p)} - \frac{s_w^2}{16e} D}{\frac{3}{8} V^{(n)} + \left(\frac{4s_w^2}{3} - \frac{3}{8} \right) V^{(p)}} + \frac{\frac{m_2}{m_1} \log \frac{m_2}{m_1} + r \frac{m_3}{m_1} \log \frac{m_3}{m_1}}{\frac{m_2}{m_1} - 1 + r \left(\frac{m_3}{m_1} - 1 \right)} \right]^{-1}$$

General structure of the rate is $\mathcal{R} \propto \operatorname{Re} \{ \bar{\mathcal{L}} \}^2 + \operatorname{Im} \{ \bar{\mathcal{L}} \}^2$

$\operatorname{Re} \{ \bar{\mathcal{L}} \}^2$ and $\operatorname{Im} \{ \bar{\mathcal{L}} \}^2$ cancel independently at $y_0^{(R,I)}$ respectively

When no cancellation happens, we find a local minima:

$$r_R = \frac{\operatorname{Re} \left\{ U_{\mu 3}^* U_{e 3} \right\}}{\operatorname{Re} \left\{ U_{\mu 2}^* U_{e 2} \right\}} \quad ; \quad r_I = \frac{\operatorname{Im} \left\{ U_{\mu 3}^* U_{e 3} \right\}}{\operatorname{Im} \left\{ U_{\mu 2}^* U_{e 2} \right\}} \quad \text{with} \quad r_R \neq r_I$$

$$y_0^{(min)} = \sqrt{\frac{2m_{(1,3)}}{\mu_0 v^2} M_W^2} \exp \left(\frac{1 - \mathcal{K}_R - \mathcal{K}_I \phi^2}{2 - \mathcal{K}_R^2 - \mathcal{K}_I^2 \phi^2} \right)$$

$$\mathcal{K}_{R,I} = - \left[\frac{\frac{9}{8} V^{(n)} + \left(\frac{9}{8} + \frac{37}{12} s_w^2 \right) V^{(p)} - \frac{s_w^2}{16e} D}{\frac{3}{8} V^{(n)} + \left(\frac{4s_w^2}{3} - \frac{3}{8} \right) V^{(p)}} + \frac{\frac{m_2}{m_1} \log \frac{m_2}{m_1} + r \frac{m_3}{m_1} \log \frac{m_3}{m_1}}{\frac{m_2}{m_1} - 1 + r \left(\frac{m_3}{m_1} - 1 \right)} \right]^{-1}$$

General structure of the rate is $\mathcal{R} \propto \operatorname{Re} \{ \bar{\mathcal{L}} \}^2 + \operatorname{Im} \{ \bar{\mathcal{L}} \}^2$

$\operatorname{Re} \{ \bar{\mathcal{L}} \}^2$ and $\operatorname{Im} \{ \bar{\mathcal{L}} \}^2$ cancel independently at $y_0^{(R,I)}$ respectively

$$y_0^{(R)} = y_0^{(I)} \Leftrightarrow r_I = r_R$$

When no cancellation happens, we find a local minima:

$$r_R = \frac{\operatorname{Re} \left\{ U_{\mu 3}^* U_{e 3} \right\}}{\operatorname{Re} \left\{ U_{\mu 2}^* U_{e 2} \right\}} \quad ; \quad r_I = \frac{\operatorname{Im} \left\{ U_{\mu 3}^* U_{e 3} \right\}}{\operatorname{Im} \left\{ U_{\mu 2}^* U_{e 2} \right\}} \quad \text{with} \quad r_R \neq r_I$$

$$y_0^{(min)} = \sqrt{\frac{2m_{(1,3)}}{\mu_0 v^2} M_W^2} \exp \left(\frac{1 - \mathcal{K}_R - \mathcal{K}_I \phi^2}{2 - \mathcal{K}_R^2 - \mathcal{K}_I^2 \phi^2} \right)$$

$$\mathcal{K}_{R,I} = - \left[\frac{\frac{9}{8} V^{(n)} + \left(\frac{9}{8} + \frac{37}{12} s_w^2 \right) V^{(p)} - \frac{s_w^2}{16e} D}{\frac{3}{8} V^{(n)} + \left(\frac{4s_w^2}{3} - \frac{3}{8} \right) V^{(p)}} + \frac{\frac{m_2}{m_1} \log \frac{m_2}{m_1} + r \frac{m_3}{m_1} \log \frac{m_3}{m_1}}{\frac{m_2}{m_1} - 1 + r \left(\frac{m_3}{m_1} - 1 \right)} \right]^{-1}$$

General structure of the rate is $\mathcal{R} \propto \operatorname{Re} \{ \bar{\mathcal{L}} \}^2 + \operatorname{Im} \{ \bar{\mathcal{L}} \}^2$

$\operatorname{Re} \{ \bar{\mathcal{L}} \}^2$ and $\operatorname{Im} \{ \bar{\mathcal{L}} \}^2$ cancel independently at $y_0^{(R,I)}$ respectively

$$y_0^{(R)} = y_0^{(I)} \Leftrightarrow r_I = r_R$$

The minima is shallower the closer r_R and r_I are

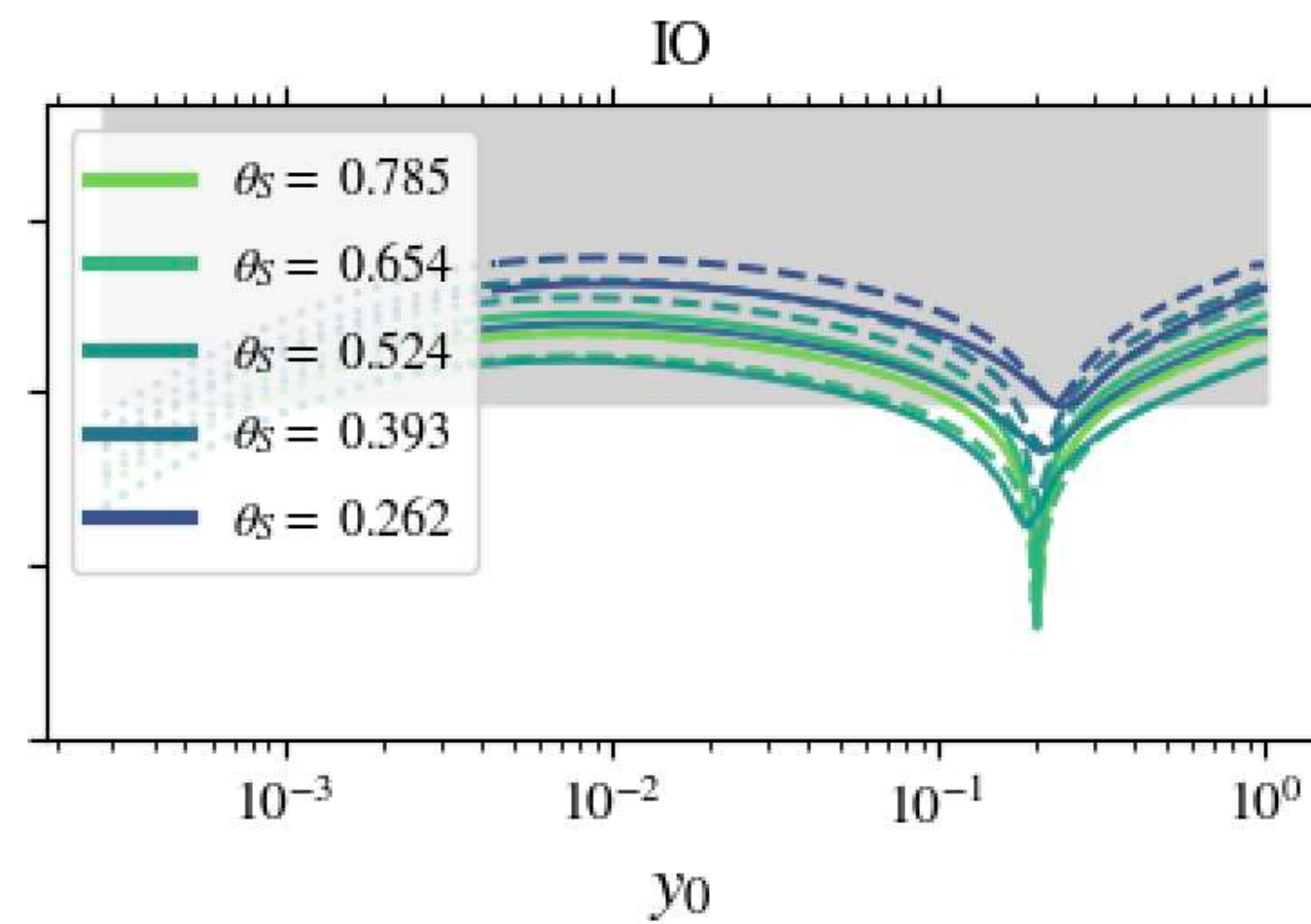
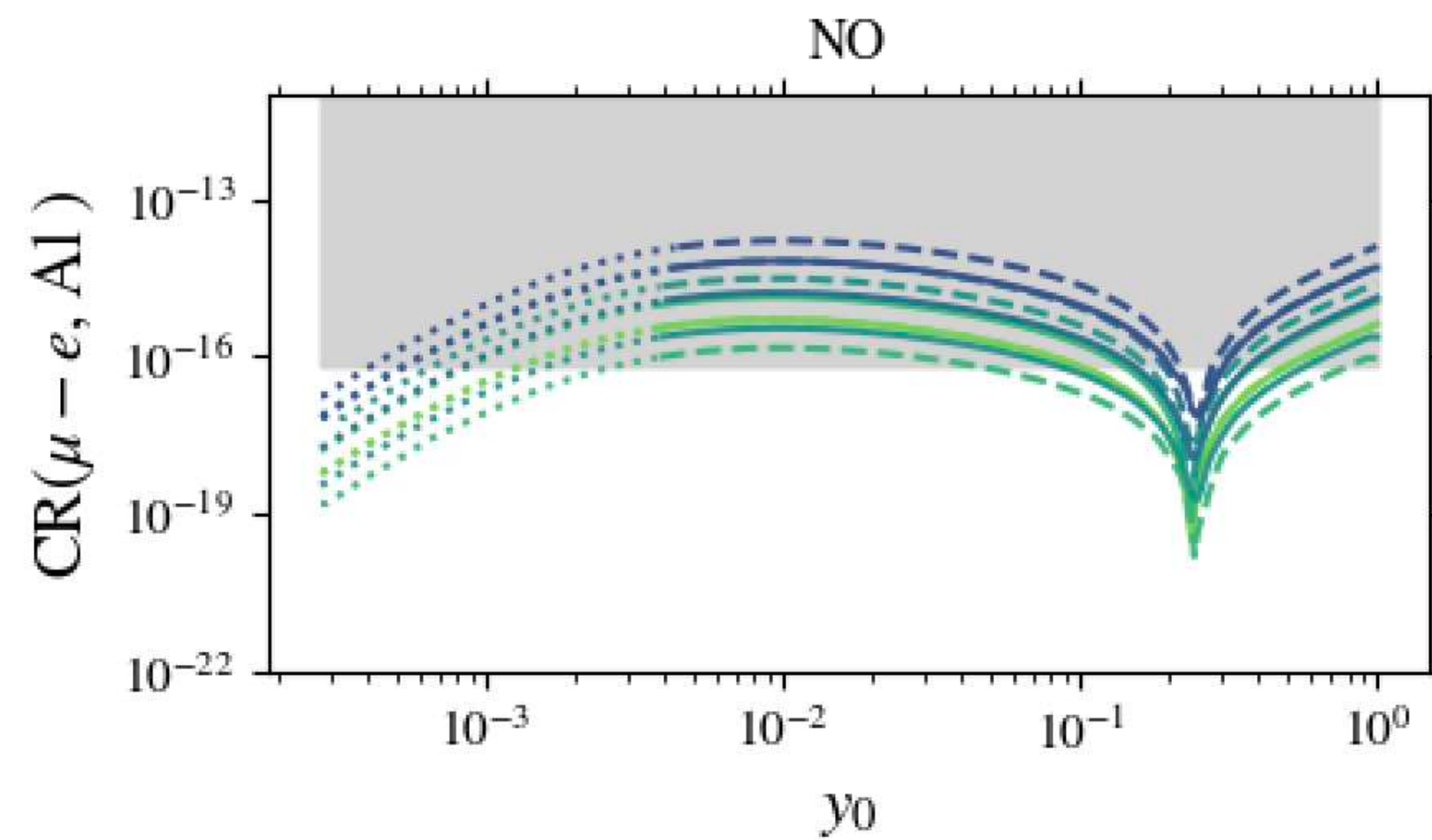
Let's see some examples!!

When no cancellation happens, we find a local minima:

$$r_R = \frac{\operatorname{Re} \left\{ U_{\mu 3}^* U_{e 3} \right\}}{\operatorname{Re} \left\{ U_{\mu 2}^* U_{e 2} \right\}} \quad ; \quad r_I = \frac{\operatorname{Im} \left\{ U_{\mu 3}^* U_{e 3} \right\}}{\operatorname{Im} \left\{ U_{\mu 2}^* U_{e 2} \right\}} \quad \text{with} \quad r_R \neq r_I$$

$$y_0^{(\min)} = \sqrt{\frac{2m_{(1,3)}}{\mu_0 v^2} M_W^2} \exp \left(\frac{1 - \mathcal{K}_R - \mathcal{K}_I \phi^2}{2 - \mathcal{K}_R^2 - \mathcal{K}_I^2 \phi^2} \right) \quad \mathcal{K}_{R,I} = - \left[\frac{\frac{9}{8} V^{(n)} + \left(\frac{9}{8} + \frac{37}{12} s_w^2 \right) V^{(p)} - \frac{s_w^2}{16e} D}{\frac{3}{8} V^{(n)} + \left(\frac{4s_w^2}{3} - \frac{3}{8} \right) V^{(p)}} + \frac{\frac{m_2}{m_1} \log \frac{m_2}{m_1} + r \frac{m_3}{m_1} \log \frac{m_3}{m_1}}{\frac{m_2}{m_1} - 1 + r \left(\frac{m_3}{m_1} - 1 \right)} \right]^{-1}$$

Case 2), $n = 14, u = 1$ ($s = 1, t = 1$)



Case 2)

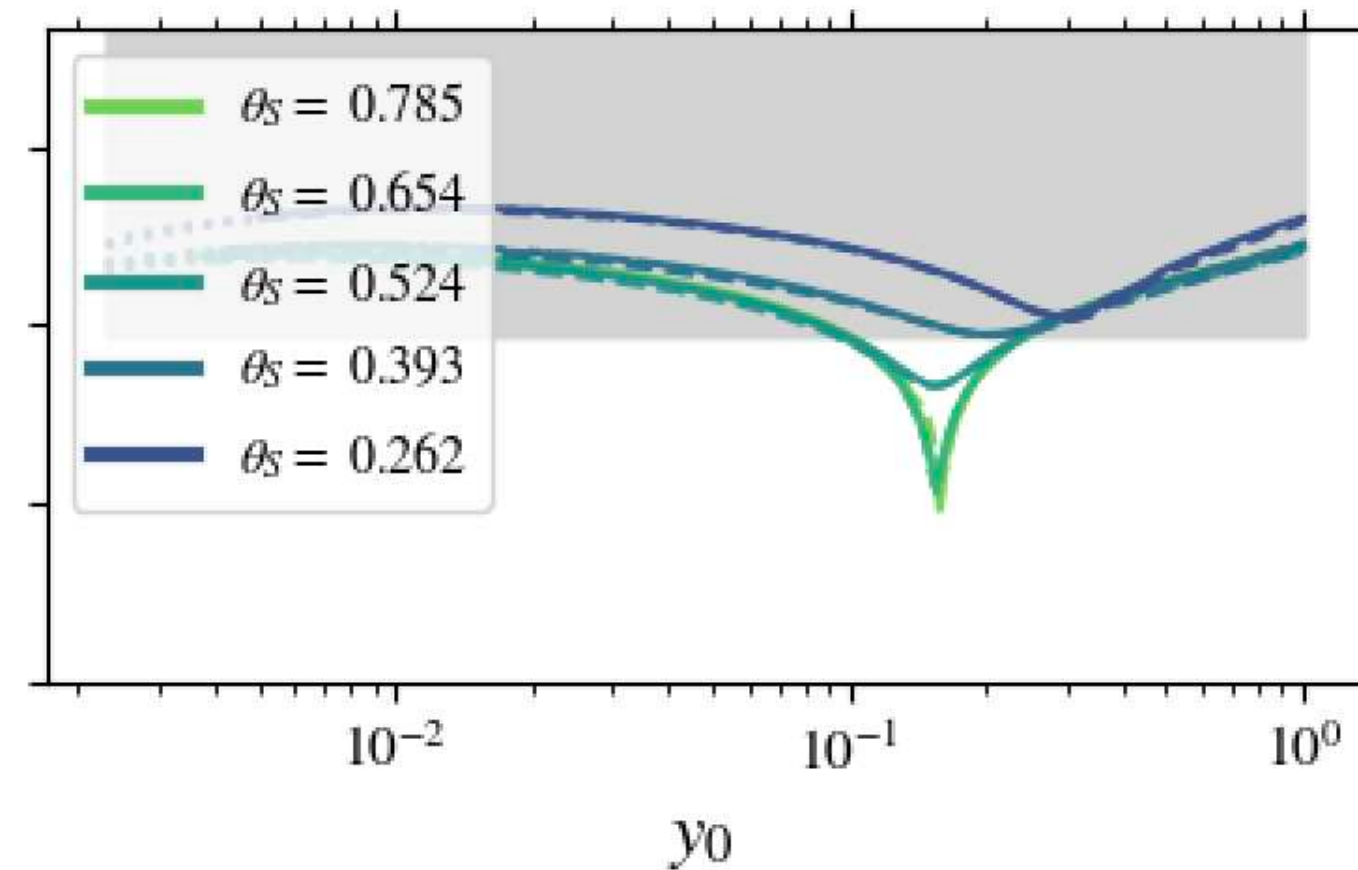
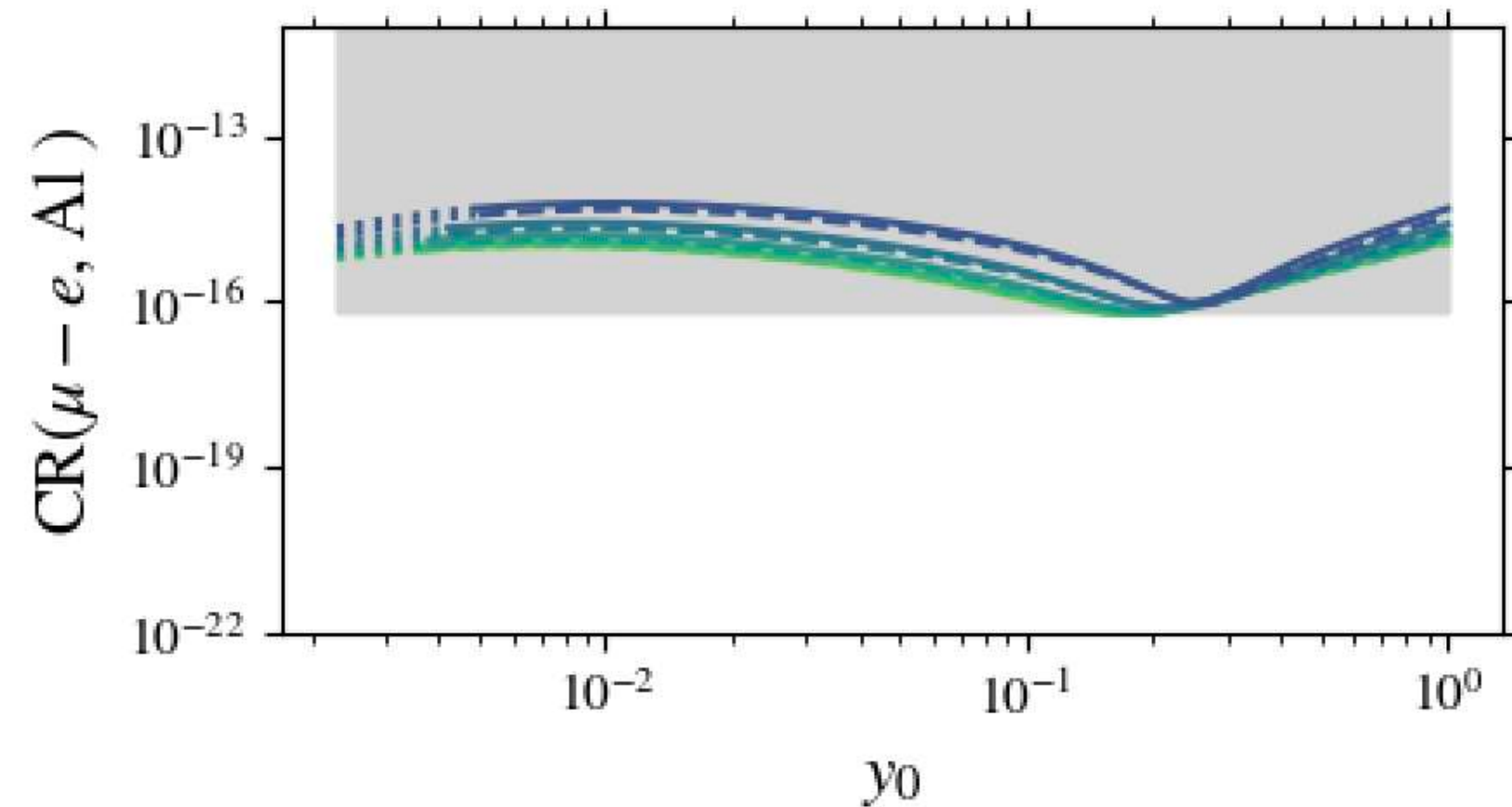
- Dependence on θ_S is rather weak
- Minima is really shallow due to $r_R \approx r_I$
- Shallower minima for IO

When no cancellation happens, we find a local minima:

$$r_R = \frac{\operatorname{Re} \left\{ U_{\mu 3}^* U_{e 3} \right\}}{\operatorname{Re} \left\{ U_{\mu 2}^* U_{e 2} \right\}} \quad ; \quad r_I = \frac{\operatorname{Im} \left\{ U_{\mu 3}^* U_{e 3} \right\}}{\operatorname{Im} \left\{ U_{\mu 2}^* U_{e 2} \right\}} \quad \text{with} \quad r_R \neq r_I$$

$$y_0^{(\min)} = \sqrt{\frac{2m_{(1,3)}}{\mu_0 v^2} M_W^2} \exp \left(\frac{1 - \mathcal{K}_R - \mathcal{K}_I \phi^2}{2 - \mathcal{K}_R^2 - \mathcal{K}_I^2 \phi^2} \right) \quad \mathcal{K}_{R,I} = - \left[\frac{\frac{9}{8} V^{(n)} + \left(\frac{9}{8} + \frac{37}{12} s_w^2 \right) V^{(p)} - \frac{s_w^2}{16e} D}{\frac{3}{8} V^{(n)} + \left(\frac{4s_w^2}{3} - \frac{3}{8} \right) V^{(p)}} + \frac{\frac{m_2}{m_1} \log \frac{m_2}{m_1} + r \frac{m_3}{m_1} \log \frac{m_3}{m_1}}{\frac{m_2}{m_1} - 1 + r \left(\frac{m_3}{m_1} - 1 \right)} \right]^{-1}$$

Case 2), $n=14, u=1$ ($s=1, t=1$), ($m_0 \rightarrow 0$)



Case 2)

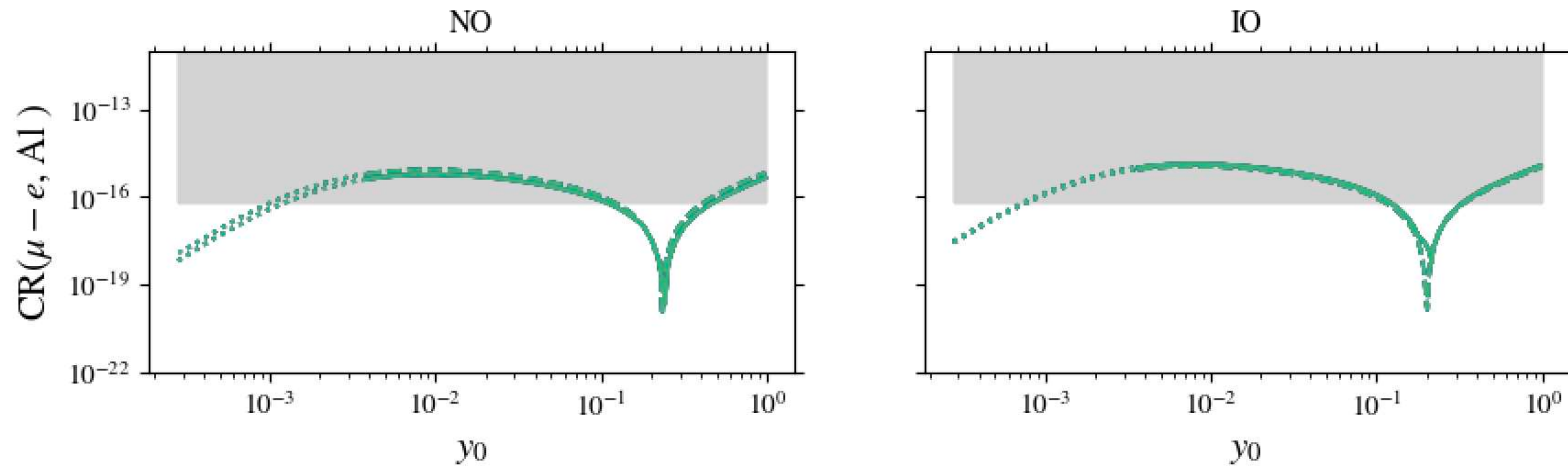
- In the decoupling limit minima is much shallower
- Stronger dependence on θ_S
- Shallower minima for NO

When no cancellation happens, we find a local minima:

$$r_R = \frac{\operatorname{Re} \left\{ U_{\mu 3}^* U_{e 3} \right\}}{\operatorname{Re} \left\{ U_{\mu 2}^* U_{e 2} \right\}} \quad ; \quad r_I = \frac{\operatorname{Im} \left\{ U_{\mu 3}^* U_{e 3} \right\}}{\operatorname{Im} \left\{ U_{\mu 2}^* U_{e 2} \right\}} \quad \text{with} \quad r_R \neq r_I$$

$$y_0^{(\min)} = \sqrt{\frac{2m_{(1,3)}}{\mu_0 v^2} M_W^2} \exp \left(\frac{1 - \mathcal{K}_R - \mathcal{K}_I \phi^2}{2 - \mathcal{K}_R^2 - \mathcal{K}_I^2 \phi^2} \right) \quad \mathcal{K}_{R,I} = - \left[\frac{\frac{9}{8} V^{(n)} + \left(\frac{9}{8} + \frac{37}{12} s_w^2 \right) V^{(p)} - \frac{s_w^2}{16e} D}{\frac{3}{8} V^{(n)} + \left(\frac{4s_w^2}{3} - \frac{3}{8} \right) V^{(p)}} + \frac{\frac{m_2}{m_1} \log \frac{m_2}{m_1} + r \frac{m_3}{m_1} \log \frac{m_3}{m_1}}{\frac{m_2}{m_1} - 1 + r \left(\frac{m_3}{m_1} - 1 \right)} \right]^{-1}$$

Case 3 a), $n = 16, m = 1, s = 1$



Case 3 a)

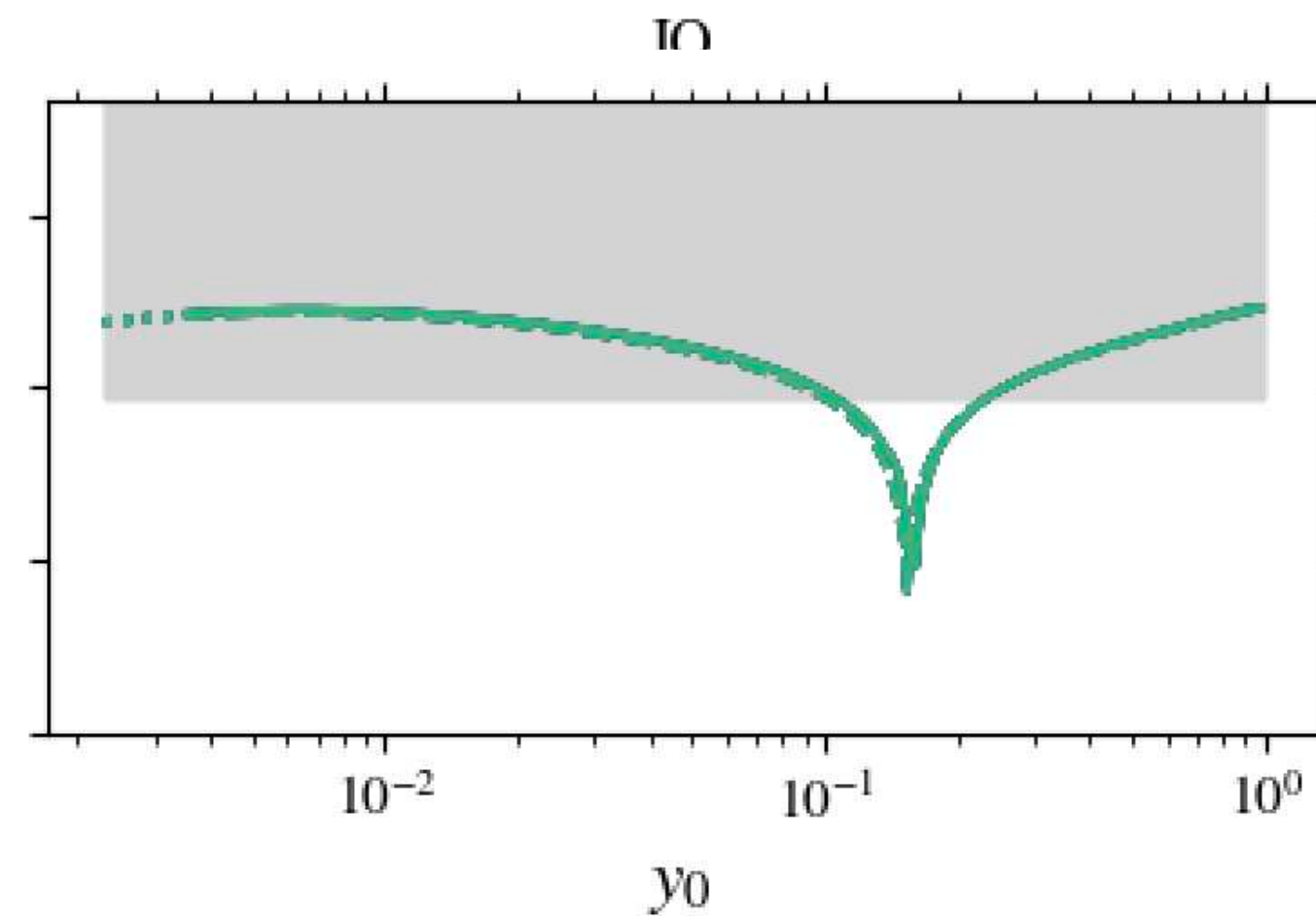
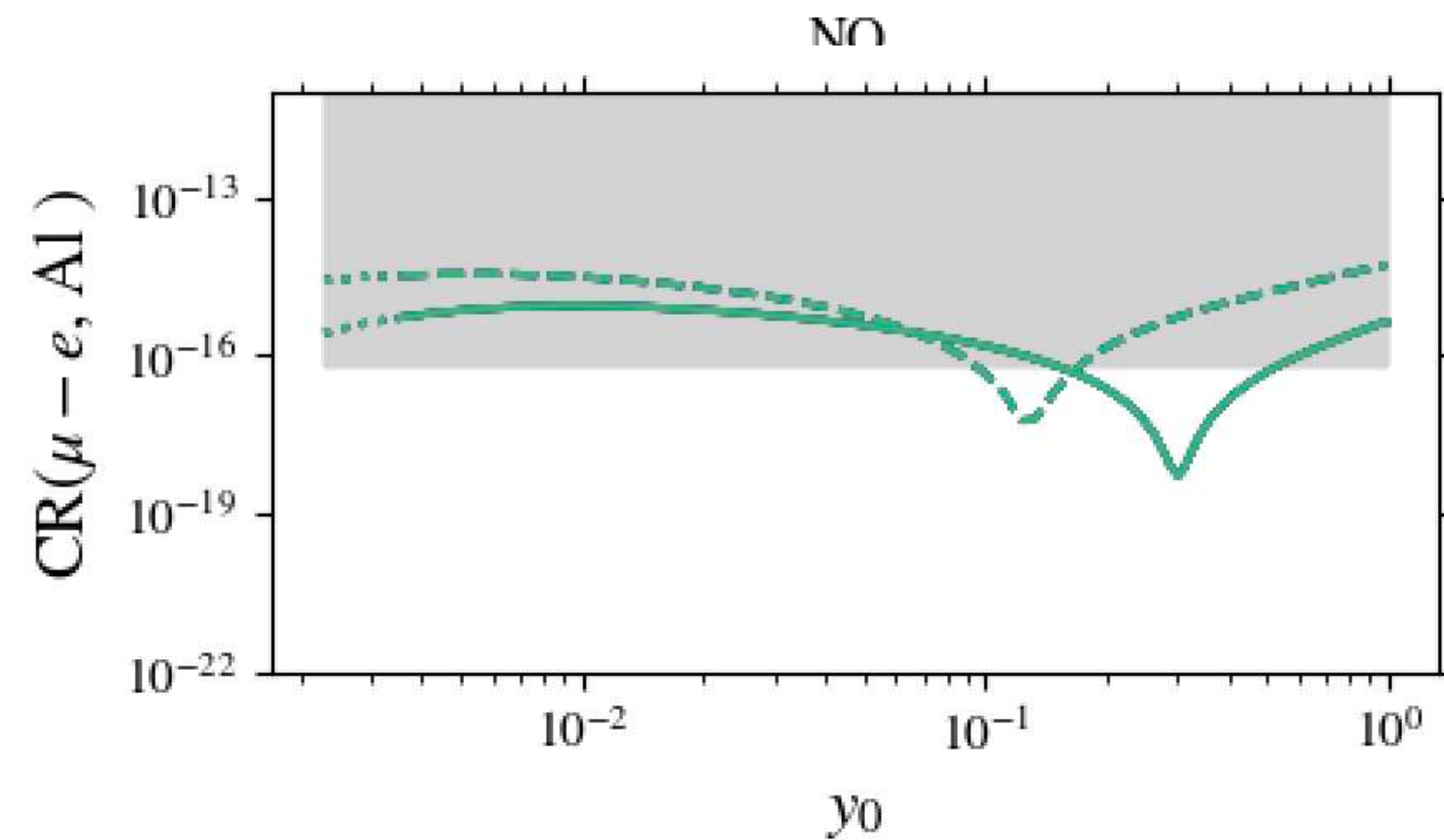
- As per Case 2, minima is really shallow due to $r_R \approx r_I$

When no cancellation happens, we find a local minima:

$$r_R = \frac{\text{Re} \left\{ U_{\mu 3}^* U_{e 3} \right\}}{\text{Re} \left\{ U_{\mu 2}^* U_{e 2} \right\}} \quad ; \quad r_I = \frac{\text{Im} \left\{ U_{\mu 3}^* U_{e 3} \right\}}{\text{Im} \left\{ U_{\mu 2}^* U_{e 2} \right\}} \quad \text{with} \quad r_R \neq r_I$$

$$y_0^{(\min)} = \sqrt{\frac{2m_{(1,3)}}{\mu_0 v^2} M_W^2} \exp \left(\frac{1 - \mathcal{K}_R - \mathcal{K}_I \phi^2}{2 - \mathcal{K}_R^2 - \mathcal{K}_I^2 \phi^2} \right) \quad \mathcal{K}_{R,I} = - \left[\frac{\frac{9}{8} V^{(n)} + \left(\frac{9}{8} + \frac{37}{12} s_w^2 \right) V^{(p)} - \frac{s_w^2}{16e} D}{\frac{3}{8} V^{(n)} + \left(\frac{4s_w^2}{3} - \frac{3}{8} \right) V^{(p)}} + \frac{\frac{m_2}{m_1} \log \frac{m_2}{m_1} + r \frac{m_3}{m_1} \log \frac{m_3}{m_1}}{\frac{m_2}{m_1} - 1 + r \left(\frac{m_3}{m_1} - 1 \right)} \right]^{-1}$$

Case 3 a), $n = 16, m = 1, s = 1$, $(m_0 \rightarrow 0)$



Case 3 a)

- In the decoupling limit, for NO, different predictions for different solutions for θ_N
- Shallow minima for NO only

Option 3: Case 2

Case 2), $n = 14, s = 1, t = 2 (u = 0)$, NO, $m_0 = 1e-14eV$

In the decoupling limit, predictions are of the same order of magnitude

Local minima is much shallower than in the non-decoupling limit

Lower limit is raised due to the shallower minima

